RHEOLOGICAL STUDIES AND SIMULATED DISTILLATION OF CRUDE OILS POST ELECTRON BEAM TREATMENT

A Thesis

by

HARIKA RAO DAMARLA

Submitted to the Office of Graduate and Professional Studies of
Texas A&M University
in partial fulfillment of the requirements for the degree of

MASTER OF SCIENCE

Chair of Committee,	David Staack
Committee Members,	Andrea Strzelec
	Berna Hascakir
Head of Department,	Andreas Polycarpou

December 2016

Major Subject: Mechanical Engineering

ABSTRACT

Use of electron beam irradiation could effectively transfer energy to crude oil, resulting in improved cracking and reduction of operating temperatures. The overall objective is to crack heavy oil and make it less viscous while avoiding generation of micro-carbon residue and olefins. A flow loop system has been built to dynamically treat extra-heavy crude oils with electron beam. Operating temperature, dose rate, dose and shear rate have been identified to be the important parameters.

This thesis focuses on analyzing the fluid properties and characterization of heavy crude oils pre and post treatment. Extra-heavy crude oil and bitumen with API gravity in the range of 7-8° (viscosity; order of 10^6cP at 40°C) have been used for this study. Rheological studies and viscosity measurements have been performed using a rheometer. Existing viscosity-temperature models have been modified and utilized to obtain continuous viscosity-temperature plots. Further, blending experiments have been conducted to understand the effect of addition or loss of different yields (lighter fractions, middle distillates, heavy residue etc.) and account for discrepancies in mass balance.

Oil characterization has been carried out using simulated distillation on a gas chromatograph. High temperature simulated distillation methods such as ASTM D6352 and ASTM D7169 have been used for the same. Polywax 655 has been employed to obtain the retention time calibration. Percentage weight off versus boiling point (% wt off vs BP) has been measured to obtain the % conversion post treatment.

Experimental process conditions were broadly tested. Temperatures in the range of 100-300°C, dose rates of the order of 15-25 kGy/s and absorbed dose in the range of 20-1700 kGy were employed during the experiments. Initial tests yielded a reduction in viscosity of 50% for oil #1 (1300 kGy, 20 kGy/s) and 39% for oil #2 (560 kGy, 20 kGy/s) measured at 100°C. Simulated distillation results indicate a sample conversion of 9.84% and residue conversion (above 1000°F) of 20.95% for oil #2 at conditions stated above. For oil #1, sample conversion was 6% and residue conversion (above 1000°F) was 16.8% at conditions stated above.

DEDICATION

To Dr. Krishnan

ACKNOWLEDGEMENTS

I am grateful to my advisor, Dr. David Staack, for presenting me with the opportunity to work under his guidance. I would like to thank my committee members Dr. Andrea Strzelec and Dr. Berna Hascakir for their valuable suggestions.

I would also like to thank all the members of the plasma engineering and diagnostics laboratory for their invaluable support and assistance.

I would like to thank Dr. Alexander Gutsol and Chevron for the sponsorship of my research. It has been a learning experience working with Dr. Yuriy Zaikin, and Dr. Raissa Zaikina.

NOMENCLATURE

API	American Petroleum Institute
ASTM	American Society for Testing and Materials
BNC	Bayonet Neill–Concelman
°C	Degrees Celsius
CAPEX	Capital Expenditure
CFM	Cubic Feet per Minute
CO_2	Carbon dioxide
cP	Centipoise (dynamic viscosity unit; 1 cP = 1 mPa.s)
eV	Electron Volt
°F	Degrees Fahrenheit
H_2S	Hydrogen Sulfide
kGy	kJ/kg (unit of radiation energy)
Ni	Nickel
OD	Outer Diameter
P&ID	Process and Instrumentation Diagram
ppm	Parts Per Million
ppmw	Parts Per Million Weight
psi	Pounds per Square Inch
UPS	Uninterruptible Power Supply
V	Vanadium

TABLE OF CONTENTS

Page

LIST OF FIGURES

Page

LIST OF TABLES

Page

1. INTRODUCTION

1.1 Background

Petroleum in its crude form is a complex mixture which is refined to obtain various products such as gasoline, diesel, fuel oil etc. With increasing demand for petroleum products and decreasing conventional crude oil resources, previously undeveloped unconventional reserves are at the forefront. Conventional crude reserves have long established production, transportation and refining techniques. Extracted using traditional oil well techniques, they are easier and cheaper to produce, typically yield significant lower boiling distillates and hence have high market value. Unconventional crude, on the other hand poses challenges in production, transportation and refining. With high amounts of residue, they have lower market value than conventional crude and upgrading forms an essential refining process. Even though heavy oils are difficult and expensive to produce, transport, and refine, they are abundant. Oil sands-bitumen, heavy and extra-heavy crude oil form part of unconventional crude reserves and amount to 70% of total oil reserves [1] as shown in Figure 1. Most of the bitumen-oil sands reserves are concentrated in Canada and extra-heavy crude reserves in Orinoco belt, Venezuela. Together they amount to an estimated 4 trillion barrels of oil in place [2]. However, recoverable oil is much lower than oil in place and varies with existing technologies. But, with improvements and technological advancements in production and refining, more unconventional oil can be produced.

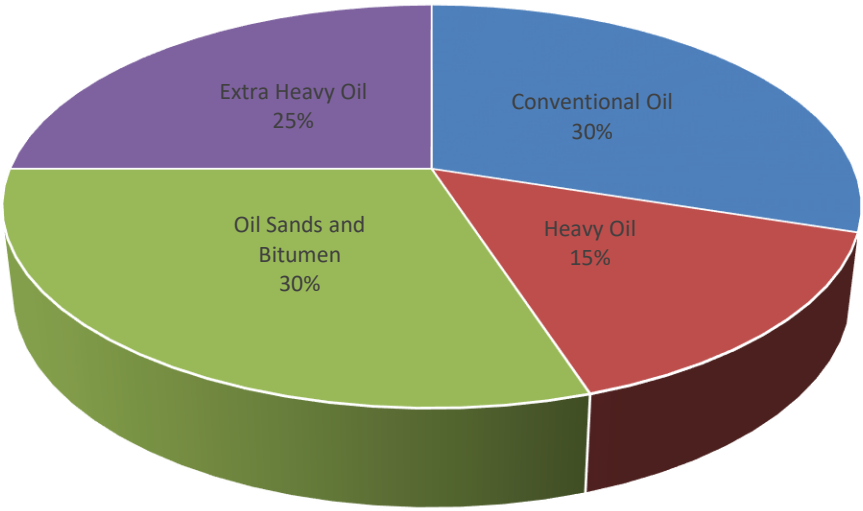

Figure 1: Total world oil reserves. Data taken from [1]

Biodegradation is considered to be a major cause for heavy oil formation. Over long geologic time scales, light and medium hydrocarbons could be degraded by microorganisms resulting in high C/H ratios, heavier molecules, and higher metal and sulfur content characteristic of heavy crude oils [1]. With viscosities of the order of 10^6 cP at ambient temperatures, they pose serious challenges in transportation. While pipelines remain the most efficient way to transfer oil, pipeline manufacturers have a maximum viscosity limit of 400 cP for the oil to be transported [3]. Other problems with heavy crude pipelining include paraffin instability, asphaltene precipitation, clogging of pipes and high pressure drops [4]. Hence, on site viscosity reduction or upgrading is required to transport extra-heavy crude to refineries where they can be further treated, distilled and sold as various petroleum products.

1.2 Motivation

Some of the approaches for transportation of extra-heavy crude and bitumen include viscosity reduction, drag reduction and upgrading[4,5]. A common viscosity reduction method employed is use of diluents. Typically, condensates or light crude oils are mixed with heavy crude oils to reduce the viscosity and sent to refineries where the diluents are separated and the heavy crude is upgraded, distilled, and sold as various products. However, this process requires use of expensive lighter crude oil and lower availability of light crude/ condensates at heavy oil production sites means diluents are separated at refineries, transported, and reused at the production site adding to the cost. Unlike upgrading processes where there is some cracking, this process does not affect the chemical characteristics of crude oil.

On-site heavy crude oil upgrading could involve partial or total upgrading using various thermal or catalytic processes. These upgrader facilities require large investments, higher operating costs, and complex facilities, and have to deal with various environmental issues. Current upgrading techniques implementing thermo-catalytic-cracking (TCC) processes require high energy. For oil sands based upgrading, it could consume almost one third of the energy of oil being processed [6,7]. Further, TCC based processes have low efficiencies, higher carbon residues, and olefin content (C=C). Due to the huge amount of coke and/or heavy residue as well as some dry gas production, net product mass output is much lower than the feedstock input. Other potential issues include the refined products not meeting the specifications for use in pipelines, insufficient increase in API, gumming of unstable products etc.

Radiation assisted cracking could be a promising alternative and potentially address the above mentioned issues with TCC based processes. The process involves use of ionizing radiation to effectively transfer energy to the molecular structure of the crude oil thereby enhancing the energy transfer process. Though in relatively early stages of development, self-sustained cracking of hydrocarbons using radiation has been observed [8]. Good mass balance and conversions have been reported with little or no carbon residue. Figure 2 shows the basic system set up for radiation assisted cracking.

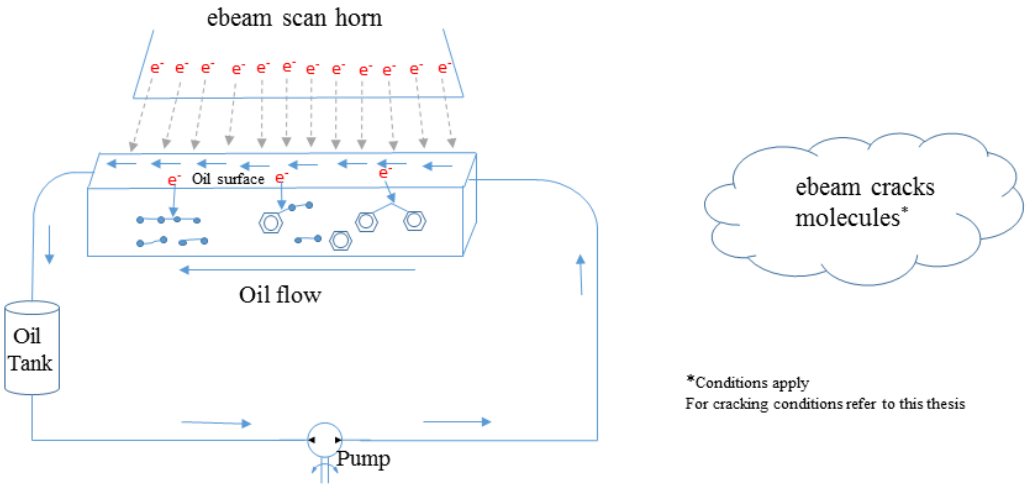

Figure 2: Radiation assisted cracking – system overview

Economic analysis reveals a comprehensive processing cost of $5.44/barrel at moderate dose and temperature of 150°C and 300 kGy. A 10° increase in API post treatment fetches a $10 per barrel increase in market price indicating the economic

viability of the process. Detailed economic analysis involving a wide range of parameters is provided in Appendix G.

1.3 Objective and Overview

The project aims at achieving radiation assisted low temperature cracking of extra-heavy crude oil and bitumen. Objectives include the development of an energy efficient process which lowers the viscosity of treated oil, has good mass balance while avoiding the formation of coke or unstable products. A flow loop system has been developed to treat heavy crude oils using electron beam irradiation. Post electron beam treatment, rheological and simulated distillation characterization techniques have been employed to analyze the effect of radiation processing.

This thesis focuses on fluid property analysis and crude oil characterization post treatment. A rheometer has been used to analyze the viscosity post treatment and compare it with that of an untreated sample. Rheological studies have been carried out to understand the effect of shear and shear history on flow properties of heavy oil at different temperatures. Viscosity-temperature models have been employed to obtain continuous viscosity-temperature plots which were used in the fluid model. Real time viscosity-temperature correlation is necessary to evaluate the residence time. Further, viscosity blending models were looked into and experiments were performed to evaluate the effect of addition of lighter fractions and/or heavier fractions. This information is required to analyze the mass balance results and account for any discrepancies.

Chemical characterization of crude oil has been carried out by performing simulated distillation on a gas chromatograph. High temperature simulated distillation methods such as ASTM D6352 and D7169 were employed to obtain the boiling point distribution. Compounds with atmospheric boiling point lower than 720°C can be detected by these techniques. Retention time calibration has been carried out using polywax 655 and an addition of nC5-nC44 standards. Using the correlations obtained between retention time and boiling points, percentage weight off versus boiling point curve has been obtained.

Chapter 1 talks about the background and motivation for this study and chapter 2 gives the details of heavy oil characteristics and prior radiation processing of crude oils. Chapter 3 presents the experimental set up that was designed to process crude oils with electron beam. Chapter 4 talks about the rheological studies carried out on untreated samples, details of viscosity-temperature models and viscosity of mixtures. Chapter 5 presents the working and details of simulated distillation as well as the boiling point and carbon number distribution for untreated oils. Chapter 6 discusses the results of electron beam processing of heavy crude oils and chapter 7 gives the conclusions and recommendations for future work.

2. LITERATURE REVIEW

2.1 Heavy Oil Characteristics

Crude oil classification is typically based on physical properties such as density and viscosity. The lighter the crude, the lower the viscosity and density and the higher the market value. The American Petroleum Institute defined a scale inversely related to density called API gravity to classify various crudes[9]. API gravity is calculated by the following equation:

$$API = \frac{141.5}{SG} - 131.5$$

where SG is the specific gravity of oil at 15.6°C or 60°F.

No consistent definition for heavy oils exists, but a commonly accepted one defines heavy crude as oil with API gravity less than 20 and in the range of 10-20 [2]. Oil having API less than 10 is further classified as extra-heavy or bitumen based on viscosity. If the viscosity of crude at reservoir temperatures is less than 10000 cP, it is termed extra-heavy crude and if the viscosity at reservoir temperatures is greater than 10000 cP, it is called bitumen. The chemical characteristics of extra-heavy crude and bitumen are similar and the distinction between extra-heavy crude and bitumen is mostly for production purposes[1]. Extra-heavy crude with lower viscosities at reservoir temperatures can be produced by enhanced recovery processes whereas bitumen is typically mined [10]. Another distinction of crude oils is based on sulfur content. Oil is sweet if the sulfur content is less than 0.5 wt% and sour otherwise.

Characterized by low H/C ratios and high molecular weights, extra-heavy crude and bitumen are comparable to atmospheric and vacuum residua. Atmospheric residuum is the left over fraction at the end of atmospheric distillation, typically at 345°C and vacuum residuum is the left over fraction at the end of vacuum distillation, at 600°C. They represent the bottom of the barrel fraction and would be upgraded to further convert heavy fractions to lighter distillates [11].

In contrast to lighter crudes, heavy crude oils contain high volume percentage of atmospheric and vacuum residue, up to 80% and 50%, respectively. With current inefficiencies in upgrading processes, lower yields of light fractions are obtained from these residua [12]. Heavy oil composition is further made complex due to presence of sulfur and metal components such as vanadium and nickel. They are highly undesirable as metal deposits can cause deactivation of catalysts and presence of mercaptans could lead to corrosion of refining equipment.

Elemental analysis of crude oils on an average yield 83-87% carbon, 10-14% hydrogen, 0.1-2% nitrogen, 0.05-1.5% oxygen, 0.05-6% sulfur and trace metals[6]. Sulfur is present in two different forms in crude oils, in the aromatic ring or as an organic sulfide. Organic sulfides are easier to remove by reaction with hydrogen. But, sulfur present in aromatic rings is not easy to remove owing to the stability of aromatic compounds[6,13]. Derivative forms of pyrrole and pyridine are the components containing high amounts of nitrogen. Higher ring nitrogen containing compounds have been identified in gas oils, asphaltenes and residues. Even though nitrogen content in crude oils is low, its presence is undesirable as it could contribute to poisoning and deactivation of catalysts[13,14]. Further,

oxygen has its presence in various forms such as carboxylic acids, furans, thiophenes, phenols, ethers, and other oxygen containing ring structures. Of all these compounds, carboxylic acids are important because they act as surfactants during extraction and the corrosion they could cause. They are usually represented by Total Acid Number (TAN), which is found by titrating crude oil samples with potassium hydroxide [6,10].

Even trace levels of metals such as nickel, vanadium, iron, copper, sodium etc. are not desirable due to their negative effect on catalysts by poisoning or deactivating. They exist as inorganic salts or organometallic complexes or colloidal suspensions of elemental metals. All the metal constituents have to be removed or brought down to acceptable levels during refining [6].

A common way of chemically characterizing crude oils is SARA analysis. SARA stands for Saturates, Aromatics, Resins and Asphaltenes. Saturated hydrocarbons are straight or branched paraffins which could make up two-thirds of volume in light crudes, but not highly present in extra-heavy crude oils or bitumen due to biodegradation [10]. They have relatively lower molecular weights and their abundance typically yields lower distillate fractions. Octane number, which is used to determine the anti-knocking quality of gasoline is based on the standard trimethyl pentane (isooctane) which is a saturated hydrocarbon. Aromatic compounds vary from single ring to up to 4 ring structures, though biodegradation tends to target lighter aromatic hydrocarbons[10]. Aromatic compounds are toxic and not desirable [6].

Resins and Asphaltenes are high molecular weight components present in large proportions in heavy crude oils. They form part of residuum and their highly complex

structures makes processing of heavy crude oils difficult[14]. Heavy crude oils have higher proportions of aromatics, resins and asphaltenes and lower saturate hydrocarbon fractions when compared to lighter crude oils[15].

Resins and asphaltenes are relatively heavy, polar, and are made of polycyclic aromatic rings[12,16]. Asphaltenes are very complex components without a unique molecular structure. They are known to be very polar with poly-aromatic characteristics and containing metals[16]. Since their chemical structure is not known, they are usually defined based on their solubility[17]. They precipitate in solvents like pentane and heptane but dissolve in aromatic solvents such as toluene[17].

Studies conducted on asphaltene microstructure reported that it is a large aromatic sheet piled one on the other to form a large associated molecule. Further metalloporphyrins are thought to be linked with the asphaltene molecules via π-electronic interactions[12].

Along with the chemical structure, molecular weight of asphaltene molecules are yet to be determined. Various researchers have worked on determining the molecular weight value of asphaltene molecules. There have been disagreements of the range, with some researchers stating in the range of 500 and 1000 g/mol while other researchers claim it to be as high as 3000 g/mol[18,19]. Nevertheless, asphaltenes remain the heaviest components of crude oils and account for the high molecular weights of heavy crude oils.

2.2 Prior Work on Radiation Processing

2.2.1 Introduction

Use of ionizing radiation is an effective means of transferring energy to the target molecules. As opposed to thermal energy which is strongly related to translational, vibrational, and rotational modes, radiation energy can transfer most of the energy to the electronic structure of the molecule. It can provide energies which are orders of magnitude higher than the amount required for bond breaking (C-H, C-C, C-S and C-N). However, using thermal energy only a fraction is used to overcome the activation energy which might be just enough for radical formation or reaction progress[20–23]. Prior work on radiation assisted hydrocarbon cracking is summarized in this section.

An important classification of radiation assisted cracking is based on the processing temperature. At temperatures greater than 450°C, cracking reactions are predominantly thermal (TC). There is enough thermal activation for both initiation and propagation reactions at such high temperatures[24,25]. However, for processing temperatures in the range of 350-450°C, there isn't enough thermal energy for initiation but the propagation reactions are thermal induced. Use of this range of temperatures classifies the processes as Radiation Thermal Cracking (RTC) where the cracking is radiation induced and thermally propagated[23,24]. At temperatures lower than 350°C, both initiation and propagation reactions are radiation induced and propagated[8,24]. Using this range of temperatures is termed low temperature radiation cracking and/or cold cracking. Some researchers[24] further divide the low temperature range into 200-350°C and less than 200°C with the latter termed cold cracking and the former low temperature radiation

cracking. Both low temperature radiation cracking and cold cracking have been used interchangeably in this thesis implying processing temperatures less than 350°C.

Use of radiation has been proven to reduce the operating temperatures required for cracking. In the case of radiative thermal cracking, use of radiation can induce the required initiation reactions when there is no thermal activation. Experiments on RTC of fuel oil by Mustafaev and Gulieva[26] indicate that the reaction rates were higher for RTC over TC for all their case studies. RTC and TC experiments conducted at the same temperature (RTC range of 350-450°C) showed cracking products only in RTC case. Further, rate of radiation induced initiation is very much greater than any thermal component in that range of temperature and hence radiation is necessary for cracking reactions to take place within operating temperatures less than 450°C.

2.2.2 Reaction Mechanism

The reaction pathway is known to occur through the free radical chain reaction mechanism. Studies conducted by various researchers corroborate this. Alfi et al[21,22] have compared RTC with TC at different temperatures. Their results show the relative amounts of products to be the same in both processes indicating the similarity of reaction mechanism. Also, it was found that the use of ionizing radiation intensifies cracking processes with no change in underlying reactions or selectivity. RTC products were 30% less viscous than TC products. However, the oil used for that particular study was deasphalted and when applied to heavy asphalted oil, the results differed widely. Even though the reaction pathway occurs through free radicals, there appeared to be selective reactions during RTC and not TC when heavy asphaltic oil was used.

In the radiation induced free radical reaction mechanism, the generally accepted pathway follows a paraffin molecule disintegrating into two radicals, a light radical and big unstable radical. This initiation step is followed by the light radical playing the role of chain carrier. The big unstable radical formed in the initiation step further disintegrates into an olefin and a light radical which could also work as a chain carrier [27]. The propagation steps are carried out by the interactions of radicals with excited molecular states which could be generated as a result of thermal or radiation activation [28].

Other studies[29] on electron beam irradiation of different heavy and sulfuric crude oils claim that radiation induced chemical conversion of complex feedstock such as crude oil is very much different from simple hydrocarbons. Given the heavy and complex nature of the feedstock, it has been theorized that they tend to have smeared transition parameters from one type of radiation induced reactions to other as well as simultaneous occurrence of various competing reactions with participation from both original and intermediate compounds [29].

2.2.3 Nature of Feedstock

Studies conducted by several researchers indicate a difference in results when using different samples implying radiation chemistry depends on the nature of the feedstock. Protecting effect, as summarized by Foldiak and Wojnarovits[30] depends on the physical and chemical interactions such as energy and charge transfer, and radical scavenging that follow the initial energy uptake. Based on their calculations, it was concluded that protecting effect is mainly due to the energy and charge transfer processes.

So, molecules better at transferring charge and energy are protected, in other words radiation resistant.

For example, aromatic compounds are known to be radiation resistant structures. With higher stability and the capability to charge scavenge, they do not degrade easily and can absorb the excess energy of the radicals generated due to irradiation.

Zaykina et al[29,31] have performed RTC experiments on highly viscous oil which support the idea of radiation resistant aromatic compounds. The oil they analyzed was from Karazhanbas field of Kazakhstan which has high aromatic and low paraffinic content along with high sulfur and metal content. With an operating temperature range of 350-450°C and use of 2MeV electrons they observed that most of the aromatic content remained after treatment. However, the paraffinic compounds reacted and lead to conversion to lighter components. It has also been observed that gasoline obtained this way has higher octane rating indicating the presence of branched alkanes (isoparaffins).

To understand the effect the initial feedstock has on the products, they further conducted experiments on a heavy paraffinic and low aromatic crude oil from Kumkol oil field[32]. Their results showed considerable difference in the yields of the two oils indicating that the characteristics of initial crude oil contents dictate the rate and yields of RTC products. In spite of providing similar experimental conditions, the yields were lesser and heavier when heavy paraffinic oil was used signifying the role of competing reactions such as polymerization. Presence of the heavy paraffin fractions might have caused the difference in reaction mechanism compared to feedstock with light paraffin fractions.

Even though aromatic content is radiation resistant and mostly remains after irradiation, it can affect the direction and results of radiation based conversion[32]. For example, studies conducted by Zaykin et al[33] indicate that the presence of heavy aromatic compounds in the feedstock could lead to increased isomerization reactions. Presence of heavy aromatic content has similar result as that of lower temperatures and dose rates. At lower temperatures and lower dose rates, there is lower radiation energy that the alkyl radicals can transfer leading to higher isomerization before disintegration or recombination. Whereas, the presence of polyaromatic compounds (which are known for their radiation resistant structures) leads to them absorbing the excess energy of radicals and providing enough time for alkyl radicals to stabilize and form isomers before disintegration or recombination. Further, heavy bitumen residua was added to lighter oil and used as a feedstock for radiation thermal cracking. They have observed considerable increase in the iso-alkane concentration in gasoline, by as high as 15% mass. Their results also indicate that the effect reaches saturation at 5-6 mass % of aromatic content as there is little increase in iso-alkane concentration with increase in aromatics from 6 to 15%.

2.2.4 Presence of Water

Effect of the presence of water was studied by Andrade et al[34]. Benzothiophene degradation reactions were carried out and it was observed that the degradation occurred mainly through hydroxyl radicals when water was present in the system. Zaykin's group[35] have also studied the effect of water by adding 5-6% water to their bitumen feedstock during RTC experiments. They have observed an increase in liquid product yield up to 95-97% of bitumen mass (mass excluding water content). Further, they have found that heavy

residue is practically absent. Presence of water could lead to radiation induced oxidation-reduction reactions and overall intensified reactions involving hydroxyl radical participation.

2.2.5 Competing Reactions

Chemical reactions are not always unidirectional or selective. There would always be competing reactions; more so when tens and hundreds of different radicals are present along with several reaction pathways. Along with cracking reactions, there exist competing reactions such as recombination, condensation and polymerization. These reactions could occur along with cracking reactions and/ or post treatment. Condensation and polymerization reactions lead to formation of heavy molecules and/ or gums. Though there is no exact theory on when and how they happen, it is generally agreed that polymerization reactions tend to continue post treatment[20,24] and some quenching processes have to be employed to suppress them.

Paraffins form the most reactive species of a crude oil with products highly dependent on the processing conditions. Zaykin et al[32] conducted experiments on highly paraffinic oil (high molecular weight) and observed polymerization and condensation reactions. They concluded that with high content of heavy paraffins, competing reactions such as polymerization and poly-condensation tend to dominate.

2.2.6 Operating Parameters

Irradiation based cracking products are complex functions of various parameters; radiation, thermodynamic and flow (in case of flow/semi-batch reactors). Radiation

parameters are the dose, dose rate and electron energy, thermodynamic parameters include temperature and pressure, and flow parameters include shear rate etc.

Arguably, the most important operating parameter is the temperature. Since, thermal effects are relevant only above 350°C, any radiation treatment at temperatures less that is called cold cracking. If the temperature range is within 350°C and 450°C, both radiation and thermal effects are relevant making the process radiation-thermal cracking. At greater than 450°C, thermal effects tend to be predominant with the processes essentially being thermal cracking[24].

Several researchers worked on optimizing the operating temperature. Studies conducted by Alfi et al[21,22] show that cracking (both radiation and thermal) is active only beyond a certain threshold temperature. Researchers have observed that during RTC and cold cracking reactions, radiation induces the required initiation reactions. Topichev et al[25] have concluded in their work that up to 550°C radiation induced initiation reactions are prominent with no thermal component involved. Even at temperatures higher than 550°C, they have observed a 4:1 relation between radiation and thermal initiation reactions. However, temperature plays a role in the chain propagation steps which are endothermic in nature. Failure to provide the required energy for the propagation reactions could lead to the free radicals stabilizing through recombination and condensation reactions thereby increasing the viscosity and heavy nature of the oil[29].

However, almost all the studies emphasizing the requirement of a minimum temperature were conducted at low dose rates. Use of high dose rates as explained by Zaikin et al[8,24] could lead to a radiation induced pathway for propagation reactions. Low

temperature radiation cracking and cold cracking along with the necessary conditions are elaborated later in this section.

Unlike a linear relation for temperature, the effect of dose on cracking products is a complex and non-linear function. Experiments conducted by Zaykina's group showed a non-linear effect of dose on the radiation chemical yields. With no change in other parameters, yield increased with dose till a value and further started decreasing which could be explained due to polymerization reactions. They have explained the non-linearity using intramolecular isomerization which stabilizes the alkyl radicals increasing the necessary activation energy for disintegration and therefore lowering the conversion[29,31].

Studies on crude oil from Karazhanbas field isolated the effect of dose but not temperature and dose rate. Two modes; one with high temperature and high dose rate and other with lower temperature and lower dose rate were used. In the low temperature, low dose rate mode, lower yields were observed indicating lower probability of big radical disintegration which could lead to higher competing reactions[29]. Their studies on heavy paraffinic oil[32] at different operating conditions isolate the effect of dose rate, clearly showing an increase in yields with an increase in dose rate. At a temperature of 400°C, both dose and dose rates were varied. Even though the effect of dose was non-linear, the curve shifted towards higher yields with increasing dose rate.

Though early studies conducted by Topichev[25] and several other researchers[22,23] talk about the thermal requirement for propagation reactions, experiments performed by Zaikin[8,28] indicate that at sufficiently high dose rates, when the concentration and life times of radiation excited molecular states and radicals are relatively high, chain reactions can

propagate without any thermal activation. This revelation is extremely crucial as it lays down the conditions for cold cracking i.e., high dose rates (of the order of several tens of kGy/s). It could also help explain the reason several other researchers could not observe cracking at lower temperatures; use of low dose rates (<< 1kGy). At low temperatures and low dose rates, there is neither thermal activation nor long radical lifetimes for propagation and radicals tend to stabilize without disintegration increasing the heavy nature of feedstock.

The commonly accepted path for cracking reactions is that a radical when interacts with a molecule, the latter decomposes into a reactive lighter radical and an unstable heavy radical. The unstable heavy radical further decomposes into an olefin and another radical thereby propagating the chain reaction[28,25]. However, Zaikin[28] has proposed a modified mechanism suiting the conditions of low temperature cracking. It has been theorized that the radical chain carriers at low temperature cracking conditions interact with excited molecular states or behave as scavengers of light alkyl radicals and hydrogen atoms thereby helping accumulation of heavy unstable radicals. These unstable heavy radicals subsequently disintegrate to an olefin and a light radical and the chain propagation continues. High dose rates are important as they increase life time and concentration of hydrogen atoms and excited molecular states leading to increased cracking reaction rates.

Based on their study[24,27,28], the reaction rate is proportional to $P^{3/2}$ (P being the dose rate) as opposed to $P^{1/2}$ as theorized by early researchers. At conditions of low temperature cracking the concentration of unstable alkyl radical-hydrogen atom pairs are important for propagation and are proportional to the dose rate. The reaction rate at such conditions is a

product of chain carrier concentration and the concentration of radiation induced reactive molecular groups leading to a $P^{3/2}$ dependence of reaction rate on dose rate.

Hence, dose rate is the major driving factor for cracking reactions at low temperatures. Further, it is known to affect the product yield and ratios. Zaikin and Zaikina[8,24] have performed cold cracking at 50°C by irradiating high viscous crude oil with 2 MeV electrons at dose rates of up to 40 kGy/s. They have also conducted experiments with dose rates as high as 80 kGy/s. They have observed considerable conversion and it was stated that the total and relative yields of lighter fractions differed for different dose rates and same dose implying the key role dose rate plays at low temperature conditions

An increase in dose rate leads to increase in conversion. However, this also leads to the complicated relationship of conversion with dose. There was no significant increase in the conversion with increase of dose in the higher dose region at 80 kGy/s indicating the effects of polymerization. Increase in dose rates increases both cracking and polymerizing reactions[28]. And, it has been theorized that accumulation of unstable by products such as olefins and asphaltene aggregates might lead to increasing polymerization and limit cracking rate. Hence, conversion reaches saturation faster at high dose rates.

The use of high dose rates plays a huge role in treating bitumen and extra-heavy crude oils because of the presence of maximums in the dose dependent studies[36]. This is explained using the competing reactions such as polymerization and adsorption of light fractions by reactive residue. Studies conducted previously indicated the phenomenon of

reactive residue adsorbing lighter fractions[32]. Increasing dose rates could help achieve higher yields at lower doses rather than using high doses and increasing the probability of polymerization[36]. Increase in dose rates resulted in increased yield at the same dose and temperature.

Even though temperature, dose and dose rates are the major processing parameters; they alone do not dictate the radiation cracking of crude oils. There are several other parameters including the structural composition that affect the results, especially with the use of extra-heavy crude oils and bitumen as feedstock.

Flow parameters such as shear come into play when the feedstock has thixotropic properties. If the decomposition of such heavy thixotropic structures can occur at lower temperatures under shear it could cause a drop in viscosity and a sharp increase in the cracking rate. Zaikin et al[24] claim that this effect could even result in an order of magnitude increase in the cracking.

2.2.7 Experimental Setup and Results

Some of the early studies on RTC of hydrocarbons were performed by Topichev and Polak[25] on heptane and various other crude oil distillates with varying dose rates. With irradiation of n-heptane under static conditions, they have observed an increase in cracked products along with an increase in olefin content with an increase in operating temperature. The yields were very less at temperatures less than 300°C and a rapid increase after that.

Alfi et al[22,23] have performed successful RTC experiments on crude oil. They have used deasphalted oil (DAO) and heavy asphaltic oil (HAO) for analysis and observed 55%

and 30% viscosity reduction respectively. No reduction was observed at temperatures lower than 380°C. However, they have used a small sample size of 30gm and low dose of 20 kGy. Even though viscosity reduced after treatment, there was no change in API and the results of mass balance haven't been provided.

Mustafaev and Gulieva[26] have performed radiative thermal cracking studies on fuel oil and observed 71% conversion to gasoline and diesel fractions. All the three major parameters; temperature (20-500°C) dose rate (11-2000 kGy/h) and dose (0-10000 kGy) were varied. They have analyzed the process in three different temperature ranges; 20-400°C, 400-450°C and 450-500°C. In the low temperature range, polycondensation reactions occurred with no net cracking observed. Even though the dose range was reasonable, the dose rates employed were too low (with a maximum of 2000 kGy/h = ~0.55kGy/s) which might have been a reason for the dominant polycondensation reactions at low temperatures. Conversion was observed at temperatures beyond 400°C with the dry gas yield increasing with temperature. Using high temperatures, 450-500°C, both high gas yields and coke were observed, implying 400-450°C as the optimum temperature range for RTC of fuel oil.

Optimum conditions were achieved at T = 430°C and dose of 3.5 kGy, resulting in a total of 71% lighter fraction yield including 16% gasoline and 55% diesel. They were one of the few authors who provided mass balance of the treated products, which has been summarized in table 1.

Component	Mass percentage
Fuel Oil Taken	100%
Dry gas yield	1.8%
Gasoline yield	16%
Diesel yield	55%
Vacuum gas oil yield	26.2%
Waste yield	1%

Table 1: Mass balance for products of fuel oil RTC by Mustafaev and Gulieva[26]

Zaykina's group[29] has conducted radiation thermal cracking experiments on crude oil from Karazhanbas field at temperatures of 350-450°C, dose rates of 0.5-1.5 kGy/s and electron energies of 2MeV. They have observed an increase in the liquid yields with increase in operating temperature and dose rate and a non-linear effect of dose. Post treatment, they have observed structural difference in both aliphatic and aromatic compounds compared to feedstock. IR spectra of products indicated destruction of long chain paraffins and formation of isomeric structures. They have observed absorption bands at 1380 and 1460 cm^{-1} implying presence of alkyl substituents. Also, high concentrations of methyl and methylene groups indicated there was considerable branching in the irradiated products. Further, they have observed that an increase in dose from 2 to 6 kGy led to decrease in aromatic content of gasoline fractions. A reaction scheme for dimerization of alkyl aromatic radicals was provided to explain the same.

The same group have used a different crude oil, a heavy paraffinic feedstock which resulted in lower yields and higher dry gas[32]. Operating temperatures in the range of 340-450°C, dose rates of 1-4kGy/s, irradiation dose of 1-4kGy, and 2 Mev electrons were used. They have observed lower yields as well as heavier products. Gasoline obtained in this study was heavier when compared to lighter paraffinic Karazhanbas crude RTC yield. It

has been theorized that competing reactions have a bigger role in case of the presence of heavy paraffins in the initial feedstock.

Further studies of the effect of heavy paraffins was conducted by using asphalt-pitch-paraffin sediments which contain high concentrations of heavy paraffins. Radiation thermal cracking of this sample exhibited polymerization reactions. Further, the paraffinic residue was found to be very reactive and interacted with lighter fractions resulting in absorption and even heavier residue[32].

Application of radiation thermal cracking to extremely heavy feedstock such as bitumen has been successful too. Zaykin et al[35] have conducted radiation thermal cracking experiments on bitumen and observed 82-86% synthetic crude, along with some coking residue and dry gases. Use of lower dose rates and lower temperature (high enough for noticeable chain reaction) resulted in pronounced isomerization effects and hence increasing the isomer concentration in gasoline yield. They have compared the results of RTC with conventional TCC methods and found that RTC yields are much higher than the conventional processes.

Though majority of their work is concentrated on RTC, Zaikin's group[8,24,28] worked on achieving low temperature radiation cracking and cold cracking. They have used high dose rates of the order of tens of kGy/s to achieve the required cracking reaction rates.

2.2.8 Time Stability

An important concern of any cracking products is their stability over time. Alfi et al[22] claim RTC products have stable viscosity over time for both DAO and HAO samples

whereas TC products of HAO sample showed increase in viscosity over time. Zaikin et al[8,24] did not provide time stability results for most of their experiments. However, the products of ebeam treated asphalt-pitch-paraffin sediments showed increase in viscosity over time[29].

2.2.9 Sulfur Content

Andrade et al[34] have conducted gamma irradiation studies on sulfur containing diesel oil and petroleum and observed the transfer of sulfur species to heavier fraction. They have observed better cracking at 30 kGy when compared to 50 kGy. But, the sample was small (20mL) and the dose rate is very low at 1.27kGy/h which might not be sufficient for cracking reactions to propagate and might have led to increasing polymerizing reactions. Dose and dose rate are not independent parameters as time required for the same dose plays a major role in cracking reactions[24].

Zaykina et al.[37] have presented a two stage radiation method for desulfurization. Experiments have been performed resulting in the initial radiation processing leading to the conversion of mercaptans and other sulfur compounds to oxidized compounds such as disulfides, sulfones, sulfuric oxides and sulfuric acids. This stage is followed by standard extraction of highly oxidized sulfur compounds. Their results show that at milder conditions (lower dose and dose rates), there were higher conversion of sulfur compounds. At severe conditions, due to the presence of higher amounts of hydrogen could result in reversing some of the conversion reactions. Using radiation treatment on heavy crude oil with 1.7% sulfur content, they have observed gasoline yields with sulfur content as low as 440 ppm. Most of the residual sulfur was concentrated in heavy liquid fractions.

2.2.10 Comparison with Other Sources of Radiation

Electron beam irradiation is the preferred radiation method for several reasons. Electron beams are produced using electricity and can be switched on and off instantly unlike other ionizing radiation such as gamma irradiation which uses cobalt-60 or cesium-137. Further, with gamma irradiation there is always the problem associated with radioactive source material. Even though they are relatively inexpensive by products of atomic fission, they have considerable radioactivity with half-life of cobalt-60 is 5.27 years and that of cesium-137 is 30 years[38].

Neutron reactors are very expensive and could lead to problems with radioactivity. Production of Bremsstrahlung radiation has very little conversion efficiency and has high penetration power[39]. Even though gamma irradiation and x-rays have higher penetration power, the associated radioactivity and lower conversion efficiency do not justify their use over electron beams. Further, gamma irradiation is not capable of achieving high dose rates necessary for low temperature radiation cracking.

2.2.11 Economics

Comparative technical and economic analysis by Mustafaev and Gulieva[26] show that RTC has more than 10% economic advantage over catalytic processes for fuel oil. Economic evaluations performed by Zaikin et al[8] use different doses and estimate industrial scale processing costs. They estimated $2-2.5 processing costs per ton of crude oil using a dose of 450-500 kGy and $5 per ton using a dose of 1400 kGy.

3. EXPERIMENTAL SETUP

3.1 Introduction

In order to process extra-heavy crude oil and bitumen using electron beam irradiation, a flow loop system has been built along with the necessary controls, fire extinguishers and fire-monitoring devices. Major components include the test cart, control cart, fire extinguisher cart and all the required electrical and pneumatic lines. The test cart is the flow loop system for oil to be treated using electron beam whereas the control cart has all the control set up such as the data acquisition system, thermometers, computers, air compressors etc. Given the potential flammability issues associated with oil treatment, a cart with fire extinguishers and pneumatically actuated valves has been assembled. Details of the constituents of the carts and their working has been provided in the later sections of this chapter.

Experiments have been conducted at the National Center for Electron Beam Research Facility at Texas A&M University. It is equipped with 18 KW linear accelerators with electron energies as high as 10 MeV. Dose rate can be modified by adjusting the height of reactor underneath the ebeam scan horn. Currently, dose rates of the order of 20 kGy/s have been achieved.

Due to the lethal consequences associated with the exposure to ebeam, all the personnel have to be away by 100ft from the processing area (ebeam vault), which is enclosed by thick concrete walls. So, the test cart and fire extinguisher carts are controlled

remotely using the control cart, which is stationed 100 ft away, at a safe distance. All the electrical, pneumatic and thermocouple lines required for the control were laid out.

3.2 Experimental Setup

3.2.1 Test Cart

Initial experiments were conducted with a semi-batch reactor and currently, a closed loop flow system is being used. Figure 3 gives the P&ID diagram for both open loop (semi-batch) and closed loop (continuous flow) configurations.

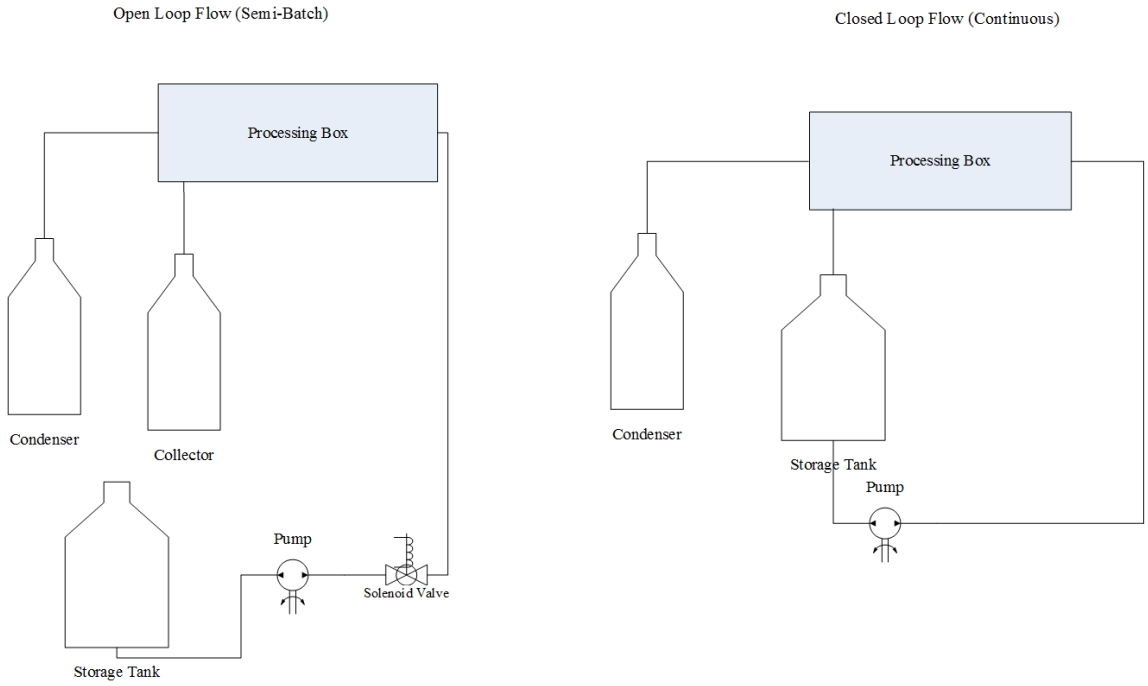

Figure 3: Open and closed loop configurations for oil processing system

As can be observed from figure 3, the major components of the test system include the storage tank, processing box, collector, condenser, pump-motor and a pneumatically

actuated solenoid valve. For the open loop system, oil flows from the storage tank through the pump and valve to the box where it is treated. Post treatment it flows into the collector and the volatile lighter fractions are collected in the condenser. For the continuous flow system, oil from storage tank is pumped to box and post treatment gravity drain allows it to flow back into the tank. Similar to the semi-batch reactor, volatile light fractions are captured in the condenser.

A rolling test cart was built to mount all the required components. It is designed to be compatible with different reactors and to handle well over 200 pounds. It is built with a steel base, aluminum body and 1 5/8in strut channels. Figure 4 shows the test cart with all the components mounted. The design and size is mostly constrained by the width of doors and hallways in the testing area of the ebeam facility.

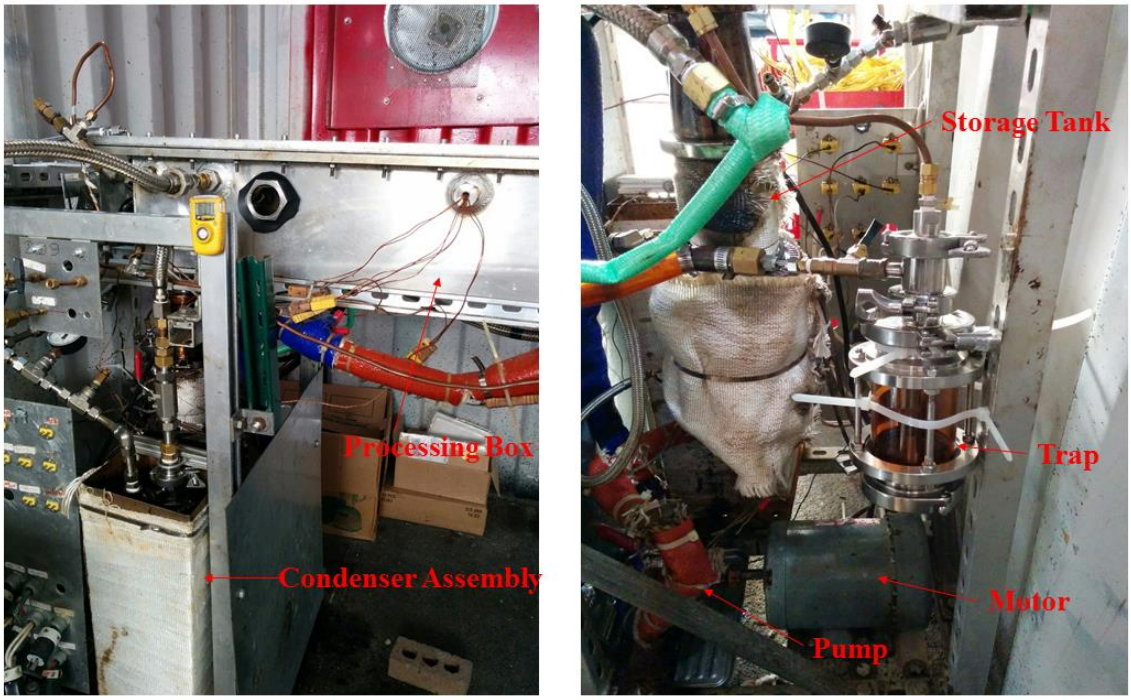

Figure 4: Test cart

The oil collector and condenser are high polish quick clamp sanitary straight tube fitting with size of 3in OD X 18in and 2L capacity. High temperature Viton gasket (rated to 600°F) has been used for the storage tank and collector, and a silicone gasket (-40-450°F) for the condenser. The storage tank has a size of 4in OD X 15 and 3L capacity. They are all made of 304 stainless steel. A 3 phase AC motor and the gear pump are connected coaxially through a shaft coupler. The pump-motor combination is powered by a variable frequency drive (VFD) mounted on the control cart. The VFD takes a normal power supply at 120AC, 50 Hz and outputs 120AC and varying frequency of 0-60 Hz. Oil flow rate is controlled by changing the output frequency of the VFD. Flow rate vs. VFD output frequency correlation is provided in the section 'Flow Modeling' of this chapter.

The processing box is rectangular with a wall thickness of 1/8in and 1in flange. It provides the reaction space for the ebeam irradiation of crude oils. An aluminum channel 1in wide is mounted along the center of the box through with the oil flows and is treated. The width of the channel is constrained by the ebeam width of 1in. Aluminum is the chosen material for the box and channel because it allows less energy loss when the electron beam passes through it. It has small stopping power and hence electrons preserve most of the energy without aluminum gaining excess heat.

Oil flows in and out of the box along the channel. An inlet nozzle guides the oil from the hose to the channel. The channel is slightly inclined (4-7°) and the oil flows down the channel to the feedthrough opening from the box to the storage tank. Gas inlet and outlet and thermocouple feedthroughs have been provided on the box. Two thermocouples have been placed on the channel to note the oil temperature while flowing; one at the inlet and the other at outlet. Due to the close exposure to the ebeam, the thermocouple connectors used in the box are ceramic and are rated to 800°F. Figure 5 shows the oil processing box and the channel.

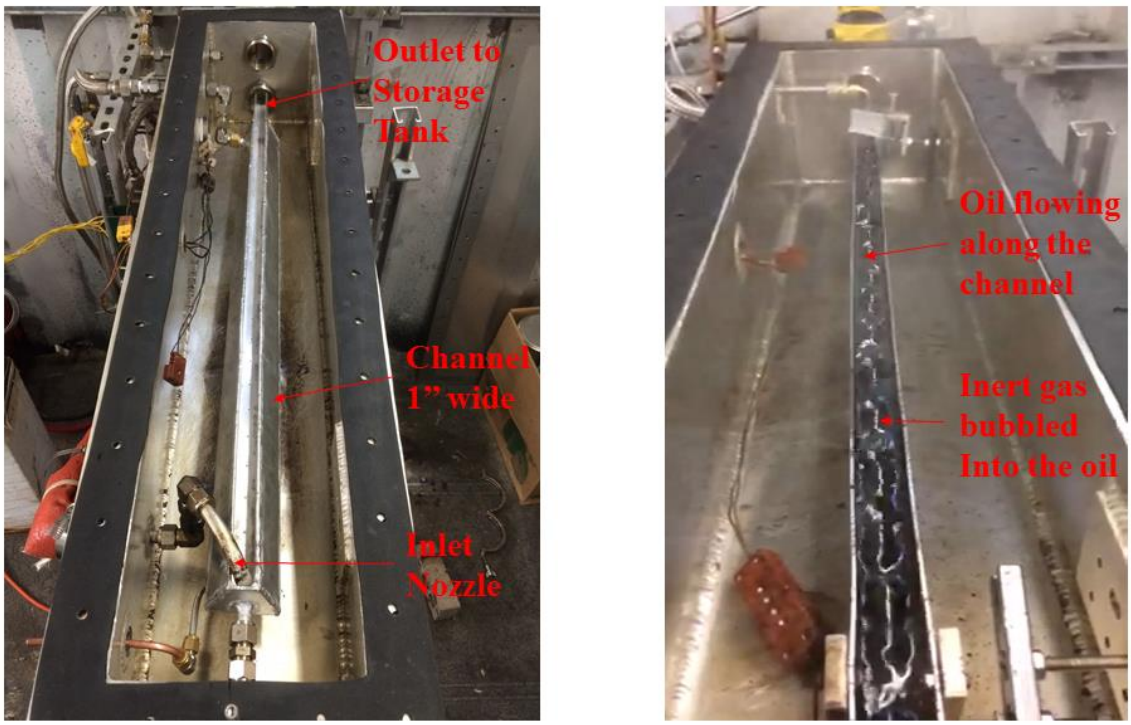

Figure 5: Processing box on the test cart

During the ebeam treatment, some of the liquid hydrocarbons evaporate, separate from the oil and condense in the box. The box being cooler than the channel acts as a condenser for the separated liquids, which are neither heavy oil nor condensate. A chamber has been designed to capture the separated liquids. It is an assembly including a pipe nipple (inner pipe), a bushing and a customized 3in OD sanitary tube. In its presence, separated liquids will flow down the box into the outer annulus of the separation chamber and be contained by the plug. The main oil stream flows along the channel and get processed by the electron beam, then travels down to the collector through the inner pipe. This design will prevent mixing of the collected light fractions in the separation chamber with the main stream on the channel. Thus the produced light fractions will not be retreated

and be polymerized. In the absence of the chamber, the separated liquids condensing in the box flow down to the storage tank and mix with the oil present in the tank. Figure 6 shows the separation chamber in place between the processing box and storage tank.

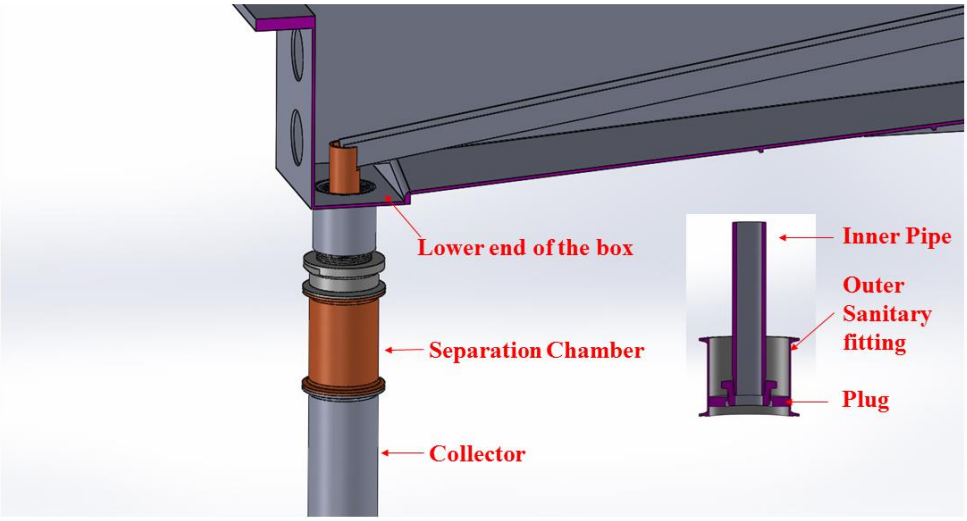

Figure 6: Separation chamber

It was observed during the initial lab tests that a significant temperature gradient exists along the tank due to natural convection and non-uniform heating. Hence, inert gas (any gas except oxygen) was bubbled into the storage tank to help mix the oil while heating. Further, gas purge to the box is required to purge any air present. Feed throughs are provided on the box for the gas lines.

The condenser assembly is placed in a square iron holder of dimensions 8in X 8in X 20in which is filled with either liquid nitrogen or dry ice or water-ice. All the gases exiting the processing box go through the condenser. Incondensable gases exit the condenser through a quarter inch pipe through a line to the exhaust system. A hydrocarbon trap is placed between condenser outlet and exhaust system to further condense the incondensable gases from the condenser. Exit of the trap is connected to the exhaust. Pressure relief valves (5-10 psig) have been placed on the gas lines and the condenser to avoid excess pressure.

Since, the oils are very viscous (solid like) at room temperature, they have to be heated in order to flow. Hence, the storage tank, pump, valve and all the lines have to be heated. This is achieved by placing ceramic insulated band heaters around the storage tank and wrapping flexible heaters around the lines, pump and the valve. Two layers of fiberglass insulation is provided above the heaters on the pump, valve and the flow lines. Heater control is detailed in the 'control cart' section.

3.2.2 Fire Extinguisher Cart

Two 10 lb capacity, CO_2 cartridge operated fire extinguishers with custom filled dispersal mechanisms are being used. Remotely controlled pneumatic valves are used to control them. A set of manual valves are also present for additional control. Once, the fire extinguishers are pressurized, the valve can be turned on to disperse the agent at the site of interest. The cart is placed close to the test cart with two metal hoses connected the end of fire extinguishers and the other end with nozzle pointed at the processing box and the storage tank (two places with high fire risk). Purple K agent which is tailored for oil fires

has been used and the extinguishers can be refilled with the agent post use. The assembly of extinguishers (along with the valves and lines) is mounted on a cast iron cart. Figure 7 shows the fire extinguisher cart used.

Figure 7: Fire extinguisher cart

3.2.3 Control Cart

All the components required for the remote control of test cart and fire extinguisher cart are mounted on a 30in X 60in steel welded rolling table which can take a load over

1500 lbs. Components mounted on the cart include the data acquisition system, computers, air compressor, VFD, thermometers, beam monitor, gas flow control, solid state relays, UPS battery etc. All the electrical, BNC, pneumatic and thermocouple lines required are laid out through the test cell over a distance of 100 ft connecting the equipment on control cart with the test cart. Figure 8 shows the control cart.

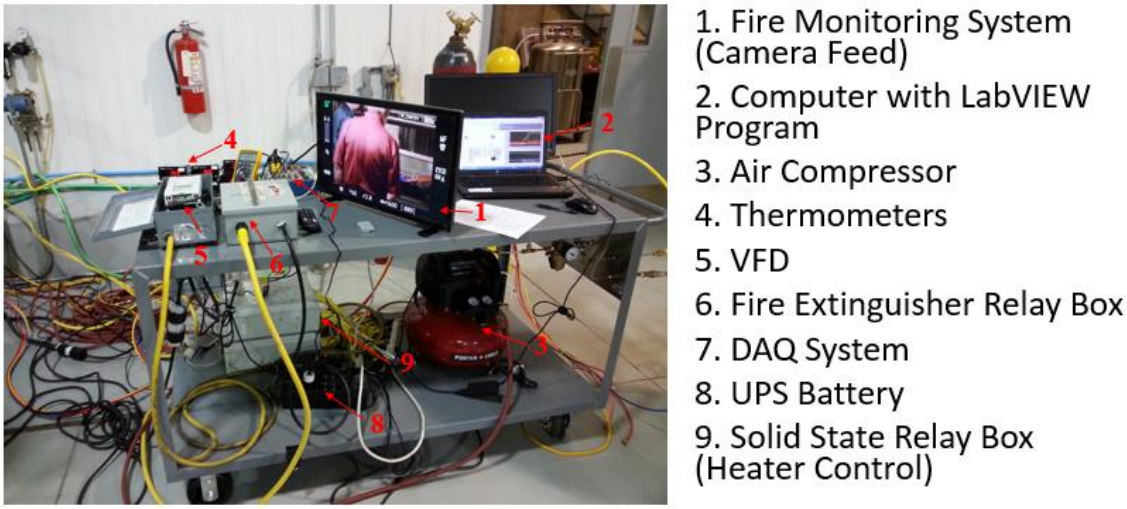

Figure 8: Control cart

A NI USB 6361 data acquisition device is used for data acquisition (DAQ) and control. It has 16 analog inputs, 2 analog outputs, 24 digital I/O etc. 8 analog inputs are used for 6 thermocouple signals, VFD signal and beam monitor. 7 digital output signals are connected to 7 solid state relays to power them. Of the 7 controls, 6 are heater controls (3 band heaters and 3 flexible heaters wrapped around valve, pump and the lines) and 1 solenoid valve on/off control. Data acquisition through analog inputs, digital outputs to

solid state relays are all controlled by a LabVIEW program. Feedback heater control as well as valve on/off are performed using the same LabVIEW program. Further, VFD and beam signals are acquired to obtain the time and duration of the flow and beam exposure.

The Variable Frequency Drive (VFD) which controls the flow of the oil on the test cart is mounted on the control cart. By varying the output frequency of the VFD, speed of the motor and hence the flow rate of the oil can be changed. Calibration tests were performed in the lab to correlate the output frequency of the VFD with the flow rate of oil.

Thermometer panels have been mounted on the table for better visual inspection along with obtaining the signal as an input to the DAQ device. The air compressor mounted on the cart provides required air pressure for all the pneumatic valves. Further, gas flow to the test cart is controlled using mass flow meters fixed to the cart. Gases used for bubbling/ purge flow from the cylinder through the mass flowmeter to the test cart. The relay box for turning on/off the fire extinguishers is also mounted on the control cart.

Along with all the required experimental controls, a fire and beam monitoring system is employed. A camera is placed a few feet away from the test cart and live image is projected on a TV screen on the control cart. This allows for monitoring the duration of ebeam and any signs of any malfunction, smoke, vapors or fire.

3.2.4 Mobile Test Cell/ Portable Walk-In Hood

Due to flammability issues and toxic volatile species associated with crude oils, there is a need to work in a continuous air-purge environment, especially during experiments conducted in the lab (shake-down, trail runs). Hence, a mobile trailer with an air-purge environment is built. It is an 8ft X 8ft X 20ft container on trailer with four wheels

fitted with two upblast ventilators (one constant speed and one variable speed), a gasoline powered generator and a lighting system.

The ventilators together can provide an air flow in the range of 1500-7000 CFM (25-100 ft/min) at small static pressure. Such high rates of air flow and face velocity classifies it as a walk in hood. It is designed such that the system can be tested in a standalone configuration in a safe manner. Trail runs are conducted in the mobile test cell prior to ebeam testing. The power generator has been used to provide electricity to all heaters, ventilator motors, flow loop system, lights etc.

3.3 Experimental Procedure

Prior to ebeam testing, trial runs have been performed in the mobile test cell to ensure proper working of all components. Once the system is pressure checked and guaranteed to work well, all the components are securely tied to the walls of the trailer and the trailer is towed to the facility. Experiments are conducted at the National Center for Electron Beam Research, Texas A&M University (ebeam facility).

At the facility, all the equipment is unloaded and moved to their respective places. The test cart and fire extinguisher cart are carefully rolled into the test cell and set in place. Alignment with scan horn is performed to make the center of the box i.e. the channel to lie exactly below the ebeam window. A laser pointer fixed on the cart is used to help set the box in the right place. Figure 9 shows the test cart set in place underneath the ebeam window. Post alignment, all the electrical lines, thermocouples and gas lines are connected to the cart as well as the lines from the fire extinguisher cart. Control cart is set up 100 ft

away from the test cell and all the devices are turned on. Live signal from the camera is verified. Hydrocarbon and H_2S gas detectors are placed 10 ft away from the test cart to alert the personnel of the presence of volatile hydrocarbon vapors and H_2S gas.

Figure 9: Test cart in place underneath the ebeam scan horn

Closed loop heater control is verified by increasing the set point to 5°C above ambient and looking for an increase in the corresponding temperature reading. Later the cartridges on the fire extinguishers are activated and manual valves opened. Further, the processing box is pre-purged with an inert gas and the system is verified to be leak free.

The condenser is filled with liquid nitrogen or dry ice. After the condenser is ready, oil is heated to a set temperature by engaging all the heaters using the LabVIEW program. An inert gas is bubbled to the tank to help mix the oil while being heated.

Dose rate is measured by placing alanine tablets (dosimeters) on the top and bottom of the processing box and exposing them to the ebeam for 2-3 seconds. Alanine tablets on exposure to the electron beam irradiation, change composition. The composition change can be measured and the result is converted to dose in kGy. As the exposure time is known, dose rate is obtained in kGy/s. Average dose rate for the experiment is obtained by performing a weighted average on the top and bottom dose rates. Further, dosimeters are placed along the width of the beam to obtain the range of irradiation. Using 5 tablets over a width of 2 inches a Gaussian fit is obtained along the width of the ebeam scan. Figure 10 provides the Gaussian curve.

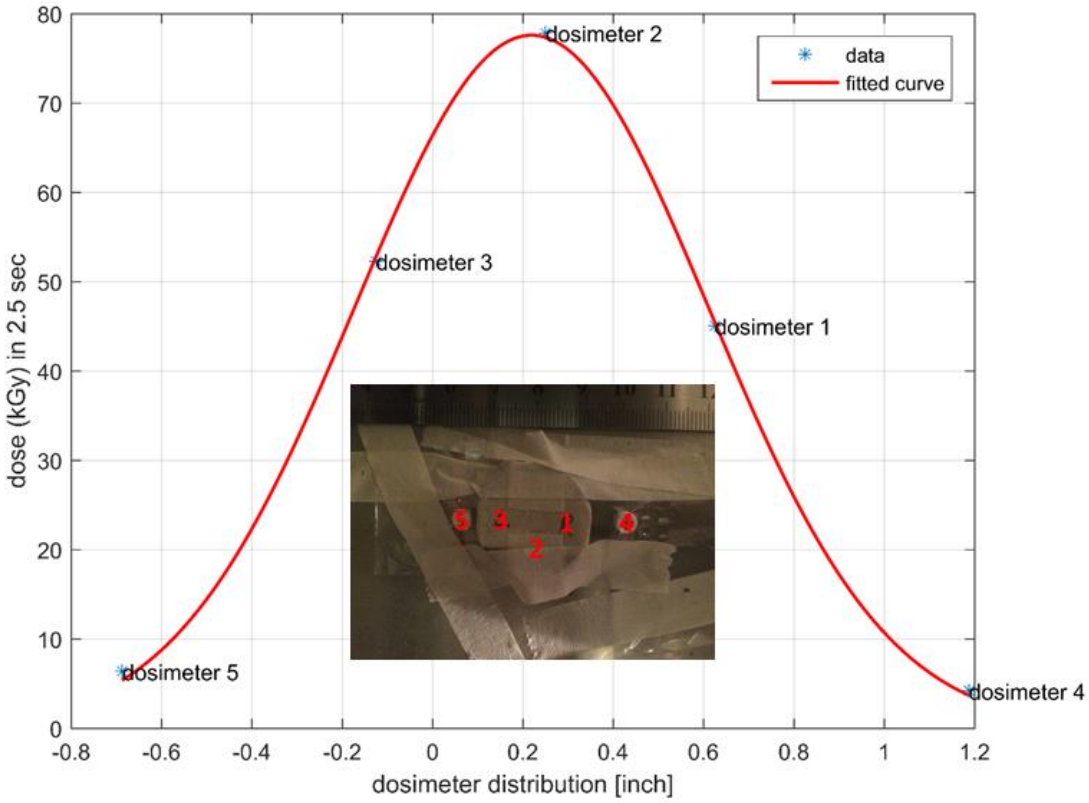

Figure 10: Gaussian fit for dose rate along width of ebeam irradiation

After the dose rate measurement is performed and the set oil temperature is reached, the motor is turned on and the oil temperature is allowed to reach a steady state (when the flow turns on, there is a sharp decrease in the temperature). Once a steady state set oil temperature is achieved, the heaters are turned off and the ebeam is turned on for a predetermined time. The heaters are turned off because the ebeam adds significant energy to oil raising its temperature. The live signal from the camera in the ebeam vault is observed on the TV screen for any signs of malfunction or smoke or vapors or fire risks.

After the beam is turned off, the system is allowed to cool down and the post purge with inert gas is started until a pre-determined time and temperature. All the data from LabVIEW program is saved and electrical cables are disconnected. Upon entering the test section, it is made sure that gas detectors are not detecting any hydrocarbons or hydrogen sulfide. All the electrical, pneumatic and thermocouple connections are detached and the carts are taken out of the vault to the trailer. The oil in the storage tank is approximately 120-150°C by this time and is decanted into a paint can in the trailer. If the collector liquids are not decanted after the experiment when it is warm enough, they would have to be heated again.

The trailer is driven back to lab where different components (liquids at the bottom of the box, separation chamber, condenser, channel) are analyzed and mass balance performed.

3.4 Operating Parameters

Careful examination of prior work and initial experiments helped identify dose, dose rate, operating temperature as the critical parameters. Shear rate and bubbling gases are further identified as other important parameters. Presence of high shear rates during the run could help unravel the highly complex asphaltene structure and help in its degradation. Role of hydrogen donation is provided by the bubbling gas such as hydrogen, methane etc. on the channel.

Operating temperature forms a big parameter whose effect is very complex. Arguably, the higher the temperature, the higher the effect. But, ebeam adds energy to the

oil thereby rapidly increasing its temperature and using an average temperature is not very informative. With current conditions, at a dose rate of 20kGy/s, temperature increase due to the ebeam is ~10°C/min in the beginning of the run and decreasing to 5°C/min at the end of the run averaging at ~7-8°C/min. To properly isolate the effect of the temperature, the oil should be irradiated at a constant temperature.

System modifications were performed to incorporate water cooling to reduce the oil temperature and the details are mentioned in the section 'Setup modifications'. Use of copper coil around the tank and a water pipe right below the channel were investigated. It has been found that with water flowing through a half inch pipe welded to the bottom of the channel decreased the oil temperature better than the water flowing through copper tube around the tank. Successful experiments were conducted with steady oil temperature of 265°C. Further modifications were performed by welding a water jacket to the channel instead of a half inch pipe and this setup resulted in a steady operating temperature of 160°C.

Experiments conducted so far were started at temperatures in the range of 180-200°C for oil #2 and 140-180°C for oil #1. Due to the energy addition by the ebeam, the oil temperature ranges during the run were 200-290°C and 140-280°C respectively.

Another important experimental parameter is the absorbed dose whose effect is even more complex. Studies conducted with different doses did not fit a linear curve although good results were observed during some tests at high doses. Wide ranges of dose values of 5-1800 kGy were used. Further, dose calculation is not straight forward either.

Various models and estimates (detailed in the later part of this section) are used to calculate the absorbed dose.

Though not very obvious, dose rate forms a vital role. At a particular temperature and dose, higher the dose rate, higher is the conversion. Studies conducted by Zaykin and Zaykina[24] corroborate this. According to their theory, reaction rate is proportional to the dose rate and so the higher the dose rate, the higher the cracking. This also helps reduce the competing polymerizing and condensation reactions. Experiments are being performed at a moderate dose rate of 20 kGy/s and to further understand its effect, high dose rate (80-100 kGy/s) experiments are planned in near future.

Even though shear rate was identified as a parameter, some of the initial experiments as well as rheological studies (detailed in Chapter 4) revealed very less (if any) effect of shear rate on the treatment. The experiments conducted to ascertain this were low dose; high shear runs where there is no significant change in viscosity post treatment. Subsequent experiments with high dose and both low, and high shear rates did show positive change post treatment implying dose and other parameters are the predominant factors, not shear.

Modifications on the channel were performed to incorporate the bubbling gases. An aluminum square pipe with a gas inlet is welded to the bottom of the channel and tiny holes are drilled on the channel for gas flow. As the oil flows down the channel and high pressure gas flows into the oil through the holes it helps mix the oil that is being treated as well as take part in some chemical reactions. However, the physical and chemical effects of bubbling gas are hard to isolate. Experiments were conducted with various gases

such as helium, argon, hydrogen and methane. Inert gases like helium and argon provide only mixing effects without any participation in chemical reactions. Use of hydrogen and methane could lead to their partaking in the chain reactions along with thoroughly mixing the oil. However, simple comparison cannot be made as there are several other important factors which could have affected the experiments in some way. To properly isolate the chemical effects, experiments should be performed with careful attention to detail ascertaining that the only change is the bubbling gas.

3.5 Flow Modeling

Knowledge of oil residence time under the ebeam is critical to estimate the absorbed dose. As the residence time is dependent on the velocity distribution, a fluid model is developed to obtain the same.

Velocity profiles are basic to any fluid modeling. Further, they are required to estimate the residence time which in turn is necessary to obtain the absorbed dose. To obtain the average velocity of oil flowing lighter particles were dropped in the flow and their path was observed using a camera. Time taken for the particle to travel a set distance is captured using the camera and is used to obtain the average velocity.

As mentioned earlier in the chapter, VFD output frequency and the oil flow rate are correlated. During the early stages of building the system, experiments were performed at various VFD frequencies and corresponding flow rates noted. This is achieved by filling the tank with a known amount of fluid and semi batch flow test is performed. Water and mineral oil were used for this test as they are clear, less viscous and with easily observable

start & stop times. As the pump is a positive displacement one, the correlation is linear and applies to any fluid.

The fluid conditions and geometry closely match poiseuille flow. From the velocity and geometric details, the flow was determined to be laminar. Experiments are conducted with laminar flow only. Turbulent regime is avoided as eddies formed could further complicate the structure of asphaltenes [Personal communication, Dr. Zaykin]. Using poiseuille flow and parabolic velocity profile shear rate is estimated.

A fluid model is set up in EES to model the flow and estimate the residence times and the absorbed dose. Conservation of mass and momentum equations make use of fluid properties such as density and viscosity which are further dependent on the temperature. As the temperature is changing over the course of the run, fluid properties as a function of temperature are required. Viscosity-temperature relations for oil #1 and oil #2 are modeled and detailed in Chapter 4. Density at various temperatures is obtained using Anton Paar 4500 density meter and a linear fit is attained. Details are provided in Appendix B.

3.6 Setup Modifications

The set up used from June 2015 to January 2016 (Oil #1 E1-11 and Oil #2 E1-7) didn't have temperature control and the oil temperature during the experiment raised by almost 80-90°C for doses of the order of 1000 kGy. If the oil temperature at the start of the run is 200°C, it raises to ~290°C by the end of the run. Due to this increase, the effect of temperature cannot be isolated very well. Hence, set up modifications were performed to obtain a controlled operating temperature.

Initial modifications were aimed at cooling the tank when the ebeam is on and is treating the oil. A quarter inch copper coil for water flow is wound all around the tank above the heaters. However, this configuration was not very effective and resulted in a steady state temperature of 295°C. To further modify it, the copper coil was placed below the heaters. This configuration has a steady state temperature of 265°C but affected the oil heating. Figure 11 shows the copper coil wrapped around the oil tank.

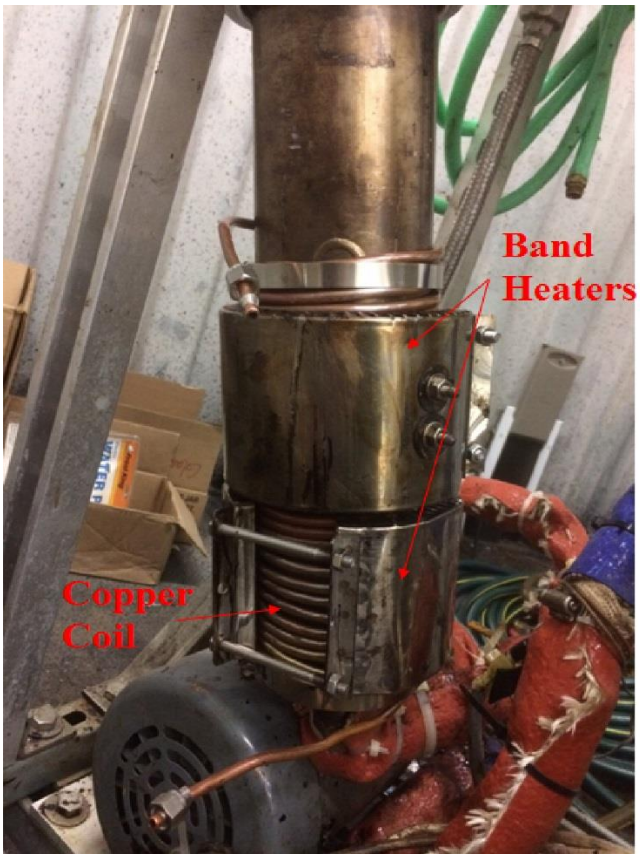

Figure 11: Storage tank with copper coil wrapped around it beneath the heaters

Due to heating issues encountered and the relatively high steady temperature achieved using the copper coil, a different configuration is designed to cool the oil when it is flowing down the channel. Owing to the larger surface area on the channel, a water jacket around it is thought to be effective. An aluminum water jacket is welded to the sides of the channel. Water flows through the jacket when the ebeam is on. This configuration resulted in a much lower steady state temperature at 160°C. Figure 12 shows the channel with water jacket and bubbling gas flow.

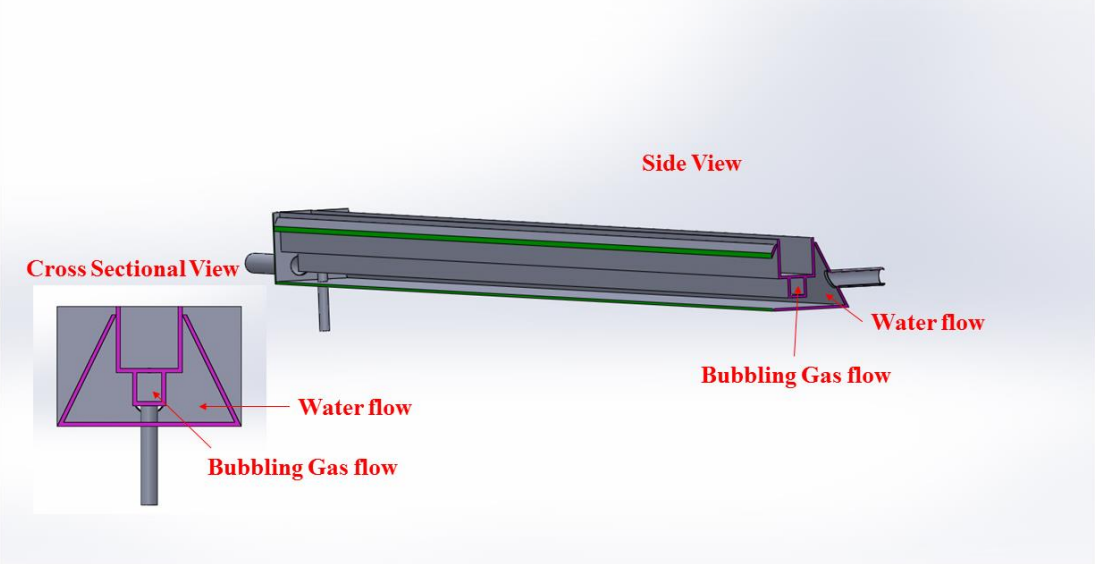

Figure 12: Modified channel to obtain cooling effect and temperature control

3.7 Mass Balance

During heating, lighter fractions volatilize and exposure to the ebeam cracks the heavy molecules. The volatile species evaporated during the course of heating and irradiation are captured in the condenser and separated liquids in the separation chamber. Further, there is some oil left in the channel and at the bottom of the box. All these components together make the treated sample and their cumulative mass should be close to the amount of oil initially put in the storage tank.

Mass balance is one of the critical analysis of the results of an experiment. Good mass balance is important along with viscosity reduction and conversion. For an industrial scale setup, mass balances close to 100% are expected whereas at laboratory scale sample sizes of 1-2kg, 95-105% is acceptable. For example, during an experiment if 90% viscosity reduction is achieved with 80% mass recovery, it is not a good result because the mass balance is bad.

Mass balance is also important because it details the relative amounts of lighter fractions, middle distillates and the heavy collector oil. The higher the amount of lighter yields, the higher the viscosity reduction achieved. Blending, as detailed in chapter 4, talks about the high sensitivity of viscosity reduction to lighter yields than to heavy compounds. Further, the error propagation due to mass balance is higher than any other instrument uncertainty.

For example, assume a case with only 95% mass balance. The 5% difference in mass could be lighter fractions like condensates or separated liquids or heavy residue. Since its origin is unknown, it is hard to evaluate the effect of 5% loss which in turn

imposes a big uncertainty in other measurements. If the 5% liquids were light (gasoline or lighter), it could lead to almost 70% decrease in viscosity. Experiments conducted to evaluate the effect of lighter and heavy yields corroborate this (more details in chapter 4). But, if the 5% were heavy residue, it would only increase the viscosity by 9%. These numbers are high when compared to rheometer uncertainty which is only 5%.

The closer the total mass balance is to 100%, the better the experiment. As mentioned above, for a lab scale sample size of 1-2kg 95-105% is allowed whereas it should be very close 99-101% at industrial scale. Apart from tests using electron beam irradiation, several tests were performed in the laboratory (mobile test cell) that match the temperature and flow profiles of the electron beam experiments. In short, they are a repeat of ebeam experiments, without the beam (also termed control experiments). Mass balance results of both ebeam and lab tests yielded similar accounted mass percentages implying no significant mass loss or gain during the ebeam experiments.

4. RHEOLOGICAL CHARACTERIZATION OF CRUDE OILS

4.1 Introduction

The famous song "The mountains flowed before the Lord" by Prophetess Deborah gave rise to the idea that at higher characteristic time scales, even solids flow. Deborah number as proposed by Reiner indicates the fluid properties of a material. It is defined as the ratio of time of relaxation and the time of observation[40]. A substance flows if this number is small, whereas it is solid like at high Deborah numbers. At the two ends of the spectrum lie ideal solids and ideal fluids. However, most substances are neither ideal solids nor ideal fluids but tend to be somewhere between them. The characteristics of non-ideal materials depend on applied forces and characteristic time. Rheology is the science of characterizing material properties i.e., flow and deformation under the influence of applied forces. The experimental techniques performed to obtain the rheological properties of materials are termed rheometry[41].

Rheological characterization is essential in providing critical flow properties of materials, more so in oil and gas industry as petroleum products and additives show a wide range of physical and chemical variation (from lighter gases and condensates to thick solid-like heavy crude oils). A very important flow property relating shear stress and the rate of deformation is viscosity which indicates the resistance of a fluid to flow. The higher the viscosity lower is its ability to flow. It is defined as the ratio of shear stress (τ) and shear rate ($\dot{\gamma}$).

Viscosity reduces with temperature, as the substance transitions from solid to liquid to gas. However, only a subset of fluids can be characterized by a constant viscosity at a temperature. Such fluids having a linear relationship between shear stress and shear rate and the plot passing through origin (zero shear stress at zero shear rate) are termed Newtonian fluids. A significant class of fluids which do not have such a linear relationship between shear stress and shear rate are identified to be non-Newtonian fluids. Non-Newtonian fluids have shear dependent viscosities, viscosity either increasing or decreasing with shear rate. Further classification of non-Newtonian fluids includes time dependent and time independent behavior[42]. Since, non-Newtonian fluids cannot be characterized by a single value of viscosity, the measured viscosity value at some particular shear rate and time is termed apparent viscosity as opposed to absolute viscosity for Newtonian fluids.

Time-independent non-Newtonian fluids could exhibit any of the following three behaviors:

a. Shear thinning or pseudo-plastic
b. Shear thickening or dilatant
c. Visco-plastic with or without shear thinning

If the apparent viscosity of a fluid decreases with increasing shear rate, it is called shear-thinning fluid whereas if the apparent viscosity increases with an increase in shear rate, it is called shear-thickening fluid. Further, a fluid could have a yield stress which must be overcome for it to deform, making it visco-plastic. Visco-plastic fluids may exhibit shear thinning behavior or have a constant viscosity beyond yield stress[43].

Application of shear over time may change the structural linkages in a fluid and could increase or decrease the apparent viscosity. Viscosity reduction of a fluid over time at some applied shear is termed thixotropy where as an increase is called rheopexy (anti-thixotropy). Thixotropic fluids have a breakdown of structure with applied shear over time and upon removal may regain the original structure and hence initial value of viscosity. On the other hand, rheopectic fluids show an increase in viscosity over time with applied shear[42,43].

Viscosity as defined above is called shear viscosity (resistance of a fluid to shear), which is the most common definition of viscosity. Resistance of a fluid to stretching is termed extensional viscosity[44]. Experiments aimed at characterizing shear flows are called Shear or Rotational Rheometry whereas others aimed at extensional flows are called Extensional Rheometry.

4.1.1 Rotational Rheometry

The subject of this research, bitumen/heavy crude oils are non-newtonian in low-moderate temperature ranges. Further they could exhibit complex rheology with time-dependent behavior. Hence, stress, shear, temperature and time are necessary to characterize their shear flow behavior. Rotational Rheometry has been employed to obtain the required correlations between applied forces and deformations. Both rheometers and viscometers could be used to characterize rotational rheological properties, but a rheometer is more precise and has a wider control compared to a viscometer[45]. Rotational rheometers could be used in two modes; controlled shear stress (CSS) or controlled shear rate (CSR).

The motor is situated above the sample and the driven spindle is supported by an air bearing in order to measure the torque. For CSR measurements, shear rate is controlled and with the gap known, it directly relates to the velocity of the spindle. The resultant torque due to spindle movement is measured which can yield the shear stress applied to the sample. Similarly, for CSS measurements, shear stress is controlled which relates to the torque and the resultant velocity (rpm) of spindle measured. With both shear stress and shear rate known, apparent viscosity of the sample is known. The following section details the different measuring systems (geometry) used in rotational rheometry.

Measuring Systems: Various measuring systems are used to carry out rotational rheometry. They include cup and bob, cone-plate and plate-plate measuring systems. Figure 13 shows the geometries of the three measuring systems.

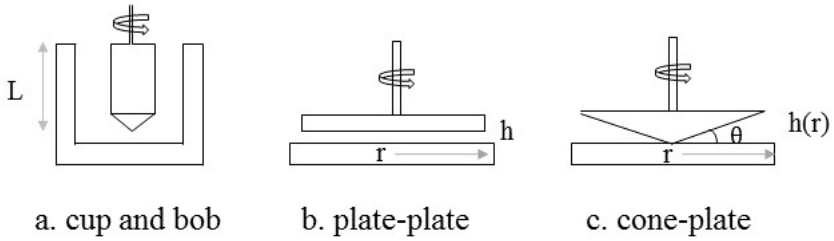

Figure 13: Measuring systems and their geometry

Cup and Bob: This kind of measuring system is usually in the form of coaxial cylinders, a coaxial cup with inner bob. They are highly useful for low viscosity fluids and

mobile suspensions. With larger and enclosed surface area, there is less chance of the liquid flowing out and easier to perform low shear measurements. However, they are difficult to clean and require larger sample sizes. Moreover, with higher mass and inertia, it is not recommended for high frequency measurements[46].

Cone-Plate: A widely used measuring system is with the cone and plate geometry. The lower end of the spindle is a truncated and the sample is placed between the truncated cone and the bottom flat plate. It is positioned such that the theoretical (missing) tip touches the bottom plate. They usually have a cone angle of 1-5°, depending on the diameter. The biggest advantage of a cone-plate system is the uniform shear rate over the sample. Due to the cone angle, the gap between the plates (gap setting) increases with increasing radius. The cone angle is provided such that the radius to gap ratio stays constant and hence shear rate is constant over the sample. It is very easy to clean, requires only small volume of sample and can be used for high viscosity materials. However, the gap setting between the plates is constant and very small, and hence should not be used for any samples with particulate matter. Further, due to the sensitivity to gap setting, it cannot be used for temperature sweeps unless equipped with an automatic system for thermal expansion compensation[46].

Plate-Plate (Parallel plates): Plate-plate measuring system has the sample placed between two parallel plates. It is very useful for high viscosity samples like polymers and can take sample in the form of a pre-formed disc. It is easy to clean, requires small volume of sample and can be used at higher shear rates. Further, it is not sensitive to the gap between plates like the cone-plate and have gap setting in the range of 0.5-2mm. Its main

disadvantage is the non-uniform shear rate across the sample. With the height being constant shear rate increases with the radius, and the software computes an average value. Also, as the gap between plates is wide, it has to be surrounded by a thermally insulating cover to avoid any temperature gradients in the sample[46].

4.1.2 Instrument Specifications

Anton Paar MCR Physica 101 rheometer has been used for obtaining rheological properties of oil #1 and oil #2. Both cone-plate and plate-plate measuring systems were used though cone-plate measuring system is favored in order to obtain constant shear rate over the sample. The cone has a diameter of 50mm and angle of 2°. Two sets of parallel plates with diameters 50mm and 25mm have been used. The cone-plate measuring system requires a sample of 1.14ml whereas the plate-plate configuration requires 1.96ml (for 50mm diameter and 1mm gap). The instrument has automatic thermal expansion compensation and a thermal insulating cover to avoid any thermal gradients and positioning errors.

The instrument is limited by a maximum torque of 0.125 Nm. This corresponds to a maximum shear stress of 3830 Pa or 8955 s^{-1} (whichever comes first) for the cone-plate system and 5093 Pa or 7854 s^{-1} for plate-plate system. Figure 14 shows the rheometer used. Rheometer calibration can be found in Appendix A.

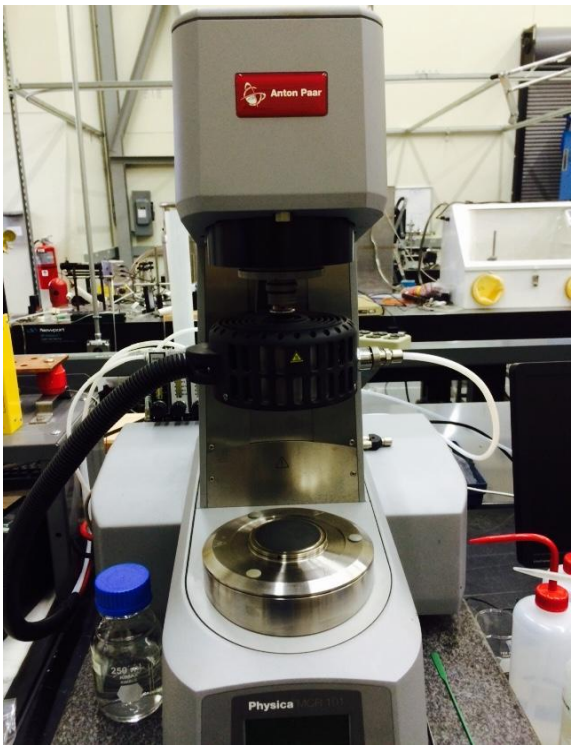

Figure 14: Rheometer used to evaluate viscosity properties of oil #1 and oil #2

4.2 Properties of Untreated Crude Oil

Extra-heavy crude oil and bitumen are characterized by very high viscosities. Further, they are known to exhibit non-newtonian (shear and time dependence) behavior at low to moderate temperatures. Steady and transient flow behaviors are examined at various temperatures for oil #1 and oil #2. This section describes the rheological properties of crude oils which are being treated using electron beam irradiation.

4.2.1 Sample Insertion

Once the instrument is initialized and the measuring system set in place, sample is inserted and the upper plate is lowered to the measuring position.

Glass syringes can be used to accurately transfer the required volume of sample but the very high viscosity of oil #2 prevents the use of one. A syringe can be used with oil #1 but with the associated high viscosity, there is shear imposed on the sample during the process and the sample hence is not fresh. To avoid unnecessary shear on the sample, oil has been scooped using a stainless steel spatula and placed on the bottom plate of the rheometer. It is made sure that the sample size is slightly more than required amount during transferring and later trimmed to ensure that exact amount of oil is present between the plates.

Temperature of the flat bottom plate plays a vital role. At low temperatures, when the oil sample is highly viscous it imposes a normal stress on the upper plate as the latter lowers to the measuring position. Any kind of stress or shear could change the structure of the oil due to shear history and should be avoided. Hence, the bottom plate is heated to 50°C for oil #1 and 80°C for oil #2 before lowering the upper plate. It has been observed that at temperatures above 50°C and 80°C for oil #1 and oil #2 respectively, there is negligible normal stress due to the sample on the upper plate.

Once the plates are set in place, the required temperature is set. Sufficient time is provided for the sample temperature to reach the set temperature. Allowed tolerance is 0.02°C. Test is started only after the sample temperature is + 0.02°C of the set temperature. The standard operating procedure for the rheometer has been provided in the Appendix E.

4.2.2 Steady Flow Behavior

Flow behavior of oil #1 and oil #2 has been investigated using the controlled shear rate (CSR) mode of the rheometer. Temperature and shear rate are varied and viscosity

measured. A temperature range of 40 - 200°C and shear rate in the range of 1-100s^{-1} has been used. The shear rate range has been selected to emulate the flow conditions during the experiments as well as real time pipe flows. At low temperatures (<50°C for oil #1 and <80°C for oil #2) the viscosity is very high and instrument is constrained by the maximum torque and could not reach the set shear rate. Though cone-plate and plate-plate measuring systems have been used, measurements using cone-plate system have been used in this thesis. Cone-plate system is preferred over the plate-plate system due to the uniform shear rate the former provides. Table 2 and Figure 15 give the viscosity of oil #1 and oil #2 at various temperatures.

Temperature [°C]	Viscosity [cP]	
	Oil #1	Oil #2
40	33400	4110000
50	9310	264000
80	774	8950
100	248	1750
120	109	494
140	59	184
150	46	122
170	31	60.6
180	26	45.7
200	20	28.3

Table 2: Viscosity of oil #1 and #2 at various temperatures and shear rate of 50s^{-1}

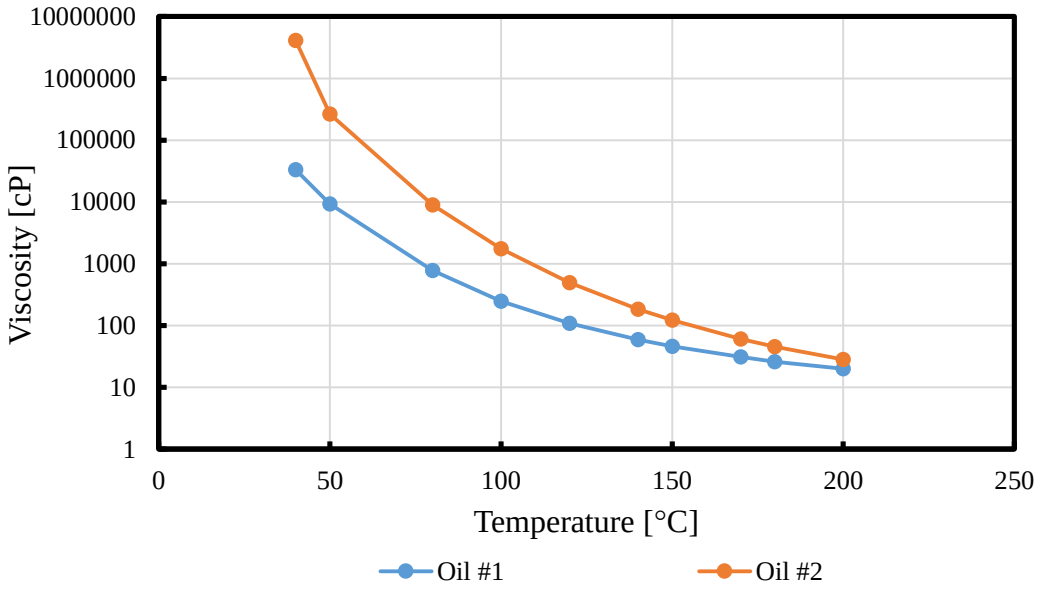

Figure 15: Viscosity vs temperature of oil #1 and oil #2

Viscosity at a shear rate of $50s^{-1}$ has been chosen for measurements in table 2 and figure 15 since it is the average shear rate during most experiments. As can be observed from figure 15, viscosity of oil #1 and oil #2 drop significantly with temperature.

Viscosities of both oil #1 and oil #2 are shear dependent, though this dependence decreases with an increase in temperature. Figures 16 & 17 give the viscosity versus shear rate plots for oil #1 and oil #2 at various temperatures. It must be noted that the instrument is constrained by the maximum torque when measuring viscosity of oil #2 at low temperatures. Given the extremely high viscosity of oil #2 at temperatures below 80°C, the rheometer couldn't reach the given maximum shear rate of $100s^{-1}$ and stops when the imposed shear stress reaches 3830 Pa (max torque by the instrument is 0.125Nm).

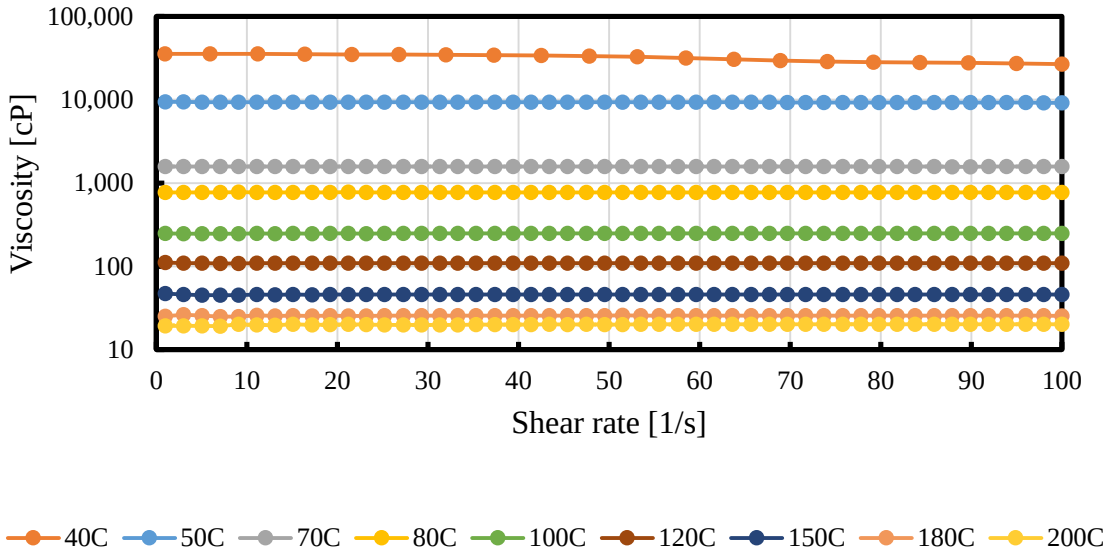

Figure 16: Viscosity vs shear rate for oil #1 at various temperatures

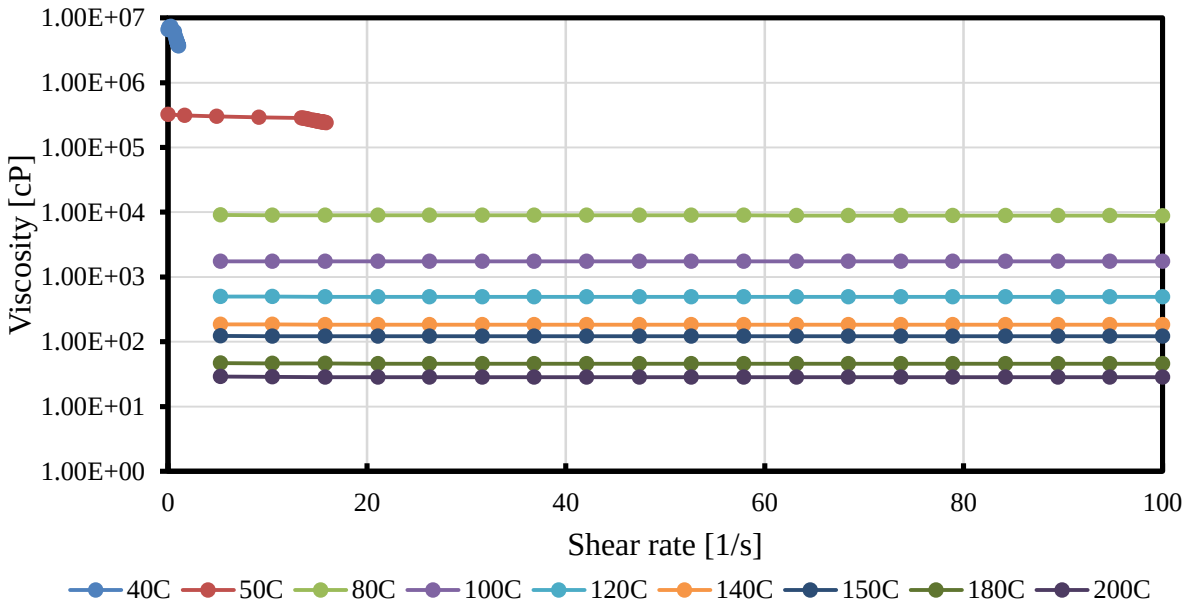

Figure 17: Viscosity vs shear rate for oil #2 at various temperatures

As it is evident from figures 16 & 17, shear stress and shear rate are increasingly linear with temperature. A linear fit has been applied to all the data and the R^2 square value noted. At lower temperatures, the fit is not quite linear. Oil #1 has an approximate linear relationship above 50°C and for oil #2 it occurs at 80°C. This indicates that both oil #1 and oil #2 exhibit shear thinning behavior (decrease in viscosity with increase in shear rate) at lower temperatures and approximate newtonian behavior beyond 50°C and 80°C respectively.

Oil #1 exhibits a 25% decrease in viscosity with an increase in shear rate from 1-100s^{-1} at 40°C. At 50°C and above this decrease drops down to less than 2%. For oil #2 above 80°C, the change in viscosity with shear rate in the range of interest (1-100 s^{-1}) is only 2-3% whereas at temperatures below 80°C the change is as high as 25%. At 50°C, the change in viscosity over 1-16 s^{-1} is 25%.

Thixotropic tests failed to reveal any apparent effect of shear on the structure of the sample. Oil #1 and #2 exhibit very low thixotropic area of 7.5 kPa/s and 12.67 kPa/s respectively. This area is very less when compared to the numbers reported in literature[47] which are of the order of hundreds of kPa/s indicating very less to no thixotropic behavior. Futher, the temperature of the sample increased by 0.1°C by the end of up curve and it might have contributed to the lower viscosity at the beginning of the down curve. It could be possible that part of the small thixotropic area is due to the slight temperature increase.

Tests were performed over a shear rate of 0.1-600 s^{-1} for oil #2 at 80°C and 0.1-150 s^{-1} for oil #1 at 40°C. Oil #1 had high viscosity at 40°C and due to maximum

instrument torque could not reach to a higher shear rate than 150 s^{-1}. Figure 18 gives the hysteresis loop results for oil #1 and oil #2.

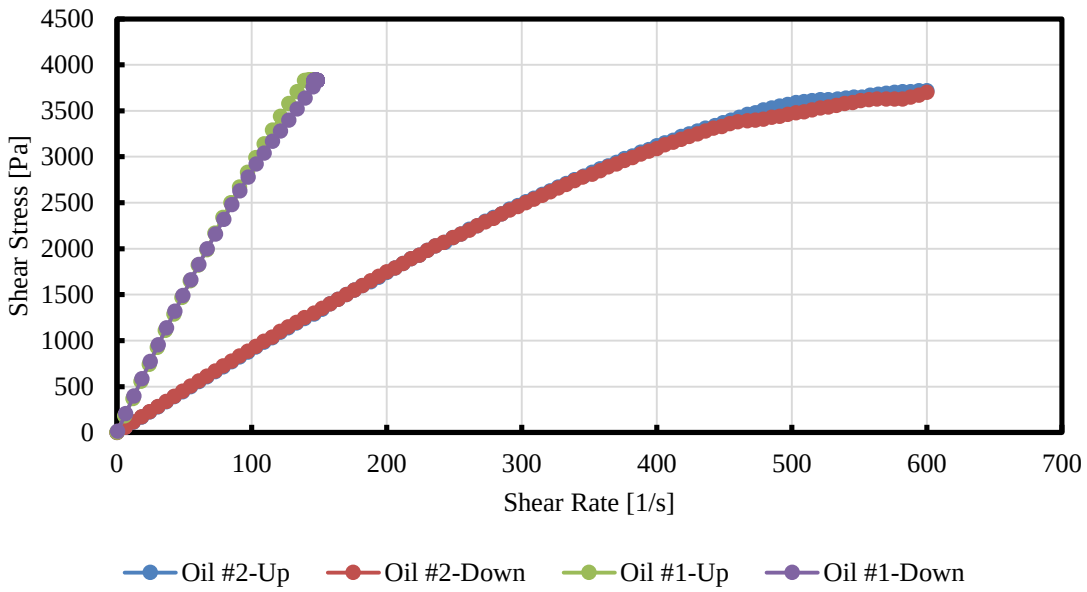

Figure 18: Hysteresis loop for oil #1 and oil #2

4.2.3 Transient Flow Behavior

Transient flow behavior of oil #1 and oil #2 has been investigated using the controlled shear rate (CSR) mode of the rheometer. Viscosity of the sample is measured as a function of time at a constant shear rate and temperature. A temperature range of 25 - 200°C and a shear rate of $20s^{-1}$ have been used. The effect of shear history is very small with a maximum difference of 3-4%. Even at low temperatures of 25°C, there is only 3-4% change in viscosity with time.

4.3 Repeatability of Measurements

An important consideration during measurements is the repeatability. In order to ascertain the repeatability of measurements, three sets of measurements spanning a wide range of shear rates (0.1-500s^{-1}) were taken and compared. Standard deviation of measurements at a particular shear rate are compared with the mean. A deviation of 2-3% was observed at 50°C and 0-2% at 100°C. Figure 19 presents the repeatability results.

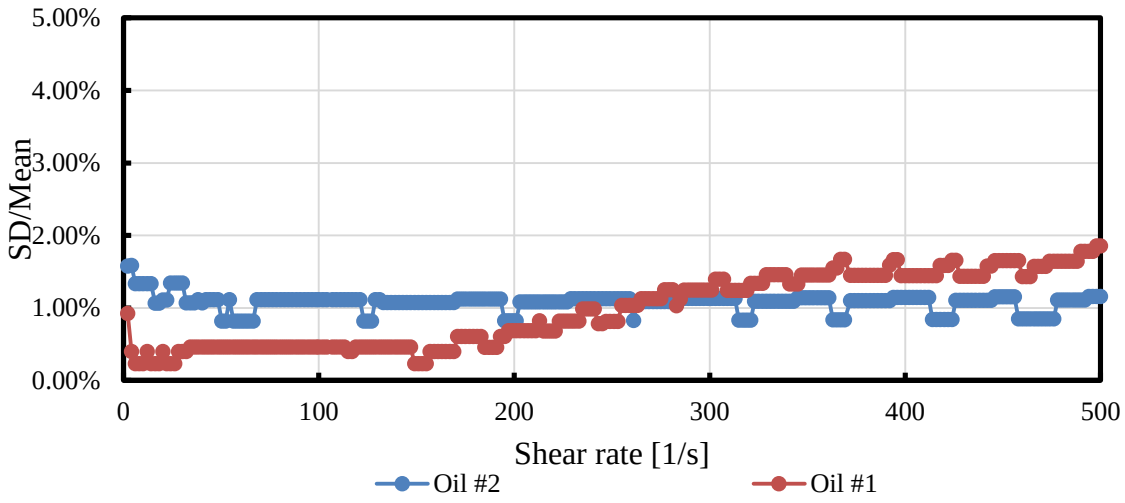

Figure 19: Repeatability (comparison of standard deviation to mean) for three data sets of oil #1 and #2 at 100°C

4.4 High Shear-High Temperature Viscosity Measurements

Viscosities of oil #1 and oil #2 have been measured at high temperatures and high shear rates. The objective is to look for a range of shear rate where there is a significant drop in viscosity. If a significant drop in viscosity is observed and if such shear rates

(termed critical shear rate for the purpose of this thesis) could be attained in experimental flow conditions, it could have a synergistic effect with the electron beam treatment. Critical shear rates could affect the asphaltene structure by unwrapping the tightly bound layered molecule and hence making it more susceptible to cracking.

Viscosity measurements were obtained at high temperatures (in the range of 190-250°C) and high shear rates. Both cone-plate and plate-plate measuring systems have been used. For a cone-plate measuring system, the maximum torque of the instrument (0.125 Nm) allows a shear stress of 3830 Pa or a shear rate of 8995 s^{-1}. The 25 mm diameter plate-plate measuring system has an allowed highest shear rate of 3920s^{-1}. In order to maintain consistency in this report, only cone-plate system data have been provided. At temperatures of interest, the oil samples are sufficiently thin to achieve the highest possible shear rate provided by the instrument. Figure 20 shows the plot of viscosity versus shear rate for oil #1 and oil #2.

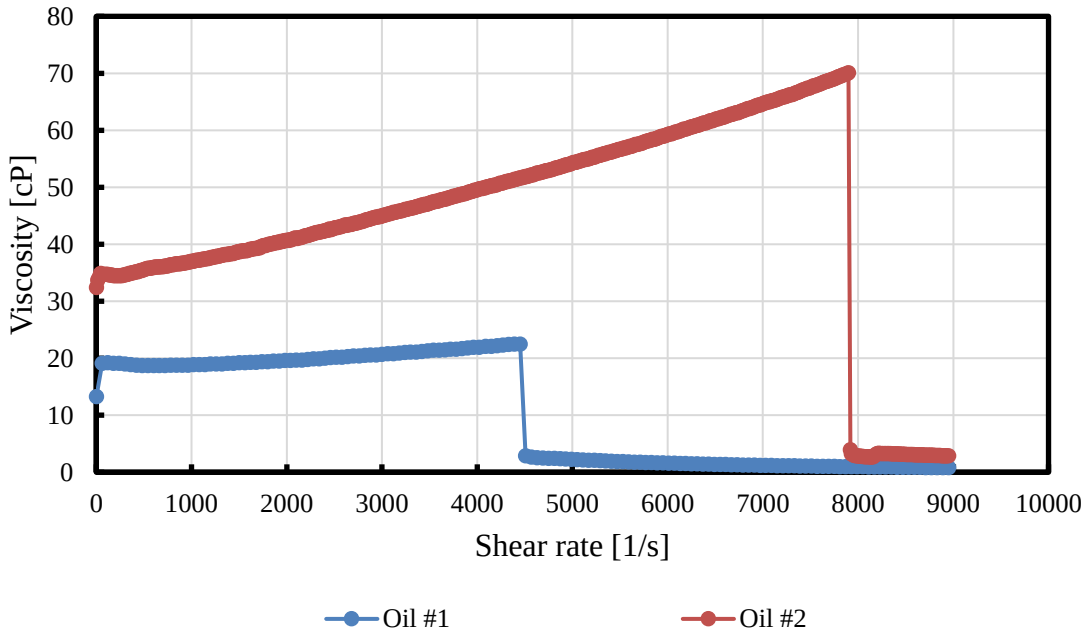

Figure 20: Viscosity vs shear rate for oil #1 and #2 at 200°C and high shear

The general trend is an increase in viscosity to a point where it drops significantly. It has been observed that by the end of experiment, the oil has flown out between the plates on to the insulating cover around it. This is the reason for the sudden drop in viscosity and could be due to either viscosity instabilities or fluid instabilities.

To better dissect the reason few other tests were conducted without the insulating cover to observe the flow pattern. At very high shear rates, the oil is explosively thrown out from between the plates. Due to the velocity being very high, the flow regime could have transitioned to turbulent flow and/ or centrifugal force too high.

As can be observed from the figure 20, the critical shear rate occurs at a few thousand s^{-1}. Further, there is no particular trend. Some of the repeatability tests performed yielded critical shear rates within a few hundred s^{-1}. It is highly plausible that the reason

behind critical shear rate is fluid instability (due to turbulence) over viscosity instability. Unfortunately, it is of very little use even if it was due to viscosity instability because the critical shear rate values are well over a few thousand s^{-1} making it practically not possible to achieve.

Interestingly, for oil #1 at 250°C and high shear rates, there was oil separation at the measuring system. It is shown in figure 21. We believe it might be asphaltene separation as they were soluble in toluene, but not pentane. If it were asphaltene separation, it would pose a different problem of cleaning. Moreover, it might even act as a nucleation site for further separation or coke formation.

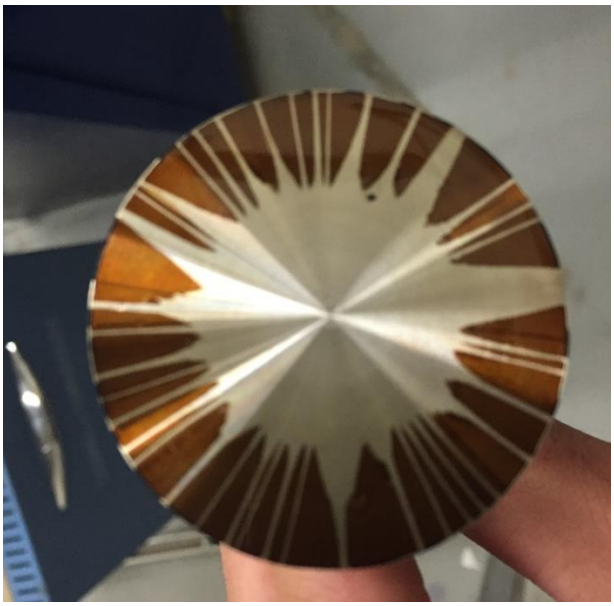

Figure 21: Separation observed for oil #1 at high shear and 250°C

4.5 Viscosity Temperature Modeling

Due to high energy addition during ebeam processing, temperature changes significantly and hence viscosity. Several experimental viscosity-temperature data points for oil #1 and #2 exist, but viscosity-temperature relations are required to predict viscosity at real-time temperature during the experiment to model the fluid flow. In order to do this, several viscosity-temperature models in literature have been examined.

Oil #1 and #2 have high proportions of aromatics, resins and asphaltenes than conventional crude yielding higher molecular weights and viscosity. Given their differences in chemical composition, structure and viscosity-temperature relationship, not all liquid viscosity-temperature models can be applied to them satisfactorily.

4.5.1 Prior Work

Some of the early viscosity-temperature models were developed using reservoir temperatures and API gravity. Beal[48] developed plots and a dead oil viscosity relation as a function of both reservoir temperature and API gravity. Different reservoir temperatures; 100-220°F and an API gravity range of 10-52^0 were considered.

$$\mu_{od} = \left(0.32 + \frac{1.8 * 10E7}{API^{4.53}}\right) * \left(\frac{360}{T - 260)}\right) * 10^{(0.43 + \frac{8.33}{API})}$$

The μ_{od}-T-API relation showed a reasonable fit at higher API, with % deviation increasing with decreasing API. In the API range of 10-19.9°, the average % deviation was 47%. Given oil #1 and #2 have API gravity less than 10, use of Beal equation could result in higher deviations.

Beggs and Robinson[49] plotted log(T) vs log(log(μ_{od}+1)) and developed a slightly different equation.

$$\mu_{od} = 10^{x} - 1; x = y(T - 460)^{-1.163}; y = 10^{z}; z = 3.0324 - 0.02023 * API$$

This equation yielding lower deviation (~14%) than Beal equation, but the study considered only API in the range of 16-58° and lower API oils like oil #1 and #2 could result in much higher errors.

Further studies on dead oil viscosity correlations were performed by Glaso[50]. But their equation was developed only from North Sea crude oil data with API range of 28-48^0.

Even though these models account for a good range of oils in terms of API gravity, they have the empirical constants generated from their data set and have higher deviation when applied to other oils. Moreover, these models are especially relevant for studies performed only with PVT data, viscosity data at reservoir temperature. For current studies on oil #1 and #2 where good number of viscosity-temperature data points exist, a two parameter viscosity-temperature model with empirical constants specific to target oils seems better equipped to relate the two.

Some of the early development of two parameter relations for viscosity-temperature modeling were brought about by MacCoull[51,52] who published viscosity-temperature plots which now form basis for the ASTM Standard D341[51]. Walther[52] was credited for developing a double logarithmic viscosity-temperature relation with two parameters.

$$\log(log(\mu)) = P - M * T$$

μ is the absolute viscosity in [cP] and T is the temperature in Celsius [°C]

One of the drawbacks of such double logarithmic relations is that they cannot be defined for viscosities less than 1. In order to correct that several additive constants and extensions have been defined by researchers[52]. Modified Walther equation has the form

$$\log(log(\mu + \gamma)) = P - M * T$$

γ is the additive constant which is typically 0.7

MacCoull's charts were based on the constant (γ) 0.7 [52].

Geniesse and Delbridge[52] proposed a similar double logarithmic linear equation with a logarithmic term associated with temperature. Moreover, they used an additive constant of 0.8 to better fit the data. Their equation takes the following form

$$\log(log(\nu + 0.8)) = A - B * \log(T)$$

Further work has been carried out by Wright and Manning[53] to extend the charts in the lower viscosity range. Current ASTM D341 standard charts use Wright's equations:

$$\log\big(log\big(\nu + \gamma + f(\nu)\big)\big) = A - B * \log(T)$$

where $$\gamma + f(\nu) = 0.7 + C - D + E - F + G - H$$

$$C = \exp(-1.14883 - 2.65868 * \nu)$$

$$D = \exp(-0.00381308 - 12.5645 * \nu)$$

$$E = \exp(5.46491 - 37.6289 * \nu)$$

$$F = \exp(13.0458 - 74.6851 * \nu)$$

$$G = \exp(37.4619 - 192.643 * \nu)$$

$$H = \exp(80.4945 - 400.468 * \nu)$$

With change of the complex f(ν) function in Wright's equation to a polynomial function, Manning has extended the chart down to 0.12cSt.

Manning's equation is of the form

$$log_{10}\left(log_{10}(\nu + \gamma + f(\nu))\right) = A - B * log_{10}(T)$$

$$\gamma + f(\nu) = 0.7 + \exp(-1.47 - 1.84\nu - 0.51\nu^2)$$

In order to further extend the existing plots without changing the historical data, Seeton[52] has replaced the exponential series functions with a zero order modified Bessel function of the second kind. The new equation takes the form:

$$ln\left(ln(\nu + 0.7 + e^{-\nu}K_0(\nu + 1.244067))\right) = A - B * ln(T)$$

Similar linear relation and a non-linear viscosity-temperature relation were developed by Mehrotra and his group[54], where the only deviation of the linear model from Walther equation is considering dynamic viscosity instead of kinematic viscosity. Linear equation proposed by Khan et al. takes the following form:

$$\ln(ln(\mu)) = A + B * \ln(T)$$

The non-linear viscosity model takes the form

$$ln(ln(\mu)) = [1 + b_1T + b_2(b_1T)^2]e^{b_1T}$$

Further, Mehrotra[55] used data from 273 pure heavy hydrocarbons to generalize constants and reduced the two parameter linear model to a single parameter model. However, such generalization is not necessary as the two empirical constants can be easily found using measured data points for oils of significance. Moreover, the hydrocarbons considered for the work have molecular weights in the range of 30-300 g/mol, which is considerably smaller than the molecular weight of bitumen (~600 g/mol)[56]

4.5.2 Development of a modified model and discussion

Oil #1 has viscosity in the range of 33400 – 20 cP over temperatures 40 – 200°C and oil #2 has a range of 264,000 – 28 cP over 50-200°C. A temperature range of 50-200°C was chosen for oil #1 and 80-205°C was chosen for oil #2. The lower temperature range; 50°C for oil #1 and 80°C for oil #2 was chosen such that the crude oils behave sufficiently Newtonian with only 2-3% difference in viscosity over the shear rate of importance (real time shear rate estimation).

All the linear viscosity-temperature models like Seeton, Manning, Wright, Mehrotra being similar mathematical expressions yield the same results. They were developed to preserve historical data and the added terms go to zero beyond 4 cSt. All the measured data points in the temperature range of 80-205°C have viscosities greater than 4 cSt and hence all the linear models give the same predicted viscosity numbers.

It was observed that non-linear models introduce a large deviation. Also, there was a slight difference between the linear models with and without additive constants, with the latter being more close to measured data. The method of least squares has been used for analysis. Use of an additive constant had a negative effect within for the oils in the required temperature ranges. Hence a negative constant has been introduced in the equation to observe its effect. The modified equation with a negative constant takes the following form:

$$\log(log(\mu + \gamma)) = A - B * logT \; ; \gamma < 0$$

where A, B are empirical constants and γ is the negative constant, all of which were fit to the experimental data set. Different negative constants (γ) in the range of -0.7 to -10 were examined and -5 has the lowest deviation.

Linear models and addition of a negative constant seem to be the best model for oil #1 & #2. Figure 22 gives the comparison between experimental and modeled data.

The modified linear model for oil #2 is:

$$log(log(\mu - 5)) = 9.7042 - 3.5748 * logT$$

The modified linear model for oil #1 is:

$$log(log(\mu - 5)) = 8.0782 - 2.9963 * logT$$

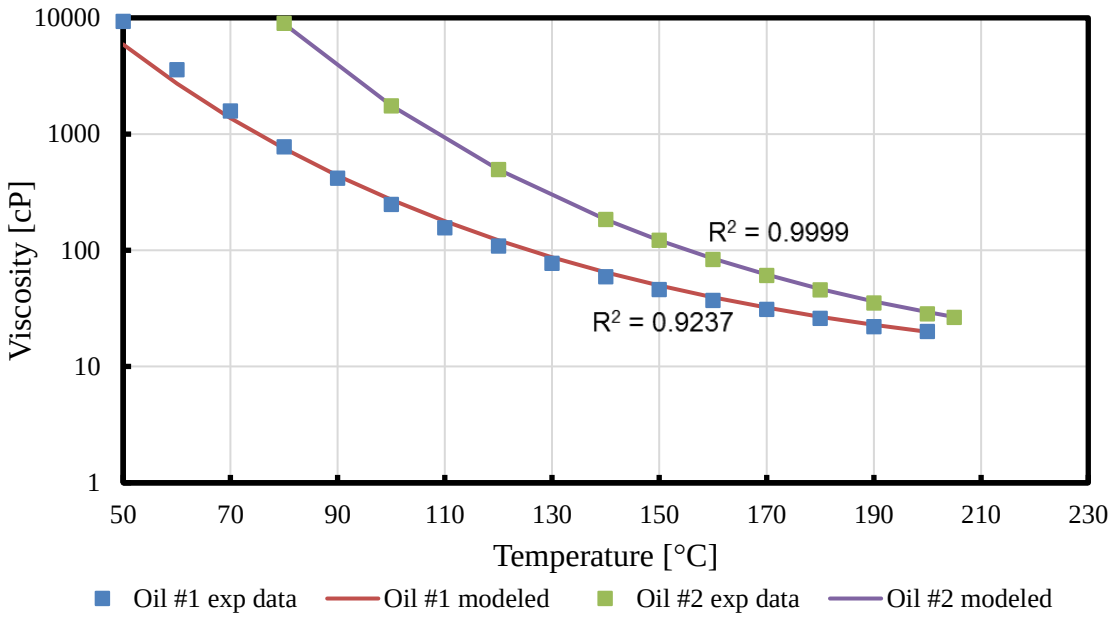

Figure 22: Modified viscosity-temperature correlation for oil #1 and oil #2

4.6 Viscosity of Mixtures

Viscosity of crude oil drops significantly when mixed with lighter fractions. In fact, blending with lighter crude or condensates is one of the widely used viscosity reduction techniques employed at production site. Crude oil blending is studied in this thesis to understand the effect of different products obtained during treatment as well as to help explain the necessity of good mass balance. Treated products obtained during electron beam irradiation include collector liquids (major portion in the storage tank), separated liquids collected in the separation chamber and the condenser liquids along with minor portions left in the box. All these components are mixed in the same mass ratios to obtain the required treated product. The higher the ratios of the lighter yields, lower is the viscosity of the product.

Typically, separation chamber liquids have the physical characteristics of middle distillates and the condenser liquids are similar to light fractions such as gasoline. The relative ratios of these lighter components determines the end result as the sensitivity to lighter fractions is much higher in blending when compared with heavier fractions. As such, good mass balance is critical because of the high uncertainty propagation otherwise.

Due to the higher sensitivity to lighter fractions, their loss has a big effect on the final viscosity. For example, post experiment if the mass balance was determined to be 95%, the 5% loss could be light fractions or heavy fractions though the former is more likely. This introduces a huge uncertainty as 5% lighter yield could further reduce the viscosity of the sample by 70%. This number is very high compared to the instrument uncertainty of 5%. Studies on blending are important to discern the error introduced in the

analysis due to the loss of light fractions. Figure 23 and table 3 show the experimental results of blending raw crude oils with both lighter and heavier compounds.

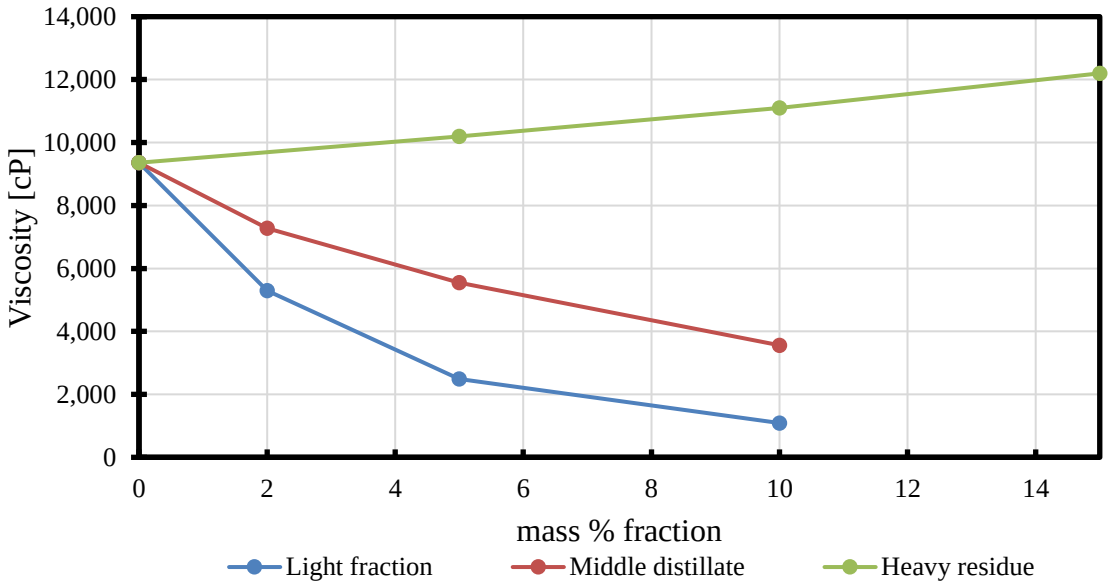

Figure 23: Blending of raw crude oil with lighter and heavier fractions at different mass fractions

Mass fraction (% wt)	Light fraction		Separated liquids		Heavy residue	
	Viscosity [cP]	% difference	Viscosity [cP]	% difference	Viscosity [cP]	% difference
0	9,360		9,360		9360	
2	5290	43.48%	7280	22.22%	NA	NA
5	2490	73.40%	5550	40.71%	10,200	-8.97%
10	1090	88.35%	3560	61.97%	11,100	-18.59%
15	NA	NA	NA	NA	12,200	-30.34%

Table 3: Blending of raw crude oil with light fractions, separated liquids and heavy residue; oil #1

Products from the same experiment were considered for this study. However, due to low amount condensates available, light mineral spirits were used as a substitute for the lighter fractions. Viscosity of light fraction is 2.8 cP and that of separated liquid is 32 cP at 25°C. Viscosity of the heavy residue is 120,000cP at 50°C.

As can be observed from the figure 23, lighter fractions have a significant effect on viscosity reduction. Addition of 5% light oil causes a drop in viscosity by 73.4% whereas 5% addition of heavy crude leads to an increase in viscosity by only 9%. So, loss of 5% light fractions could lead to errors as high as 70%. Even the loss of a modest 2% light fractions could introduce an error of 20-40% which is very high compared to the instrument error of 5%. Hence, good mass balance forms an essential part of the experimental results. For a sample size of 1-2kg, 95-105% is acceptable but as the system is scaled higher, the mass balance should be close to 100% of feedstock.

Most of the models for predicting the viscosity of mixtures are employed based on the mole fractions of the components[57]. However, knowledge of the molecular weights of crude oils is not always known and there could be a significant error in the estimates. Walace-Henry method is one of the few models which incorporate the use of mass fractions rather than mole fractions[58]. It makes use of the following equation:

$$\boldsymbol{\mu = a * e^{\frac{1}{I_{blend}}}}$$

where $I_{blend}= \frac{x_A}{\ln(\mu_A/a)} + \frac{x_B}{\ln(\mu_B/a)}$ and a=0.01, x_A, x_B and μ_A, μ_B are the mass fraction and viscosity for individual petroleum components respectively. Figure 24 plots the predicted viscosity of the blend and the % change in the viscosity due to the addition of a different hydrocarbon. Assumed viscosities are 200 Pa.s for heavy crude (viscosity of oil #1 at

25°C) and 0.0028 Pa.s for the diluent (the one used for experiments). It provides a reasonable fit when compared to the experimental results.

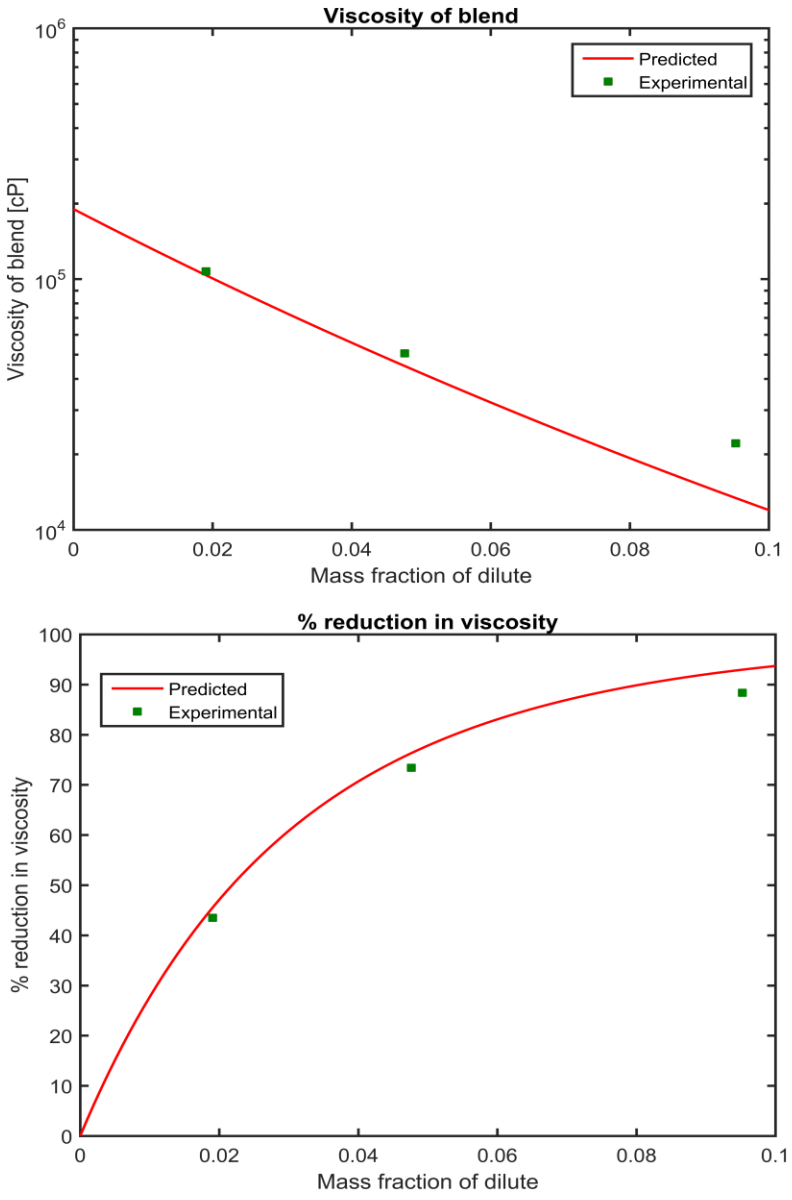

Figure 24: Effect of blending, as predicted by Wallace-Henry method

5. SIMULATED DISTILLATION

5.1 Introduction

Oil in its crude form is of little use and has to be refined into various products before sold in the market. Gasoline, naphtha, diesel, gas-oil, fuel oil etc. are all various refined crude oil products obtained through several separation and conversion processes followed by some secondary treatments. The major separation process employed by crude oil refineries is distillation which separates constituents of crude oil based on their boiling points. Hence, physical distillation is a widely used technique employed to characterize crude oils.

Laboratory scale distillation techniques are aimed at obtaining the boiling point distribution which in turn dictates various cuts i.e. lighter fractions, middle distillates and residue. Relative proportions of lighter and middle fractions directly translates to market value of the crude. Further, knowledge of boiling point distribution is essential for upgrading processes such as vis-breaking, cracking etc. Relative amounts of various distillates and residue when compared with the raw sample yield the % conversion of residue to lighter fractions.

However, use of conventional physical distillation techniques require larger samples and several hours to complete[59]. To overcome the disadvantages of physical distillation, simulated distillation techniques have been developed to simulate the process. It is carried out on a gas chromatograph (GC) and operates on the principle that hydrocarbons elute according to their boiling points on a non-polar column[60]. Also, it is

the only characterization technique that is capable of analyzing the wide range of volatile hydrocarbons in crude oils (n-C3 to n-C120)[61]. Studies conducted by researches show close overlap between physical distillation and simulated distillation (SimDis) curves[62].

5.2 GC-SimDis

Simulated distillation is very rapid, automated, reliable and equivalent to 100 plate theoretical physical distillation requiring only a few microliters of sample. As opposed to traditional GC, which is a high resolution chromatographic method, simulated distillation employs a low resolution method trying to simulate physical distillation. Using SimDis, the components are not separated as individual peaks but appears as one large Gaussian peak that resembles a big lump[60].

5.2.1 ASTM Simulated Distillation Methods

American Society for Testing and Materials (ASTM) has laid out several methods to carry out simulated distillation analysis of crude oils. These methods span different temperature ranges and are used to analyze different fractions i.e. gasoline components, mid-range distillates, vacuum, and atmospheric residues etc.

Oil #1 and oil #2 are extra-heavy crude oils with high molecular weight and containing very low lighter fractions. In order to analyze these oils, high temperatures are required. Some of the high temperature SimDis methods include ASTM D6352[66] and D7169[67]. ASTM D6352 is used to analyze 'petroleum distillate fractions having an IBP greater than 174°C and a FBP of less than 700°C using capillary GC'. A temperature of 700°C corresponds to elution of n-C90. ASTM D7169 can analyze 'boiling point

distribution of samples with residues such as crude oils and atmospheric and vacuum residues by high temperature gas chromatography'. This method gives the distribution through 720°C corresponding to elution of n-C100. Both these methods have been used to analyze the raw and treated crude samples. They have been modified by increasing the final temperature hold time for residue elution. Table 4 gives the summary of the methods employed.

	Modified ASTM D7169	Modified ASTM D6352
Initial Oven Temperature	30°C	50°C
Initial Oven Time	0 min	0 min
Oven Temperature Program	15°C/min	10°C/min
Final Oven Temperature	430°C	400°C
Final Oven Hold Time	~150 min	~180 min
Initial Injector Temperature	50°C	Track oven mode (always 3°C more than oven)
Initial Injector Time	0 min	0 min
Injector Temperature Program	15°C/min	Oven track mode
Final Injector Temperature	430°C	Oven track mode
Final Injector Hold Time	~150 min	~180 min
Column Flow	20 mL/min	18 mL/min
Carrier Gas Control	Constant Flow	Constant Flow
Detector Temperature	435°C	430°C
Detector Hydrogen Flow	40 mL/min	32 mL/min
Detector Air Flow	450 mL/min	400 mL/min
Detector He makeup Flow	15 mL/min	24 mL/min
Injection Volume	1 µL	1 µL
Sample Concentration	1:100 m/v in DCM	1:100 m/v in DCM
Data Acquisition Rate	10 Hz	10 Hz
Qualitative Calibration	Polywax 655	Polywax 655

Table 4: Summary of high temperature SimDis methods used for this study

5.2.2 Instrument Requirements

Requirements for performing simulated distillation on a GC are laid out by ASTM D6352, D7169, D2887[66–68].

Column: In order to obtain sample elution according to the boiling point distribution, a non-polar column should be used. Use of capillary columns are recommended over packed columns as packed columns have higher bleed at high temperatures required for ASTM methods. Baseline compensation tends to be difficult for columns with high bleed. It is for this reason that capillary columns are preferred even though they have higher resolution than the requirements of ASTM methods. ASTM D6352 calls for a resolution between three and ten using the specified conditions. Typically capillary columns with high flow rates are employed to get the resolution within the specified range of the methods[69].

High temperature ASTM methods[66,67] require the use of a non-polar wall coated open tubular columns and a stationary phase of crosslinked or bonded 100% dimethylpolysiloxane. Simulated distillation techniques require thin films of stationary phase to obtain the resolution within the specified range. Typical film thickness range from 0.09 to 0.15 μm and can elute components equivalent to n-C110. Even though glass, fused silica and stainless steel columns are recommended, metal tubing is preferred as fused silica cannot withstand the high temperatures of the order of 430°C required for analysis[70].

Oven: The oven should be capable of obtaining and maintaining high temperatures up to 450°C and the temperature programmer should reach linear rates up to 20°C/min.

Detector: Both thermal conductivity detectors (TCD) and flame ionization detectors (FID) are used for GC applications. But FIDs are preferred because of their higher sensitivity, reliability and low noise. Further, in SimDis analysis, detector is the end point and hence, a destructive detector can be used[71]. SimDis require the use of a flame ionization detector (FID) with linear range of the order of 10^6.

Injector: Programmable temperature vaporization (PTV) and cool-on-column injections systems are recommended.

Carrier/ Detector Gases: Helium, hydrogen or nitrogen are preferred carrier gases. Hydrogen and air are used for FID. High purity gases should be used along with additional purifiers.

5.2.3 Instrument Specifications

Agilent 6890N series gas chromatograph is used for simulated distillation analysis. It is equipped with an autosampler (Agilent 7683B series) and a flame ionization detector. A 5 µL micro-syringe with a 23 gage stainless steel needle has been used for injection. The instrument comprises of a cool-on-column (COC) injection system. A high temperature non-polar simulated distillation metal column of length 5m and diameter 0.53mm has been employed. The capillary column has a stationary phase composed of 100% bonded dimethylpolysiloxane and the film thickness is 0.09µm. The oven is capable of reaching high temperatures of 450°C and programs up to 35°C/min. The data acquisition can acquire signals in the range of 5-30 Hz. Ultra-high purity Helium is used as a carrier gas along with hydrogen and air for the detector. Along with using high purity gases, additional gas purifiers are set in place to prevent any minute amount of

contamination possible. The gas chromatograph is equipped with electronic pneumatic controls to achieve and maintain the flow rates necessary.

5.2.4 Sample Preparation and Injection

1 gm of sample is transferred to a glass vial and is dissolved in 100ml of solvent. The mixture is shaken or vortexed for a few minutes to ensure proper dissolution. Glass vials with Teflon lined lids are used for this purpose. A concentration of 1:100 m/v is chosen in order to obtain a good signal without overloading the column. Once the samples are prepared, they are placed in the injection tray in the order of sequence.

No sample injection (baseline-blank) is performed initially to make sure there is no residual left on the column. It is followed by a blank run (solvent-injection) and a sample injection. Blank runs are performed after every sample injection to ensure that the column is clean.

5.2.5 Integration

An important assumption with usage of SimDis methods is that all hydrocarbons have the same relative response factors regardless of the composition or retention time[67]. Further, the detector response factor is assumed to be unity. Addition of a mixture of hydrocarbons in the same mass ratios (5% wt/wt) resulted in similar responses solidifying this assumption. Retention time calibration has been detailed in the section 'Qualitative Calibration of GC-FID'.

Some of the terms associated with integration are area slices and sample area. Area slice is the area from the integration of the detector signal within a specific retention time

interval and total sample area is the cumulative area starting from the initial area point to the final point (return of chromatographic detector signal to baseline after sample elution).

Since the chromatographic area of importance is only due to the oil sample, solvent-only injection should be subtracted from the sample chromatogram. Before doing that sample and blank offset have to be performed to negate any possible signal displacement from origin during injection. The area slices during the first second are noted and average, and standard deviation computed. Any of the slices during the first second which are out of one standard deviation are thrown out and the average recomputed. The average computed in this manner is subtracted from the chromatogram. Any negative signals are made zero. Offset is performed on both sample and blank signals and then blank signal is subtracted from the sample signal.

After blank subtraction, total sample area is found by adding all the area slices between initial and final points. Initial area point is the end of solvent elution and final area point is when the signal level reaches the baseline. In order to obtain the % wt off, cumulative area slices spanning over the time of temperature ramp are calculated and divided by the total sample area. This gives the plot of % off versus retention time. Retention time is correlated with atmospheric boiling point using retention time calibration and the procedure is elaborated in section ‘Qualitative Calibration’. Once, the retention time-boiling point relation is obtained, % wt off vs BP can be plotted and boiling point distribution obtained. The code used for integration is provided in Appendix F. It should be noted that % wt off is calculated only till the end of temperature ramp. However, residue plays a role in the total sample area.

5.3 Detector Linear Response Check

A flame ionization detector is one of the widely used detectors for analyzing hydrocarbons in gas chromatographic applications. Elution of carbon compounds out of the column into the hydrogen flame in the FID leads to their combustion and formation of ions. These ions produce a current between the electrodes, which is recorded as the signal. The concentration of ions produced depends on the concentration of compounds in the sample. Compounds eluting at different times produce ion current at different times and several peaks could be recorded[72]. Some of the many advantages of an FID include its high sensitivity, linear response over a wide range (10^7 – 10^8) and rugged construction. Given its high sensitivity, linear response and molar response factors, an FID has been used to detect the concentration of hydrocarbons eluting during the simulated distillation of crude oils.

5.3.1 Discussion

A linear response check has been performed to verify proper working of the FID. As part of evaluating the linear response, samples with different injection volumes were introduced and the signals recorded. Since, the current application involves simulated distillation of heavy crude oils, raw samples of oil #1 crude and oil #2 crude were used for the linear response check. 1 gm of oil crude has been dissolved in 100 ml DCM (dichloromethane) and different sample volumes have been introduced. A range of 0.5-1.5µl has been chosen in order to have good signal without overloading the column.

For change in sample injection volume at the same concentration, a linear response of 1.0949 has been recorded. Since the crude oil samples form unresolved complex

mixtures, integration was performed over the time range of compound elution. It should be noted that the temperature hold time is greater than the compound elution time to make sure there is no residue left in the column.

The temperature ramp follows the one stated in ASTM D6352. An initial temperature of 50°C with an increase of 15°C/min to 400°C (this takes 35 min) and a hold time of 265 min. Sample eluting after 35 min (end of temperature ramp to 400°C) are considered residue. Since this time corresponds to an atmospheric boiling point of 700°C (obtained from qualitative calibration), residue has a boiling point of over 700°C.

Given the highly complex and weathered oils, sample elution significantly happens in the range of 5-35 min and residue elution happens during 35-105 min. For analysis, signal with and without residue have been included. An average signal value has been found that has been used to relate to the injection volume. Also, the average signal has been normalized to 1µL (typical injection volume for analysis). Figure 25 gives the normalized average signal (including the residue area) vs sample injection volume.

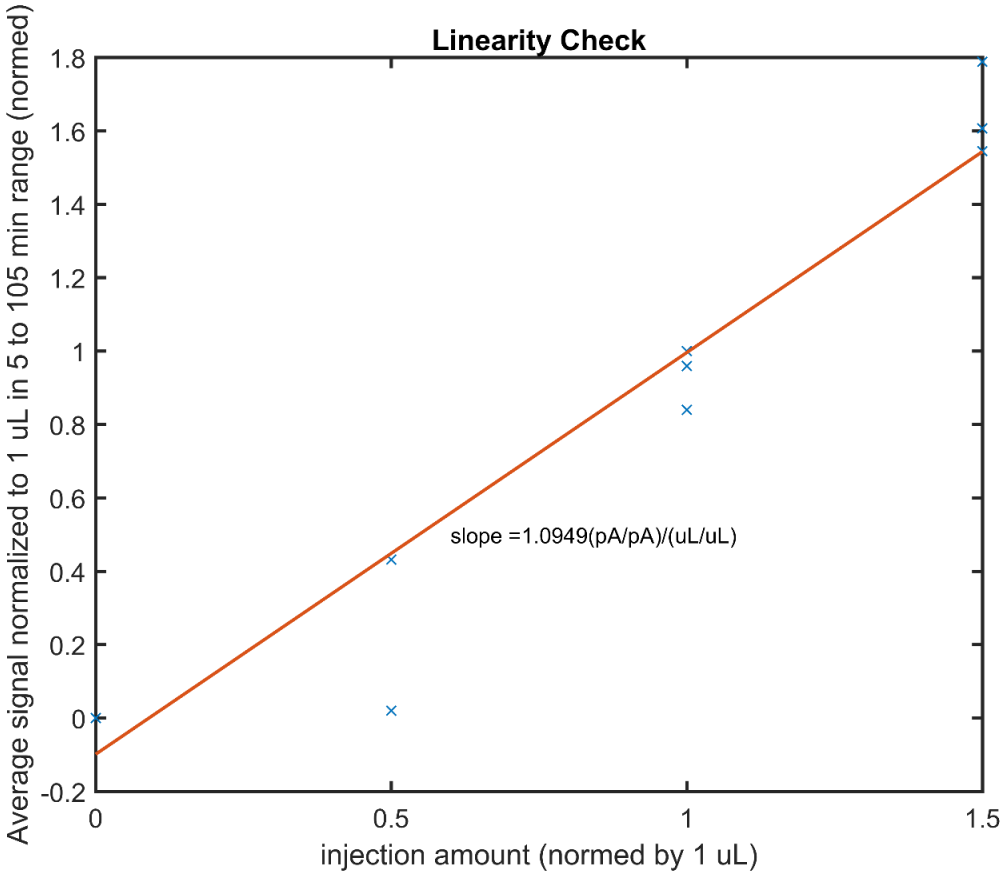

Figure 25: Normalized average signal vs injection volume for oil #1

5.4 Retention Time Calibration of GC-SimDis

Typical representation of simulated distillation signals is a plot of percent off versus atmospheric boiling point (% wt off vs BP). When cumulative area till time t is compared to the total area under the signal the percentage of sample eluting before time t is obtained. This gives % off vs retention time. Details are integration are provided in the section 'Integration'. To obtain % off vs BP, atmospheric boiling point and retention time

should be related. In order to do that qualitative calibration is performed using polywax 655.

Qualitative calibration is performed by using a mixture of known n-alkanes with the SimDis (simulated distillation) method of choice. The SimDis method employed has to be the one used to characterize crude oil samples. As the mixture of n-alkanes in the sample is known; each of the peaks in the chromatograph have been identified and corresponding retention times noted. Also, with the boiling points of each of the n-alkanes in the mixture known, relation between peaks and boiling points is obtained and the retention time (RT) vs boiling point plot generated. A linear fit ($R^2 = 0.9935$) was applied to obtain an equation for RT vs BP.

Different waxes (mixtures of n-alkanes) are available for qualitative calibration. They vary in their n-alkane range. Since oil #1 and oil #2 are heavy, elution at high temperatures is required (400-430°C). A typical calibration mix used for this range is polywax 655 which has a mixture of even n-alkanes from C20 to C100. C90 has an atmospheric boiling point of 700°C and elutes at a GC oven temperature of 400C corresponding to a retention time of 35 min as per the temperature ramp of method ASTM D6352.

Polywax 655 has been used for the calibration in this study. One of the disadvantages of such waxes is their insolubility in most solvents. However, it is known to dissolve in toluene at moderate temperatures. Hence, polywax 655 in toluene has been warmed slightly prior to injection. Figure 26 gives the chromatograph of polywax 655 using ASTM standard D6352. The n-alkane numbers have been marked. The atmospheric

boiling points corresponding to the carbon numbers were plotted against the retention time.

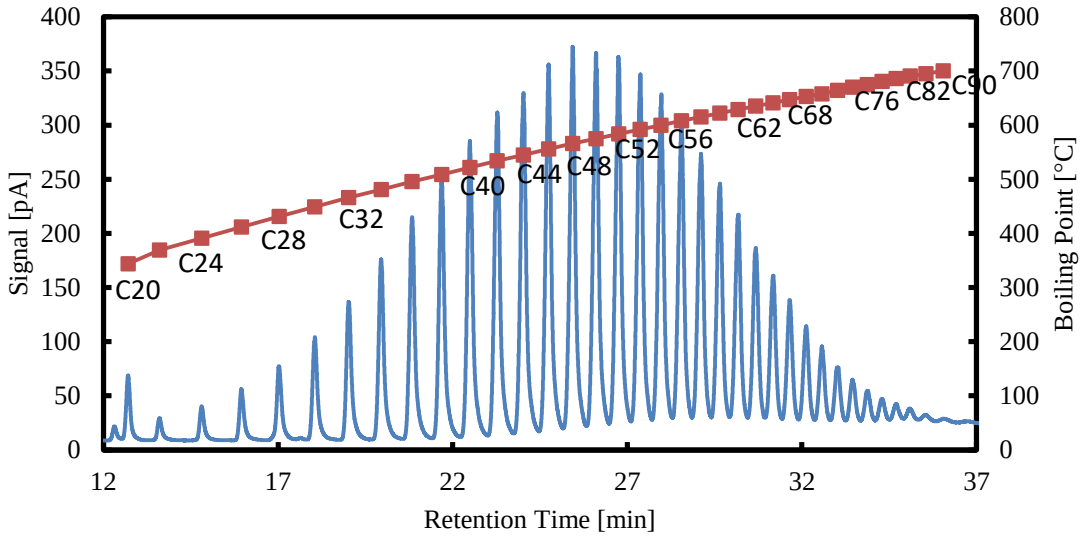

Figure 26: Chromatograph of polywax 655 using method ASTM D6352 along with the calibration curve

However, polywax 655 has a lowest carbon number of C20 and cannot be used to calibrate in the lower carbon range. Hence, a different standard with 20 compounds in the range of nC5-nC44 has been used. Use of this standard helps in calibrating the lower carbon number range. Additionally, it helps to identify the peaks in the polywax chromatogram. Due to the non-uniform mass distribution of compounds in polywax, peak height is lower for few components in the lower and higher carbon range making it slightly difficult to identify them. On the other hand, nC5-nC44 mixture has equal mass

distribution of 5% wt/wt and results is similar peak heights for all the components. Hence, it is easier to identify all the twenty peaks and use the retention time of one of the peaks to identify peaks in the polywax chromatogram. Figure 27 gives the chromatogram for nC5-nC44 mixture and figure 28 gives the boiling point versus retention time plot as well as the carbon number distribution chart using both the hydrocarbon mixtures.

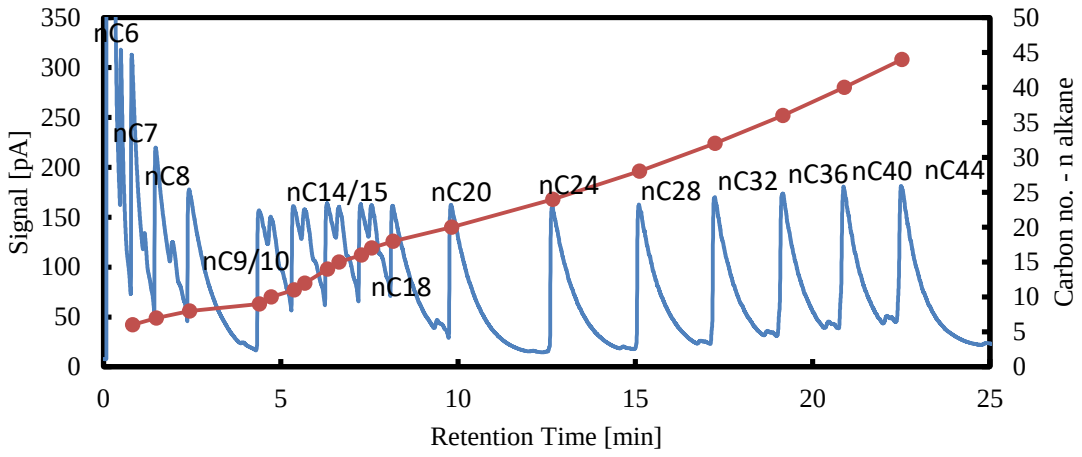

Figure 27: Chromatograph of nC5-nC44 mixture using method ASTM D6352 along with the carbon no. distribution

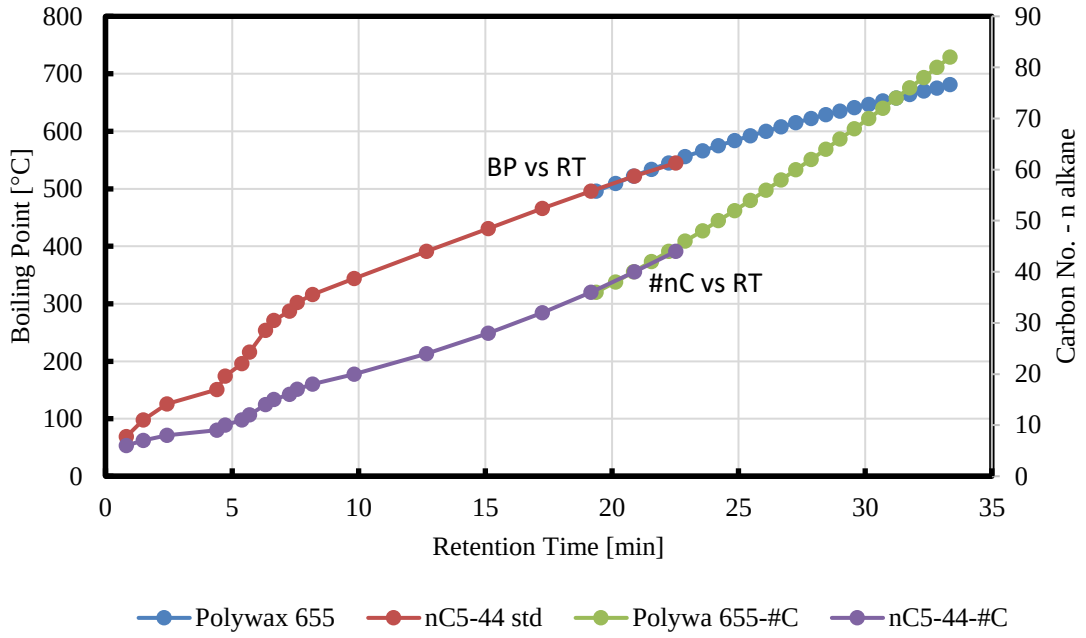

Figure 28: Retention time calibration and carbon number distribution in the range nC5-nC100

5.5 Properties of Raw Crude Oil Samples

Crude oils are comprised of thousands of individual components making it impossible to resolve them using one-dimensional chromatography. It is further complicated when highly weathered crude oils are used as they have a significant amount of heavier fractions which do not elute during the method. Due to the presence of the huge number of compounds, the sample doesn't resolve but forms one large hump termed 'unresolved complex mixture'[74]. Simulated distillation techniques which do not require resolution of individual components are employed to obtain the boiling point distribution[60].

ASTM D6352 was used to analyze the oil samples. The temperature of the column was increased from 50 to 400°C at 10°C/min. Due to the use of a cool-on-column inlet, all the sample is injected on the column. It is necessary to get the sample out of the column so as not to affect the subsequent samples. Hence, hold time at the final temperature is increased to ensure the elution of all the heavier compounds. However, sample eluted during the temperature ramp is the portion recovered and any sample eluting during the hold time is residue. It should also be noted that residue elutes due to the hold time and not temperature ramp.

Typical representations of boiling point distribution of crude oils is plotting the % wt off vs BP as well as comparison of the chromatograms. To obtain % wt off, cumulative area slices are compared with the total sample area for various retention times. Total sample area is the total area under the chromatogram and includes both sample recovered as well as the residue. However, % wt off calculation ends at the end of temperature ramp. For more details on the integration, refer to the section 'Integration'. Using the correlation between retention time and atmospheric boiling points, % off versus boiling point is obtained. Figure 29 illustrates the elution chromatogram and figure 30 gives the % off vs BP plots for both the oils.

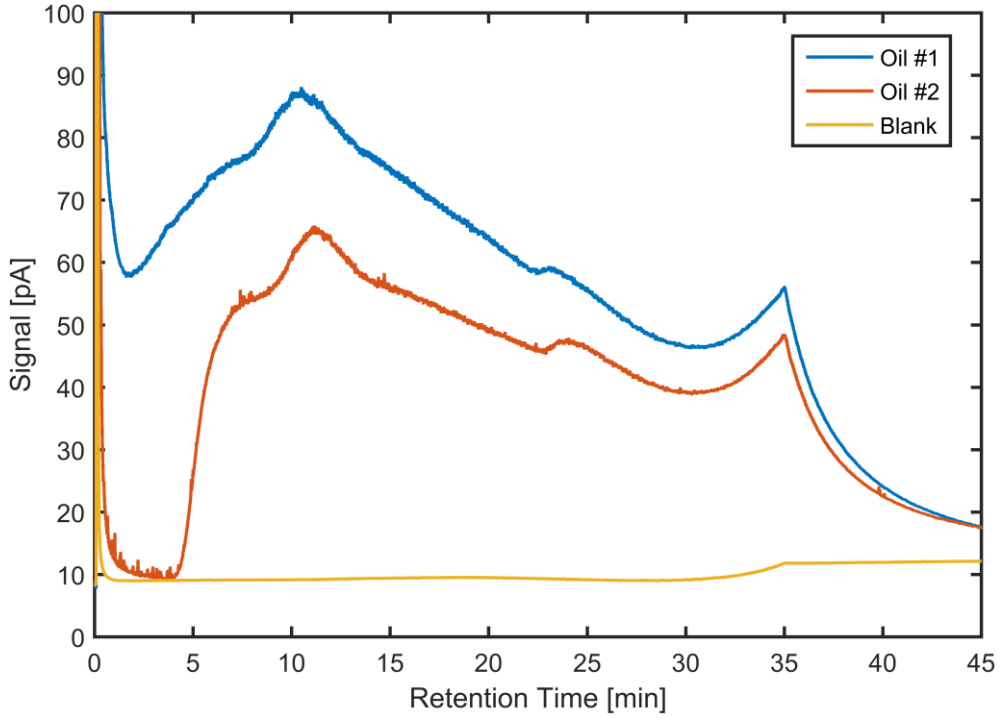

Figure 29: High temperature simulated distillation chromatogram for oil #1 and #2

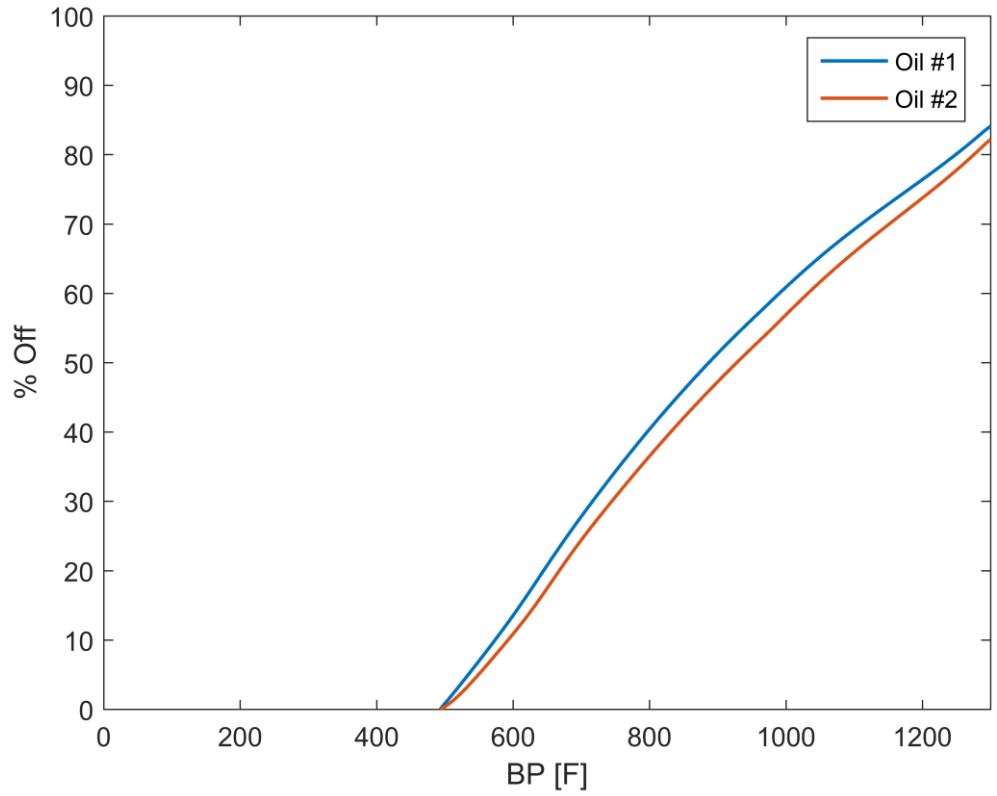

Figure 30: % weight off vs boiling point for oil #1 and #2

As can be observed from figures 29 & 30, oil #1 and oil #2 have a significant amount of sample not eluting before 35 min which corresponds to an atmospheric boiling point of 700°C (1292°F). This portion is called residue which is the non-eluting sample and should not be confused with the industrial definition of residue which is typically at 1000°F. Oil #1 has 15% and oil #2 has 18% of the sample with boiling points greater than 700°C.

At lower range of 600°F (315°C) there is only 15% of oil #1 and 12% of oil #2 has eluted whereas at 800°F (427°C) 40% oil #1 and 37% of oil #2 have eluted. At the

industrial definition of residue (1000°F), only 62% of oil #1 and 58% of oil #2 have eluted implying 38% and 42% residue for oil #1 and oil #2 respectively.

The signal level for oil #2 reaches baseline after solvent elution before rising again after 5 minutes implying very little to no components boiling in that range. Oil #2 is a heavily weathered oil with very little lighter fractions. On the other hand, oil #1 has some lighter fractions. Majority of the sample elutes between 5-25 min corresponding to 250-550°C; 60% of oil #1 and 56% of oil #2.

5.6 Repeatability of SimDis Results

Repeatability of results is essential to any scientific investigation. In order to evaluate the repeatability of heavy crude samples, simulated distillation of both oil #1 and oil #2 has been carried out several times according to method ASTM D6352 with a sample injection of 1 µL. Signal values have been normalized and integrated over the range of sample elution. Figures 31 & 32 plot the normalized integrated signal vs retention time for oil #1 and oil #2 respectively. A difference of 2% for different injections has been noted.

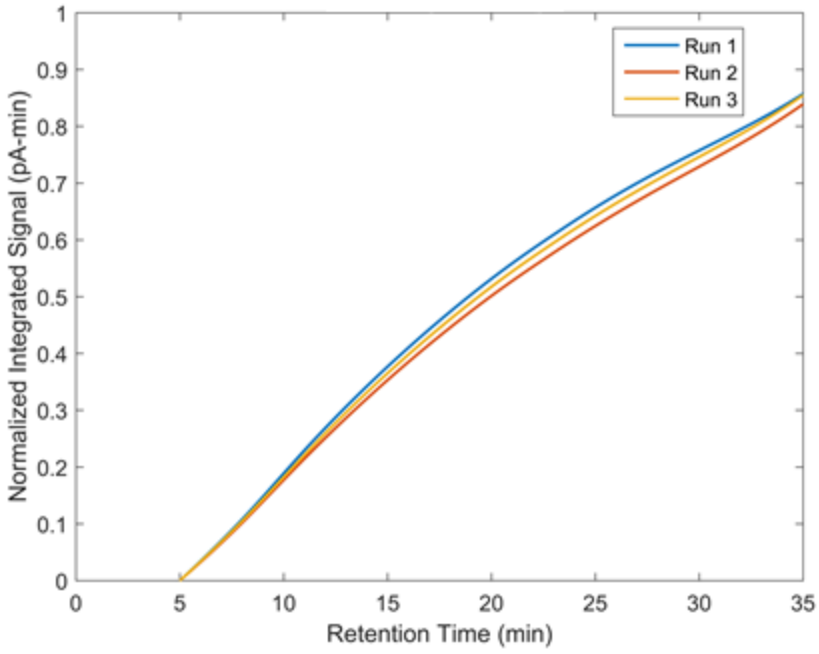

Figure 31: Repeatability check for oil #1 results

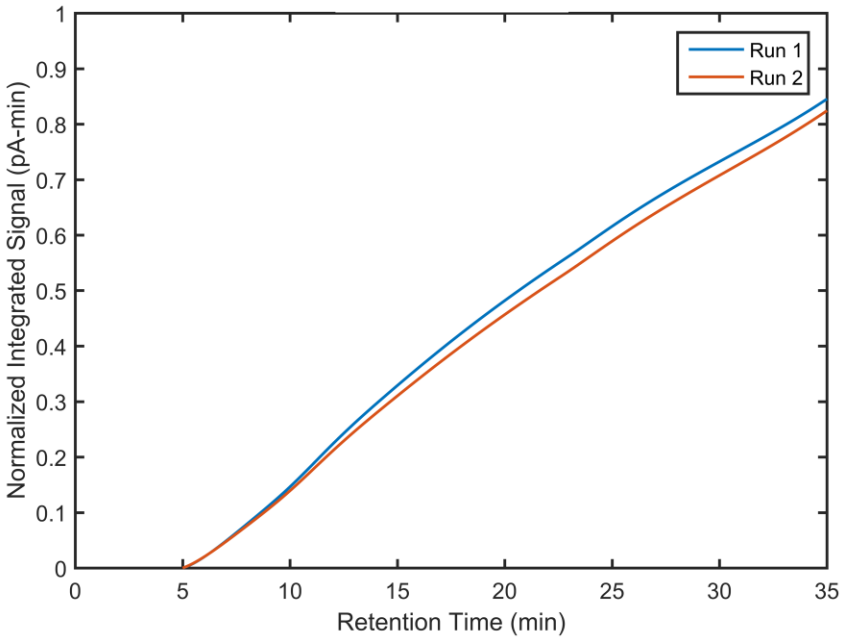

Figure 32: Repeatability check for oil #2 results

Average difference between different runs is 2% with highest individual difference of the order of 6% for oil #2 and 3% for oil #1. Figure 34 give the percentage difference in signals for oil #1 and oil #2. Percentage difference is calculated by comparing the individual signal with the mean of measured values [(Signal-Mean)/Mean].

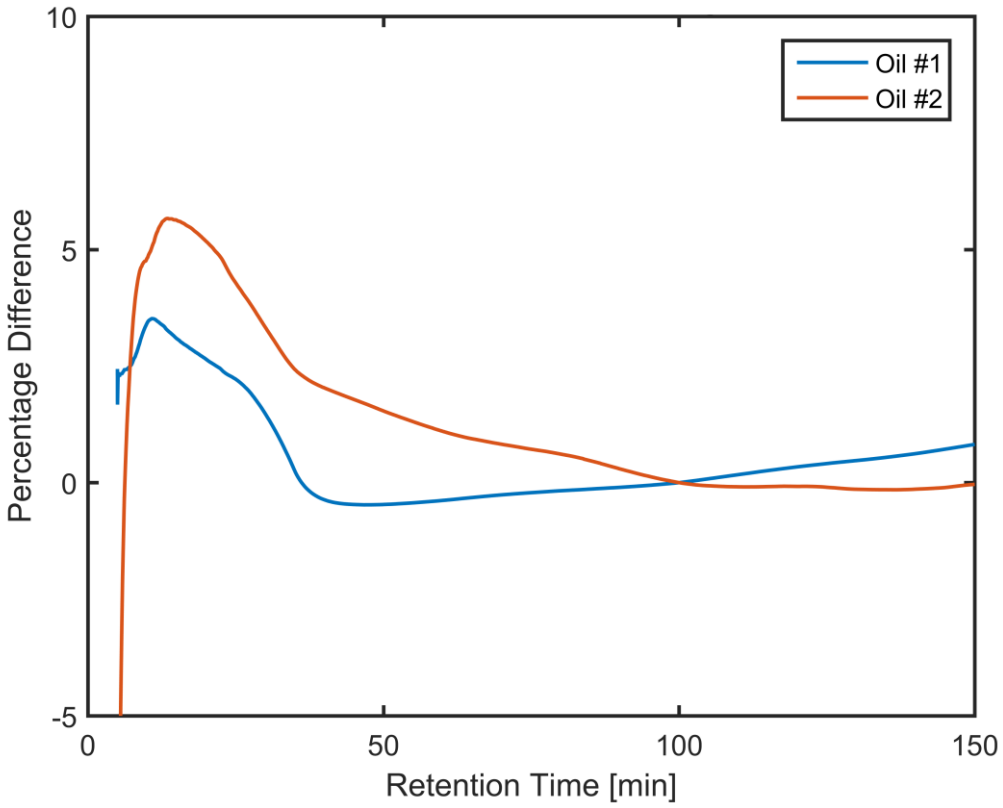

Figure 33: Absolute % difference in the signal for oil #1 and #2 simulated distillation

6. RESULTS AND DISCUSSION

6.1 Product Yields and Mass Balance

Post treatment, most of the crude oil is concentrated in the storage tank (collector; for the purpose of this discussion). However, a moderate portion of liquids are found in the condenser, separation chamber, the channel and at the bottom of the box. All these different liquids are collected and mixed in the same mass ratios to obtain the treated sample. This section talks briefly about the different liquid products and their properties.

Collector liquids make up the majority of treated sample and is the crude oil left in the storage tank post treatment. They average about 85% of the treated crude oil and are typically heavier than the raw sample. For experiments with very low doses, they were similar to raw crude whereas for moderate to high doses, collector liquids exhibited up to an order of magnitude higher viscosity than raw crude oil.

During the course of the experiment, the box is cooler than the channel due to its interaction with cooler ambient atmosphere. As such, it acts as a secondary condenser to help condense the separated liquids which are neither light nor heavy. As these liquids condense, they make their way down to the separation chamber. Chapter 3 details the design where the channel outlet opens into a pipe and the annular portion around the pipe serves as an entrance to the separation chamber.

Separation chamber liquids exhibit physical properties closer to mineral oil or light no.5 fuel oil with typical dynamic viscosity of approximately 30 cP. Being orders of magnitude lighter than the raw crude, these liquids when mixed with the residual oil in the

collector, help reduce the viscosity of treated sample. The mass percentage of separated liquids varied with the severity of experimental conditions, averaging around 4-8% for moderate doses of 250-350 kGy, 11-13% for high doses (<1250 kGy) and 15% for very high doses.

Condenser liquids being the lightest fraction of the product yields have a significant effect on the viscosity reduction. As chapter 4 explains the blending sensitivity, mass ratios of collector liquids have a direct correlation to viscosity reduction. All the gaseous fractions obtained during heating and during the presence of electron beam travel through the box to the condenser chamber where they condense and any incondensable dry gases present would flow out through the exhaust line. Typical mass ratios of condenser liquids are approximately 1-3% for moderate doses and 3-4% for high doses.

Both water-ice and liquid nitrogen have been used to maintain the condenser temperature and they are efficient in condensing very light fractions. Water-ice (water and ice mixture frozen using liquid nitrogen) has been used instead of liquid nitrogen when methane is used as the bubbling gas to avoid condensing methane.

Bottom of the box is the square section at the end of the box which has the opening from the box to the storage tank. The opening has the pipe for the oil flow from the channel to the tank and the annulus area that opens to the separation chamber.

Most of the separated liquids flow to the separation chamber, but some separated liquids which do not drain into the chamber stay in the region. The mass ratio varies depending on the presence of separation chamber as well as the set up.

Post treatment, a small amount of oil is left on the channel as a thin layer that hasn't made its way down to the tank. This mass is typically around 25 gm and makes up to approximately 0.5-1.3%, depending on the processing temperature.

Simulated distillation of the products outlines the chemical (boiling point) differences. Figure 34 elaborate on the chemical differences of various products.

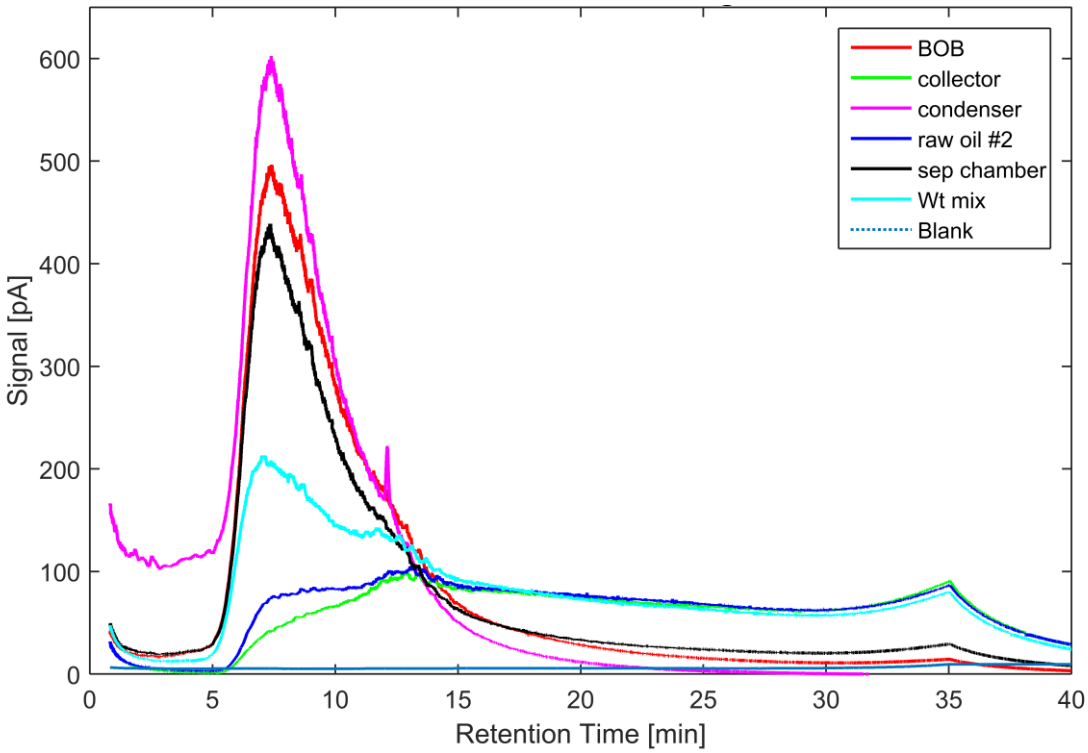

Figure 34: Simulated distillation chromatogram of various products obtained during ebeam processing

As can be observed from figure 34, condenser, bottom of the box (BOB) and separation chamber liquids are lighter than raw crude, collector liquids and treated mixture (Wt mix). Signal levels for all the three fractions; condenser, BOB and separation

chamber reach the baseline halfway through the method. On the other hand, raw crude, collector liquids and treated mixture have significant residue which do not completely elute during the temperature ramp. Temperature ramp extends only till 35 minutes (oven temperature at 35 minutes is 400°C when using ASTM D6352) and the signal beyond 35 minutes is the residual sample eluting. Signals from samples used for this plot were from oil #2-E1 which has 39% viscosity reduction post treatment at 100°C.

It should also be noted that the lighter the sample, the higher the signal level. Condenser liquids being the lightest of all product yields, have a narrow peak and hence, the highest signal level associated. Wt mix which is obtained by mixing all products samples in the obtained mass ratio is 39% physically lighter than the raw crude and similar chemical change can be expected. As the treated sample is lighter than the raw sample, its peak is less broad and signal level is higher than the raw sample. Quantitative chemical change post treatment can be obtained by comparing the % off vs BP plots. Figure 35 gives the % off vs BP plots for oil #2-E1.

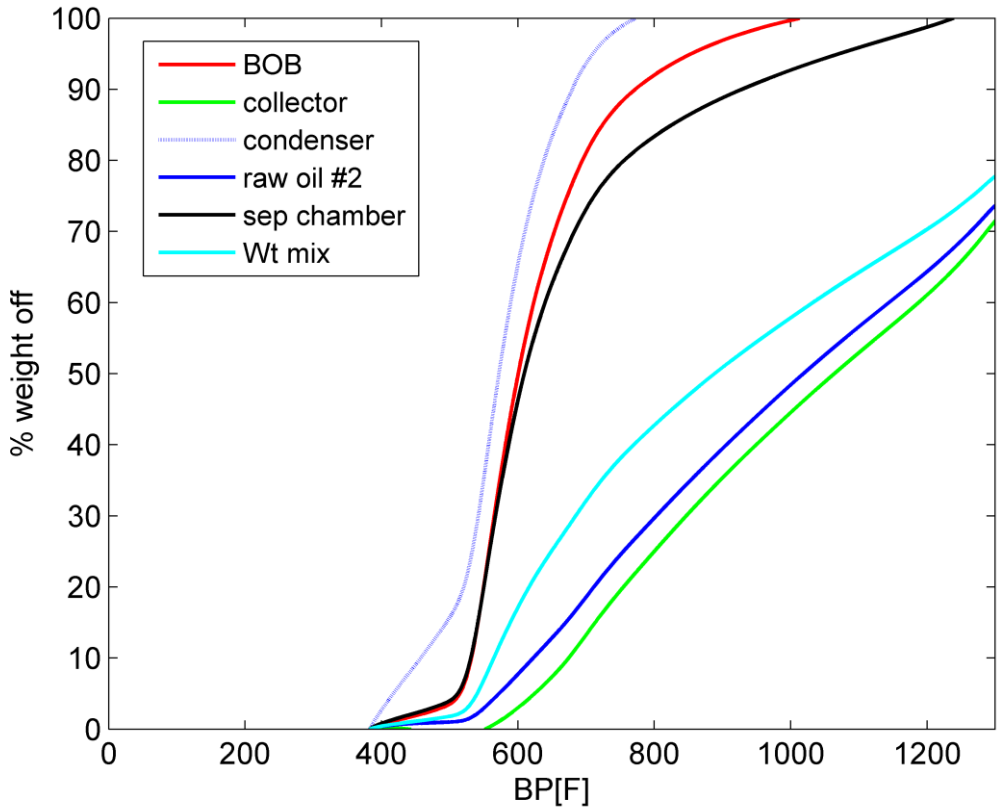

Figure 35: % off vs BP curves for various product yields

Figure 35 gives the % weight off vs atmospheric boiling point for various products which can be used to compare them quantitatively. Sample conversion is obtained by subtracting the sample recovery from the raw sample recovery at the temperature of interest. Similarly, residue conversion is the % of residue converted which is obtained by subtracting the sample recovery from the raw sample recovery and divided by the residue mass of raw sample.

$$Sample\ Conversion = \frac{(m_T)_{treated} - (m_T)_{raw}}{total\ mass\ raw\ sample}$$

$$Residue\ Conversion = \frac{(m_T)_{treated} - (m_T)_{raw}}{total\ residue\ (m_{>T})\ raw\ sample}$$

At an atmospheric pressure and a temperature of 700°C (1292°F), only 79.6% of raw sample is boiled off. On the other hand, for treated sample at 700°C, 83.9% of sample is boiled off implying 4.3% additional lighter fractions in the treated sample over raw sample. At 1000°F (537°C), % raw sample eluted is 53% and for treated sample it is 62.8% indicating 9.8% conversion. It amounts to a residue conversion of 20.95%.

As expected, condenser, separation chamber and bottom of the box samples are lighter and exhibit 100% sample boiling at temperature much lower than 700°C. All of the condenser liquids evaporate before 410°C whereas other lighter fractions evaporate before 537°C.

6.2 Experimental Conditions and Results

23 experiments have been performed so far using both oil #1 and oil #2. Various temperature ranges, shear rates and dose ranges were used. Further, the experimental set up has been modified to achieve better temperature control, incorporate the use of bubbling gases etc. This section talks briefly about the experimental conditions and summarize the results.

A wide range of doses have been used, 5kGy – 1750 kGy. They could be categorized as low dose range (<200 kGy), moderate dose range (200-700 kGy), high dose range (700-1200 kGy) and very high dose range (>1200 kGy). Both low and high shear rates have been employed. High shear rates had a range of 45-180s^{-1} whereas experiments

performed using low shear rates had a range of 20-50s^{-1}. The accelerator and electron energy configurations at the facility allowed little control over the dose rate. A highest dose rate of 20 kGy/s was achieved while few initial experiments were performed at lower dose rate of 15 kGy/s. Some experiments had bubbling gases such as methane or hydrogen pumped into the oil during treatment to help mix and assist the cracking process.

Since, the experiments were aimed at understanding the process and the effect of parameters, wide ranges were employed and did not have good temperature control. So, based on the time of exposure, the temperature increased proportionally during the run. Moreover, different start temperatures were used leading to a wide range of processing temperatures (140-300°C).

Test cart set up modifications were performed to achieve better temperature control. Use of a water jacket around the channel resulted in lower operating temperatures. The jacket uses approximately 3 gallons of water per minute and could achieve a steady operating temperature of ~160°C. Figure 36 list out the various experimental conditions used and the results.

Exp No	Reactor	Flow rate (LPM)	Sep Chamber	Shear rate [1/s]	Dose rate (KGy/s)	Dose (KGy)	Temperature range	Viscosity Reduction (%)	
							50C	100C	150C
Oil #1-E13	Loop	1	No	61-68	19.5	440	257-279°C	-1.31	-0.35	NA
Oil #1-E12	Loop	2	No	15-27	19.5	757	140-156°C	-0.71	-1.79	NA
Oil #1-E11	Loop	2	Yes	25-126	21.64	648	140-280°C	37.56	24.63	NA
Oil #1-E10	Loop	2	Yes	21-130	20	1308	140-280°C	72.4	49.8	NA
Oil #1-E9	Loop	2	Yes	30-60	19	198	150-215°C	16.27	14.52	NA
Oil #1-E8	Loop	2	No	15-134	14.75	691	120-260°C	2.36	-0.53	NA
Oil #1-E7	Loop	2	Yes	18-155	17.68	605	130-300°C	17.09	9.19	NA
Oil #1-E6	Loop	2	Yes	48.6-134	18.37	270	177-278°C	7.49	2.04	NA
Oil #1-E5	Loop	2	Yes	48-181	17	348.5	175-310°C	20.73	12.58	NA
Oil #1-E4	Loop	2	No	90.3-98	15	525	178-225°C	-21.9	-5.49	NA
Oil #1-E3	Semi-batch	1	No	11.2	15	36.8	200°C	6.18	2.06	NA
Oil #1-E2	Semi-batch	2	No	73	18.2	24.65	200°C	0.26	-4.88	NA
Oil #1-E1	Semi-batch	1	No	27	6.9	4.91	160°C	0.06	-1.28	NA
Oil #2-E8	Loop	1.5	No	20-50	20	757	200-250°C	NA	16	10
Oil #2-E7	Loop	2	Yes	19-89	20	1774	200-290°C	NA	27.25	15.7
Oil #2-E6	Loop	2	Yes	16-90	20	910	200-298°C	NA	16.7	10.5
Oil #2-E5	Loop	2	Yes	16-90	20	1342	172-294°C	NA	-27	-22.5
Oil #2-E4	Loop	2	Yes	16-90	20	1200	174-295°C	NA	35.8	21.8
Oil #2-E3	Loop	2	Yes	16-90	20	1200	174-287°C	NA	-3.65	-0.23
Oil #2-E2	Loop	2	Yes	15-85	19.5	1200	180-300°C	87.42	69.63	NA
Oil #2-E1	Loop	2	Yes	28-137	19.5	562.8	180-300°C	56.82	38.97	NA

Figure 36: Experimental conditions and results

6.3 Operating Parameters

A wide range of operating conditions have been employed.

Dose: Experiments were performed with absorbed dose in the range of 5-1750 kGy. Figures 37 & 38 give the viscosity reduction achieved (measured at 100°C) versus absorbed dose for oil #1 and oil #2 respectively. Successful runs are experiments which were executed as planned whereas in the 'not as planned runs' some uncontrolled parameter change took place. Not as planned runs do not imply unsuccessful runs; it is merely a different value of parameter than was originally intended and are very valuable data points.

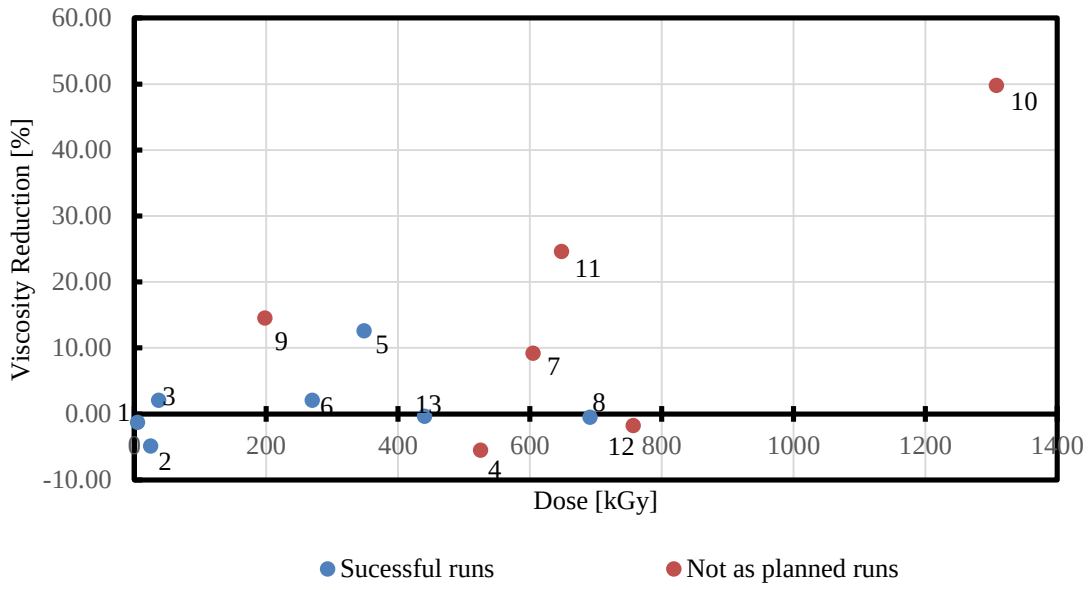

Figure 37: Viscosity reduction vs dose for oil #1. Not as planned runs have low parameter control of bad mass balance

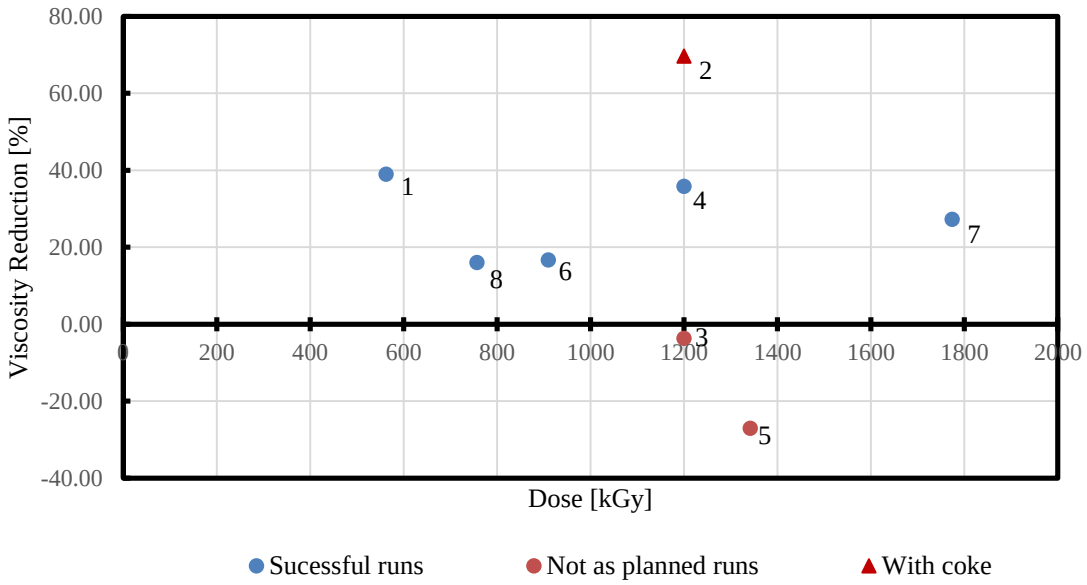

Figure 38: Viscosity reduction vs dose for oil #2. Not as planned runs have some low parameter control or bad mass balance

Due to the huge set of parameters involved, dose dependence cannot be easily isolated. However, an effort has been made to understand the effect of absorbed dose on viscosity reduction. For both oil #1 and oil #2 there is a strong non-linear effect of dose, i.e. no apparent increase in viscosity reduction with an increase in dose. Oil #2 has 5 successful runs at different doses; 560, 757, 910, 1200 and 1774 kGy and there was a non-linear dose dependence. For all the five successful experiments dose rate is the same and temperature ranges are similar. If other minor changes in the experimental set up are ignored, the dose dependence curve has maximums associated. Further optimization is required to understand the dose for maximum conversion at the allowed dose rates and temperatures.

Moreover, 3 experiments performed with oil #2 at same dose reveal the huge role played by some smaller uncontrolled parameters. Oil #2 E2, E3 and E4 had an absorbed dose of 1200 kGy but very different viscosities post treatment. E2 had some oil pooled under the channel in the beam region resulting in it's over exposure and turning to coke. Lighter fractions from the oil could have been captured in the condenser and separation chamber leading to increased mass ratios of lighter fractions and thereby increased viscosity reduction to 70% (at 100°C).

Oil #2 E4 has a leak at the funnel that guides the oil from the channel to the tank leading to only a portion of oil being treated by the electron beam. This resulted in an uneven distribution of dose in the oil. E3 has a broken gasket at the sanitary fitting of separation chamber and some light liquids were lost due to this. These uncontrolled events could have affected the experiment in a major way and led to a big difference in the results.

For E5 of oil #2 which has 27% viscosity increase post treatment, Argon was used as the bubbling gas instead of Helium. It could be possible that the bigger Argon molecules could have contributed to the quenching reactions of radicals.

Oil #1 has been used for more experiments and has more data points to compare. From viscosity reduction versus dose plot, it can be observed that moderate to high doses of the order of 200-750 kGy had good viscosity reduction. 9 experiments were performed with dose in the above mentioned range. Of the 9, 4 resulted in increased viscosity, whereas the other 5 had a positive viscosity reduction. Experimental similarities of the 4 negative result runs (E4, 8, 12, 13) is the lack of separation chamber. It is highly possible that separation chamber liquids had a big impact on reducing the viscosity. During the

experiment oil #1-E4, the irradiation was not provided continuously but in three different time slots. At these conditions, the highly reactive oil with no irradiation could have condensed to form bigger structures leading to a viscosity increase.

The experiment oil #1-E10 with an absorbed dose of 1300 kGy had the highest viscosity reduction of about 50% but had bad mass balance with only 86% accounted mass. There was little to no change in viscosity at low dose implying the need for higher doses provided other parameters stay the same.

Experiments performed with oil #2 has successful runs in the range of moderate to high doses providing us with the dose dependent data in that region. Further experiments in the low dose region should be performed to obtain a comprehensive knowledge of dose dependence.

Dose rate: Studies conducted by Zaikin and Zaikina[8,24,28] emphasize the importance of using high dose rates during the processing of bitumen and extra-heavy crude. However, due to the limitations at the ebeam facility, only a maximum of 20 kGy/s could be reached. Most of the experiments were conducted at a dose rate of 20 kGy/s though few initial experiments were performed at a slightly lower dose rate of 15 kGy/s. Hence, the effect of dose rate could not be studied in this experiment, but experiments have been performed at a moderate dose rate of 20 kGy/s.

Temperature: Electron beam adds energy to the oil during the course of the run. It is as high as 7-8°C/min leading to a significant temperature increase during the course of the run. For a 20 min run, there is almost 140°C increase in temperature making it difficult to interpret the effect of temperature. 7 of the oil #1 experiments had a starting temperature

in the range of 130-140°C and 3 runs had a starting temperature of 170-180°C. The initial semi-batch experiments were performed at 200°C and with lower dose and time of exposure, the temperature was constant. As several studies claim, increase of temperature leads to better cracking conditions with other parameters held same. However, even small changes in other parameters and some uncontrolled events seemed to affect the results and it is challenging to understand the effect of temperature. Both viscosity reduction and viscosity increase were observed in both sets of experiments with different starting temperatures.

Experiments conducted with oil #2 have two different starting temperatures; 180°C and 200°C. At high doses with longer residence time energy addition due to the ebeam resulted in the end temperatures of ~300°C. Apart from E3 and E5, all other experiments with oil #2 had positive viscosity reduction associated. Figures 39 & 40 plot the viscosity reduction achieved versus the average temperature.

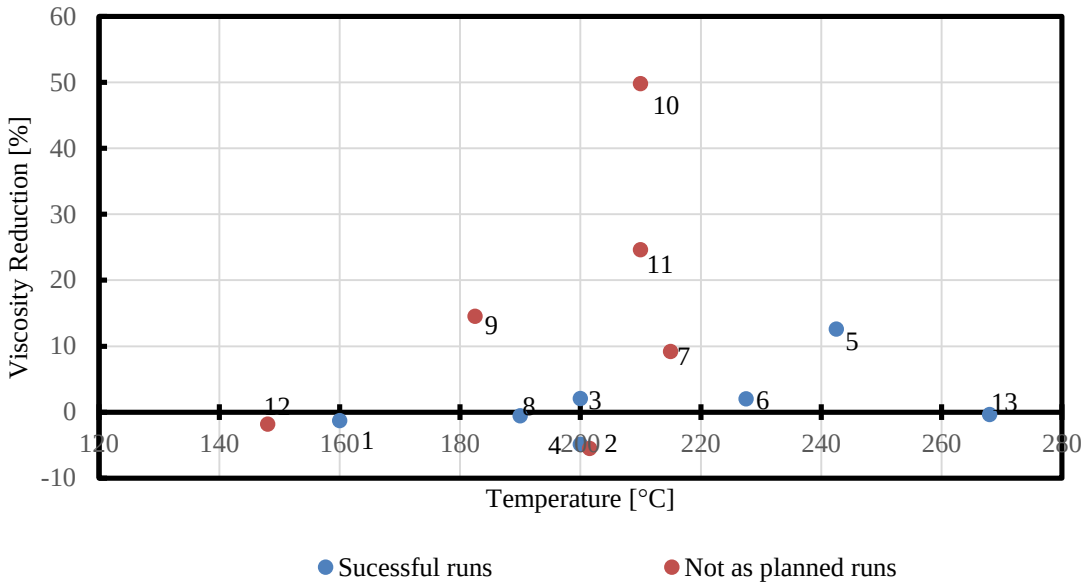

Figure 39: Viscosity reduction vs average temperature for oil #1

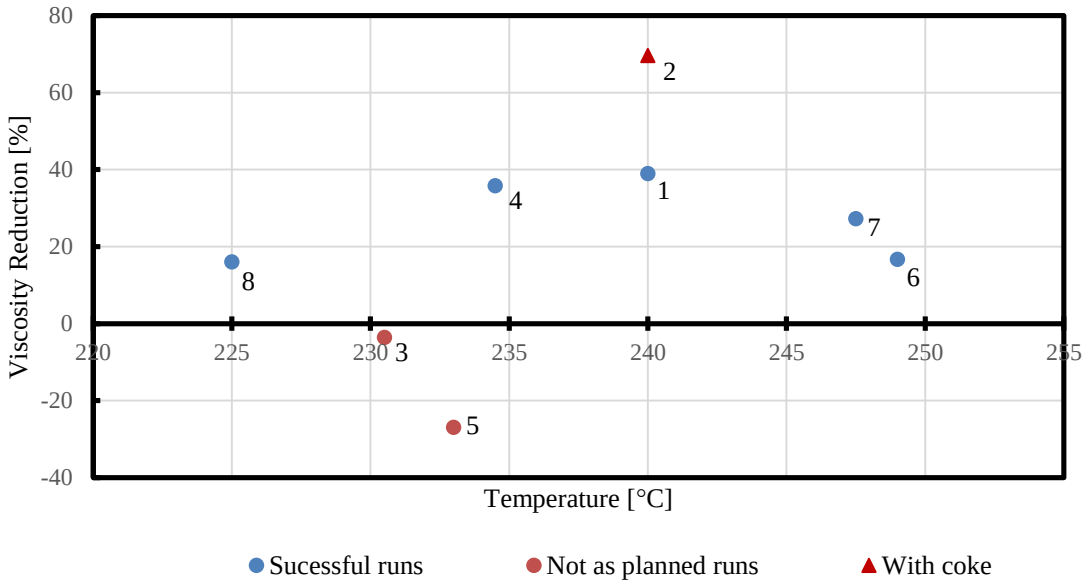

Figure 40: Viscosity reduction vs average temperature for oil #2

As can be observed from figure 39, temperature and dose are not the sole indicators of good results. For example, oil #1-E4, 12, 13 have high temperatures and absorbed dose, but due to some other uncontrolled parameters, the viscosity reduction achieved was very low. Hence, it is important to optimize all the parameters and execute the experiments with control.

To properly isolate the effect of operating temperature, experiments should be conducted at steady temperature. Currently, system modifications are underway to achieve better temperature control. Water cooling around the tank was not very effective with an operable steady temperature of 265°C. A water jacket around the channel provided a steady temperature of 160°C. Further experiments would be aimed at steady operating temperatures.

Electron energy: Electron energies of 10 MeV have been employed for this study. Typical energy loss for electrons in water is about 2 MeV/cm[75]. With the crude oil densities similar to water, the electron energy loss in oil could be estimated to be similar. The system is designed such that the maximum depth of oil is less than an inch at 2.22cm, well within the penetration depth of 10 MeV electrons.

Other electron energies have not been tested, but lower electron energies which are typically associated with high power accelerators require the use of thin films to ensure the thickness is smaller than the penetration depth of electrons.

Shear rate: An important flow parameter to consider during electron beam treatment of heavy crude oils with significant asphaltene content is the shear rate. Researchers have talked about the synergistic affect shear could play during the treatment

by decomposing the heavy thixotropic structures[24]. If shear helps in breaking down or unraveling the complex structures of bitumen during the presence of the ebeam, it could lead to more reactive sites and increased cracking. Zaikin et al[24,28] claim that this effect could even result in an order of magnitude in cracking rate.

However, rheological studies performed in the lab as well as experiments with ebeam fail to reveal the thixotropic properties of the crude or the synergistic effect of shear with ebeam irradiation. Thixotropy studies have been performed on both oil #1 and oil #2 at shear rates spanning over a range of 0.1-750 s^{-1} showed little or no area between the up and down curve implying very less thixotropic property. Even at low temperatures, when the fluid is non-newtonian, there was no apparent structural change due to shear.

This led to further investigation at high temperatures and high shear rates. Shear rates up to 8900 s^{-1} were employed in the temperature ranges of 150-250°C to look for structural changes. At such high shear rates, it was observed that oil was thrown out from between the plates. It is highly possible that at shear rates termed critical shear rate, fluid instabilities arise causing the oil to flow out. Nonetheless, the critical shear rate observed was too high (4000-5000 s^{-1}) to be of any practical importance. Initial experiments had channel set up adjusted to achieve moderate to high shear rates in the range of 15-180 s^{-1}. However, there was no indication of a synergistic effect of shear with the ebeam.

Liquid Yields: Mass ratios of lighter yields have a significant impact on the final result. As detailed in chapter 4 and the first section of this chapter, the higher the lighter yield mass ratios, the higher the viscosity reduction. Figures 41 & 42 plot condenser and separation chamber yields versus viscosity reduction for oil #1 and #2 respectively.

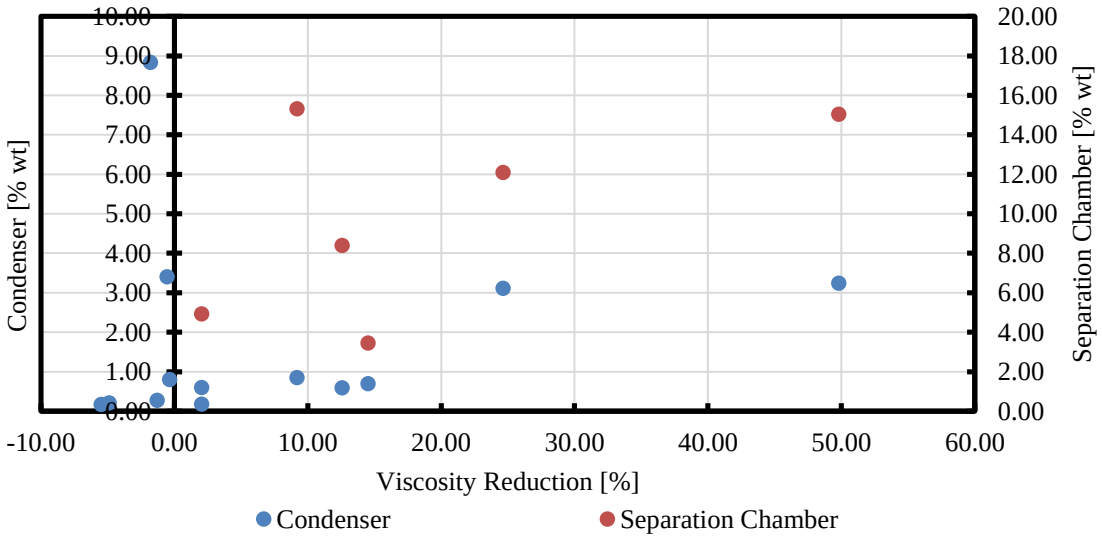

Figure 41: % light fractions vs viscosity reduction for oil #1

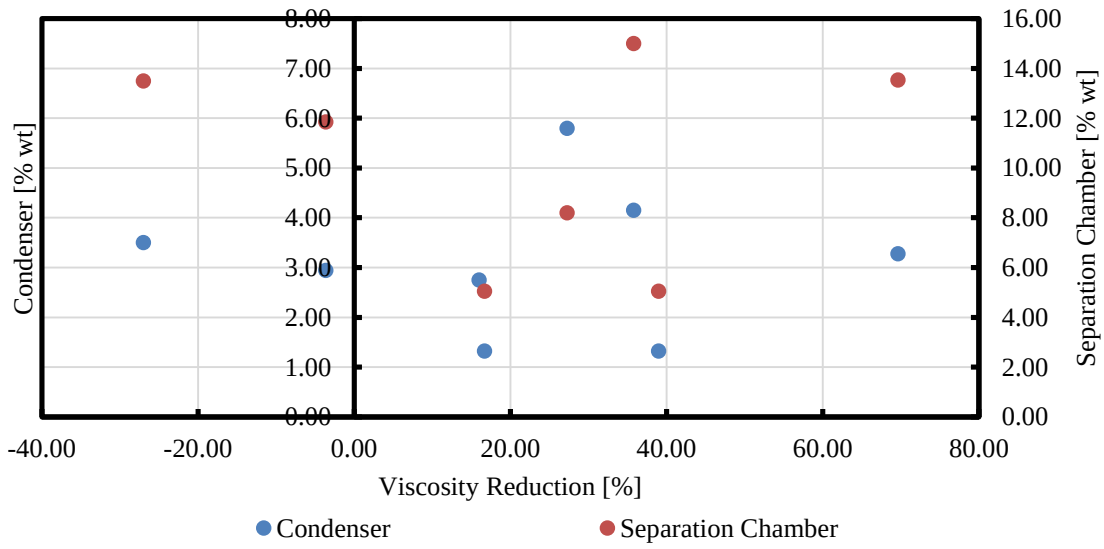

Figure 42: % light fractions vs viscosity reduction for oil #2

As explained previously in this section, some uncontrolled parameters affected few experiments adversely. But the common trend in the plots 65 & 66 is the increase in viscosity reduction with an increase in lighter fractions, more so with separation chamber liquids.

Presence of separation chamber leads to capture of ~5-15% lighter fluids which would help reduce the viscosity of treated sample further. Experiments conducted with and without chamber, oil #1 E7 and E8 had similar collector oil properties, but the presence of separation chamber in E7 led to increased viscosity reduction. Further, separated liquids were captured in almost all experiments with positive viscosity reduction implying that it might be advantageous to capture the liquids over letting them mix with the heavy oil during treatment.

Bubbling gas: Various gases were bubbled into the oil through tiny holes on the channel. The objective was to provide excess radicals (hydrogen donors) as well as mixing. The flow rates were adjusted to maintain laminar flow. Different gases were used for this purpose. Use of hydrogen provides hydrogen donors while use of methane provides excess methyl radicals for reactions. Use of inert gases such as helium provides only mixing effects with no radical addition. Though experiments have been conducted with various bubbling gases their effect could not be properly isolated due to change in other parameters involved.

6.4 Time Stability

Apart from viscosity reduction, time stability of treated compounds is of paramount importance. Presence of reactive compounds in the treated sample such as olefins and/or reactive residue might lead to continuing reactions post processing and formation of gums etc. which are undesirable. Several researchers[6,32] observed increased viscosity of radiation treated samples over time. Hence, it is important to monitor the viscosity of treated samples over time and observe for any increase. In case of an observed increase, reasons should be isolated and necessary modifications should be incorporated into the operational parameters. This section details the viscosity of treated samples over time.

One of the reasons for viscosity increase over time is the loss of lighter fractions. This is relevant for heavy crude oils with reasonable amount of lighter fractions. Raw samples of oil #1 and oil #2 have been monitored for viscosity change over time post decanting from the barrel. Oil #2 being severely weathered and almost no lighter fractions did not exhibit any viscosity increase over time. Oil #1 however, did show some viscosity increase over time; change from 9350 cP to 9960 cP at 50°C (6.5% increase). This could be attributed to the loss of lighter fractions as oil #1 has lighter fractions. The change in viscosity for oil #1 was observed in case of improper container sealing; in the case of the jar being opened frequently to obtain sample. On the other hand, in a perfectly sealed container, the viscosity change is less than 2%.

Several treated samples were monitored for viscosity increase over time. Oil #1 treated samples have shown an average 10% increased viscosity over a period of 8 weeks.

Figures 43 & 44 provide the time stability plots for oil #2 and oil #1 respectively. Detailed measurements can be found in Appendix C.4.

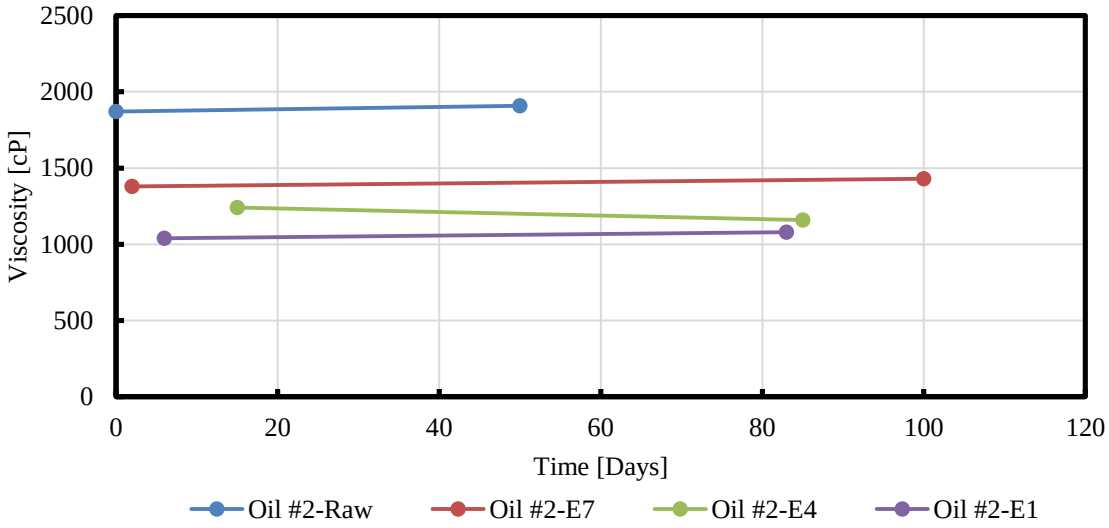

Figure 43: Oil #2 product time stability

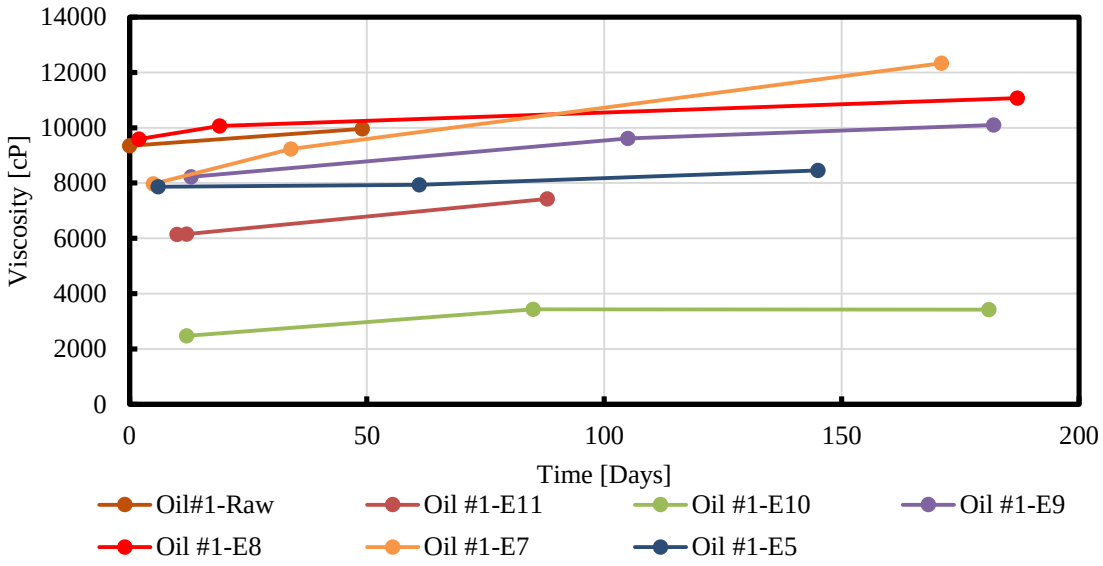

Figure 44: Oil #1 product time stability

There are several reasons that could explain this increased viscosity:

1. Loss of lighter fractions
2. Reactive residue (compounds heavier than C_{100})
3. Unstable compounds (compounds lighter than C_{100})

Increased viscosity in the raw sample could be attributed to the loss of lighter fractions. However, that alone might not be the reason for the time instability of the treated samples. As Zaikin et al[32] point out, present of high asphalt-pitch sediments in the treated collector liquids might still be reactive post experiment and could lead to 'absorbing reactions' i.e. addition of lighter fractions on to reactive heavy molecules. Further, the presence of lighter unstable compounds such as olefins etc. could lead to formation of gums or heavy components over time. It is highly possible that the time instability observed for oil #1 samples could be a combination of the one or more of the three factors.

For example presence of reactive residue as well as loss of light fractions together could explain the higher viscosity increase in the treated sample over raw crude.

However, the steady viscosity of oil #2 with time downplays the effect of loss of light fractions. Treated oil #2 sample has significant light fractions (obtained from condenser and separation chamber) with little to no change in viscosity over time. Further, with the differences in feedstock, the product composition could be highly different implying the possibility of reactive residue and/or unstable compounds in oil #1 samples and not in oil #2 samples.

6.5 Significant Result

Due to the uncertainties associated with instruments, mass balance and other estimates, the error bars for the results tend to be high. Hence, an evaluation of the same is necessary to determine good results i.e. results significantly outside the error bars. Major uncertainties arise from the mass balance and rheometer. The instrument error associated with the rheometer is approximately 5% due to sample insertion etc. by the personnel. However, error induced by mass balance is much higher.

Results of blending tests have been used for this analysis. For the purpose of this evaluation, it has been assumed that loss of yields would have the same numerical change as gain of yields. Change in viscosity has been evaluated with respect to raw sample.

$$\%\, reduction\ in\ viscosity\ = \frac{(raw\ sample\ viscosity - treated\ sample\ viscosity)}{raw\ sample\ viscosity}$$

For the case of mass loss, i.e. accounted mass <100% of sample put in, the imbalance could be due to loss of lighter fractions or heavy residue; though the former is more likely. Considering a case of 95% mass balance which resulted in x% viscosity change post treatment. Blending results can be used to isolate the effect of loss of crude. If the mass lost is entirely condensates, the actual viscosity change is x+73.4% post treatment (5% lighter fractions result in 73.4% reduction in viscosity). If the mass lost is entirely heavy residue, this change is x-8.97%. Hence, to be certain about cracking, x-8.97% should be greater than zero implying the need for x >8.97%. Similarly, to observe polymerizing x+73.4% should be less than zero indicating polymerization for x<-73.4%.

It is not to say that cracking did not occur if the viscosity reduction is the above mentioned range (>8.97%). However, due to the uncertainties involved with the 5% mass loss, it cannot be concluded with certainty that cracking reactions significantly occurred. In fact, a combination of cracking reactions, polymerization as well as loss or gain of fluid leads to the end result. In order to ascertain the occurrence of significant cracking reactions, the final result should be above the error range. Similarly, to conclude substantial polymerization, the final result should be below the error range.

However, due to the unavailability of light fractions for experiments on oil #2, Wallace-Henry method has been used to come up with the lower bound for cracking and upper bound for polymerization. In the Wallace-Henry method for oil #2, a viscosity of 40 cP was used for separation chamber liquids, 3 cP for lighter fractions and $50*10^6$ cP for heavy residue. These values are based on a combination of direct measurements of the separated components for a particular experiment and an analysis of general trends in these

values from many experiments. For oil #1, they are direct measurements as elaborated in chapter 4. Figures 45 & 46 provide the plots to identify significant results based on mass balance for oil #1 and oil 2 respectively.

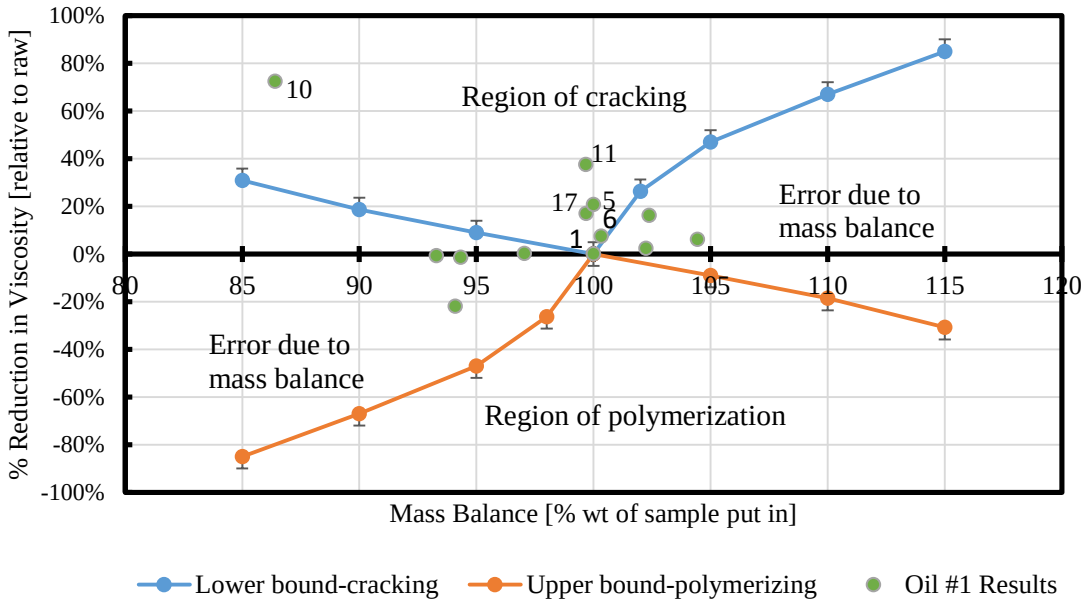

Figure 45: Plot to ascertain the significance of results based on mass balance for oil #1

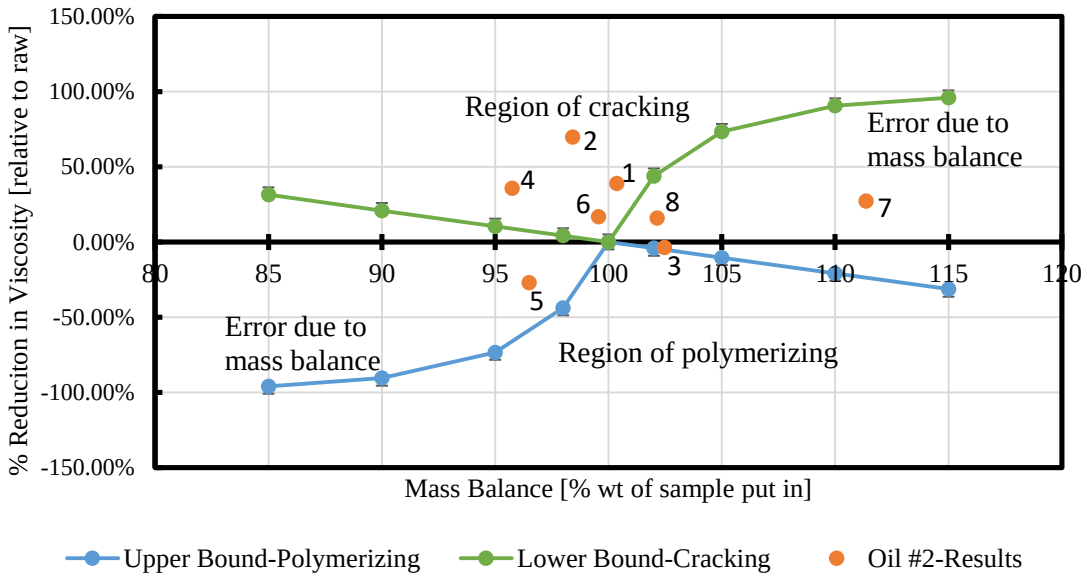

Figure 46: Plot to ascertain the significance of results based on mass balance for oil #2

Figures 45 & 46 lay out the region of cracking, polymerization as well as the region of significant uncertainty due to mass balance. A result is good and significant only if it lies in the region of cracking. A weighted averaged effect of condensates and separation chamber are considered during the analysis. Further, error bars have been used to indicate the rheometer uncertainty.

7. SUMMARY, CONCLUSIONS, AND FUTURE WORK

7.1 Summary and Conclusions

The broad objective of the research project is to achieve low temperature heavy crude oil cracking using electron beam irradiation. Several operating parameters have been identified and system modifications were performed to achieve the same. The goal of this thesis is to accurately characterize crude oil samples pre and post treatment.

Rheological studies and simulated distillation of raw crude oil samples reveal the heavy viscous nature of oil #1 and oil #2. Both oil #1 and oil #2 have extremely high viscosities at ambient temperature; 33400cP for oil #1 and 4110000cP for oil #2 at 40°C. Viscosity dependence on shear rate can be ignored at moderate temperatures of 50°C and 80°C for oil #1 and oil #2 respectively. Further, no thixotropic effects were observed implying Newtonian behavior beyond 50°C and 80°C for oil #1 and oil #2 respectively. Simulated distillation curves indicate that only 86.55% of oil #1 and 79.58% and oil #2 samples have boiling points lower than 700°C (1292°F). At 1000°F (537°C), the numbers amount to 64.2% and 53% revealing oil residues of 35.8% and 47% for oil #1 and oil #2 respectively.

Various viscosity temperature models were examined and modified to arrive at a better correlation for oil #1 and oil #2. These models are used to predict the viscosity of crude oils at varying temperature during the experiment. Relations on viscosity of hydrocarbon mixtures were also looked at and validated with experiments in order to arrive at a viscosity blending equation. The viscosity of blends are important as they lay

out the effect of addition or loss of different product fractions and help examine the discrepancies in the mass balance. Lastly, uncertainties in mass balance and instruments have been evaluated to calculate the minimum value beyond which a result is considered significant.

Comparison of physical and chemical properties of crude oils pre and post treatment reveal some interesting aspects. They are summarized as follows.

1. The higher the yields of lighter fractions, the better the result. Experimental results as well as various blending studies show the higher sensitivity of mixtures to light compounds. Hence, experiments should be designed with increased capacity to capture light fractions (condenser, separation chamber etc.)

2. Prior work by other researchers and some initial studies helped identify temperature, dose and dose rate to be primary operating parameters. Further, shear rate and bubbling gases are also considered to be important.

3. Effect of dose is observed to be non-linear. Experiments performed on oil #1 at low doses showed little to no change post treatment. Use of moderate to high doses did not reveal any particular trend. Oil #2 results show the presence of maximums in the dose dependent result curve. At a particular temperature and dose rate, these maximums should be identified to achieve better results. However, no data in the low dose region is available for oil #2. Experiments should be conducted at low doses to obtain a comprehensive understanding of the effect of dose. Dose is complexly related to competing reactions and hence hard to isolate. Optimized parametric studies are necessary to evaluate and identify the range of absorbed dose which results in the highest amount of yields.

4. Initial experiments were tested at a wide range of temperatures with no proper control making it difficult to isolate its effect. Experiments at a steady operating temperature are necessary to arrive at a conclusion on the effect of temperature. Due to the constraints at the ebeam facility, dose rates were maintained at 20 kGy/s.

5. Hysteresis curves and other rheological studies as well as high shear experiments indicate that shear has little to no effect on the hydrocarbon structure of both oil #1 and oil #2. Hence, shear rate can be eliminated as an operating parameter.

6. Bubbling gases serve different purposes. Inert gases such as helium help mix the oil during treatment so that there is uniform radical concentration over the depth. Use of hydrogen containing gases such as methane, hydrogen etc. serve as hydrogen donors along with providing mixing effect. Studies could not conclude the effect of these gases. Results do not indicate any difference when using helium or methane. However, further examination is required before arriving at a conclusion.

7. Some of the good results for oil #2 point to a 39% reduction in viscosity and 20.95% residue conversion. Similarly, for oil #1, 50% viscosity reduction and 16.8% residue conversion were observed.

8. Blending and uncertainty analysis indicate the requirement for a good mass balance. Mass balance should be closer to 100%. At 95% mass balance, the minimum value beyond which a result is considered significant is 14%. At 105% mass balance, this no. is as high as 52% whereas it is only 5% at 100% mass balance.

7.2 Future Work

Temperature, dose and dose rate being the most important parameters, should be studied well. Temperature and dose rate are known to have a linear effect with yields. However, since absorbed dose does not have a linear effect, it should be evaluated at optimum dose rates and temperatures i.e. at the maximum temperature and dose rate that economics and the accelerators allow.

High dose rate experiments would be carried out to validate the increase in yields with an increase in dose rates. Dose rates up to 100 kGy/s (as pointed out by some researchers[8,24]) would be used for the same. System modifications are underway to achieve steady operating temperature. Future experiments would be aimed at achieving temperature control. Further, the role of bubbling gases in cracking would be investigated. With adequate temperature control, other parameters can be optimized to achieve maximum yields.

REFERENCES

(1) Alboudwarej, H.; Felix, J.; Taylor, S.; Badry, R.; Bremner, C.; Brough, B.; Skeates, C.; Baker, a; Palmer, D.; Pattison, K.; et al. Highlighting heavy oil. *Oilf. Rev.* **2006**, *18* (2), 34–53.

(2) Meyer, R. F. World heavy crude oil resources. In *Proceedings of the 15th World Petroleum Congress*; John Wiley & Sons, 1998; pp 459–471.

(3) Argillier, J.; Hénaut, I.; Gateau, P.; Héraud, J.; Français, I.; Glénat, P.; A, T. S. Heavy-Oil Dilution. In *SPE International Thermal Operations and Heavy Oil Symposium*; Society of Petroleum Engineers, 2005.

(4) Martinez-Palou, R.; Mosqueira, M. de L.; Zapata-Rendon, B.; Mar-Juarez, E.; Bernal-Huicochea, C.; de la Cruz Clavel-Lopez, J.; Aburto, J. Transportation of heavy and extra-heavy crude oil by pipeline: A review. *J. Pet. Sci. Eng.* **2011**, *75* (3-4), 274–282.

(5) Hart, A. A review of technologies for transporting heavy crude oil and bitumen via pipelines. *J. Pet. Explor. Prod. Technol.* **2014**, *4* (3), 327–336.

(6) Zhussupov, D. Assessing the potential and limitations of heavy oil upgrading by electron beam irradiation, Texas A&M University, 2006.

(7) Raseev, S. *Thermal and Catalytic Processes in Petroleum Refining*; Marcel Dekker Inc: New York, 2003.

(8) Zaikin, Y.; Zaikina, R. Self-sustaining cracking of hydrocarbons. US 8192591 B2, 2012.

(9) US Energy Information Administration. Petroleum & Other Liquids

http://www.eia.gov/dnav/pet/tbldefs/pet_pri_wco_tbldef2.asp (accessed Jul 21, 2016).

(10) Gray, M. R. *Upgrading Oilsands Bitumen and Heavy Oil*, 1st editio.; The University of Alberta Press: Edmonton, 2015.

(11) Ancheyta, J.; Rana, M. S. Future technology in heavy oil processing. *Encycl. Life Support Syst.* **2004**.

(12) Rana, M. S.; Samano, V.; Ancheyta, J.; Diaz, J. A. I. A review of recent advances on process technologies for upgrading of heavy oils and residua. *Fuel* **2007**, *86*, 1216–1231.

(13) Gray, M. R. *Upgrading petroleum residues and heavy oils*; Marcel Dekker Inc: New York, 1994.

(14) Speight, J. G. *The chemistry and technology of petroleum*, 3rd editio.; Marcel Dekker Inc: New York, 1999.

(15) Speight, J. G. Natural Bitumen (Tar Sands) and Heavy Oil. In *Coal, Oil Shale, Natural Bitumen, Heavy Oil and Peat, from Encyclopedia of Life Support Systems (EOLSS)*; Jinsheng, G., Ed.; Oxford: UNESCO, EOLSS, 2005; Vol. II.

(16) Punase, A.; Prakoso, A.; Hascakir, B. The Polarity of Crude Oil Fractions Affects the Asphaltenes Stability. In *SPE Western Regional Meeting*; 2016.

(17) Prakoso, A.; Punase, A.; Klock, K.; Rogel, E.; Ovalles, C.; Hascakir, B. Determination of the Stability of Asphaltenes Through Physicochemical Characterization of Asphaltenes. In *SPE Western Regional Meeting*; 2016.

(18) Stratiev, D. S.; Dinkov, R. K.; Shishkova, I. K.; Nedelchev, a. D.; Tasaneva, T.;

Nikolaychuk, E.; Sharafutdinov, I. M.; Rudney, N.; Nenov, S.; Mitkova, M.; et al. An Investigation on the Feasibility of Simulating the Distribution of the Boiling Point and Molecular Weight of Heavy Oils. *Pet. Sci. Technol.* **2015**, *33* (5), 527–541.

(19) Cunico, R. L.; Sheu, E. Y.; Mullins, O. C. Molecular Weight Measurement of UG8 Asphaltene Using APCI Mass Spectroscopy. *Pet. Sci. Technol.* **2004**, *22* (7 & 8), 787–798.

(20) Laboratory, N. E. T. A Literature Review on Cold Cracking of Petroleum Crude Oil. *Energy Policy Act 2005 Sect. 1406* **2006**.

(21) Alfi, M.; Silva, P. F. Da; Barrufet, M. A.; Moreira, R. G. Electron Induced Chain Reactions of Heavy Petroleum Fluids — Effective Parameters. In *SPE Heavy Oil Conference*; 2012.

(22) Alfi, M.; Barrufet, M. A.; Da Silva, P. F.; Moreira, R. G. Simultaneous application of heat and electron particles to effectively reduce the viscosity of heavy deasphalted petroleum fluids. *Energy and Fuels* **2013**, *27* (9), 5116–5127.

(23) Alfi, M.; Barrufet, M. A.; Moreira, R. G.; Da Silva, P. F.; Mullins, O. C. An efficient treatment of ultra-heavy asphaltic crude oil using electron beam technology. *Fuel* **2015**, *154*, 152–160.

(24) Zaykin, Y. A.; Zaykina, R. F. *Petroleum radiation processing*; CRC Press, 2013.

(25) Topchiev, A. V; Polak, L. S.; Glushnev, V. Y. E.; Popov, V. T. the Radiation-Thermal Cracking of Petroleum Hydrocarbons. *Neftekhimiya* **1962**, *2* (2), 196–210.

(26) Mustafaev, I.; Gulieva, N. The principles of radiation-chemical technology of refining the petroleum residues. *Radiat. Phys. Chem.* **1995**, *46* (4), 1313–1316.

(27) Zaikin, Y. A. On the nature of radiation-excited unstable states of hydrocarbon molecules in heavy oil and bitumen. *Radiat. Phys. Chem.* **2013**, *84*, 2–5.

(28) Zaikin, Y. A. Low-temperature radiation-induced cracking of liquid hydrocarbons. *Radiat. Phys. Chem.* **2008**, *77* (9), 1069–1073.

(29) Zaykina, R. F.; Zaykin, Y. A.; Mamonova, T. B.; Nadirov, N. K. Radiation-thermal processing of high-viscous oil from Karazhanbas field. *Radiat. Phys. Chem.* **2001**, *60* (3), 211–221.

(30) Foldiak, G.; Wojnarovits, L. the Influence of the Cyclic Structure of Hydrocarbons on Radiation Protection. *Int. J. Radiat. Phys. Chem.* **1972**, *4*, 189–197.

(31) Zaykina, R. F.; Zaykin, Y. A.; Mirkin, G.; Nadirov, N. K. Prospects for irradiation processing in the petroleum industry. *Radiat. Phys. Chem.* **2002**, *63* (3-6), 617–620.

(32) Zaykin, Y. A.; Zaykina, R. F.; Silverman, J. Radiation-thermal conversion of paraffinic oil. *Radiat. Phys. Chem.* **2004**, *69* (3), 229–238.

(33) Zaikin, Y. A.; Zaikina, R. F. Effect of radiation-induced isomerizationon gasoline upgrading. In *Eight International Topical Meeting on Nuclear Applications and Utilization of Accelerators*; Pocatello, Idaho, USA, 2007.

(34) Andrade, L. dos S.; Calvo, W. A. P.; Sato, I. M.; Duarte, C. L. Petroleum and diesel sulfur degradation under gamma radiation. *Radiat. Phys. Chem.* **2013**, *115*,

196–201.

(35) Zaykin, Y. A.; Zaykina, R. F. Bitumen radiation processing. *Radiat. Phys. Chem.* **2004**, *71* (1-2), 469–472.

(36) Zaikin, Y. A.; Zaikina, R. F. Polymerization as a limiting factor for light product yields in radiation cracking of heavy oil and bitumen. *Radiat. Phys. Chem.* **2013**, *84*, 6–9.

(37) Zaykina, R. F.; Zaykin, Y. A.; Mamonova, T. B.; Nadirov, N. K. Radiation methods for demercaptanization and desulfurization of oil products. *Radiat. Phys. Chem.* **2002**, *63* (3-6), 621–624.

(38) NUTEK CORPORATION. E-Beam vs . Gamma Sterilization. *NUTEK Corp.* **2008**.

(39) Green, M.; Cosslett, V. E. The Efficiency of Production of Characteristic X-radiation in Thick Targets of a Pure Element. *Proc. Phys. Soc.* **2002**, *78* (6), 1206–1214.

(40) Reiner, M. The Deborah Number. *Phys. Today* **1964**, *17* (1), 62.

(41) Dimitriou, C. J. The Rheological Complexity of Waxy Crude Oils: Yielding, Thixotropy and Shear Heterogeneities, Massachusetts Institute of Technology, 2013.

(42) Cengel, Y. A.; Turner, R. H. *Fundamentals of thermal-fluid sciences*, 1st editio.; McGraw-Hill: Boston, 2001.

(43) Chhabra, R. P. Non-Newtonian fluids: An introduction. In *Symposium on Rheology of Complex Fluids*; Chennai, India, 2010.

(44) Hinch, E. J. *Lecture Notes Woods Hole GFD Summer School 2003: Introduction to Non-Newtonian Fluids*; 2003; Vol. 1.

(45) Carrington, S.; Langridge, J. Viscometer or rheometer ? Making the decision. *Laboratory News*. 2005.

(46) Rheosys. Selecting Measuring Systems http://rheosys.com/Help_system/selecting_measuring_systems.htm (accessed Apr 10, 2015).

(47) Ghannam, M. T.; Hasan, S. W.; Abu-Jdayil, B.; Esmail, N. Rheological properties of heavy & light crude oil mixtures for improving flowability. *J. Pet. Sci. Eng.* **2012**, *81*, 122–128.

(48) Beal, C. The Viscosity of Air, Water, Natural Gas, Crude Oil and Its Associated Gases at Oil Field Temperatures and Pressures. *Transactions of the AIME*. 1946, pp 94–115.

(49) Beggs, H. D.; Robinson, J. R. Estimating the Viscosity of Crude Oil Systems. *J. Pet. Technol.* **1975**, 1140–1141.

(50) Glaso, O. Generalized Pressure-Volume-Temperature Correlations. *J. Pet. Technol.* **1980**, *32* (5), 785–795.

(51) ASTM D341-09. Standard Practice for Viscosity-Temperature Charts for Liquid Petroleum. *ASTM International, West Conshohocken, PA*. 2009.

(52) Seeton, C. J. Viscosity-temperature correlation for liquids. *Tribol. Lett.* **2006**, *22* (1), 67–78.

(53) Manning, R. E. Computational Aids for Kinematic Viscosity Conversions from

100 to 210 ° F to 40 and 100 ° C. *ASTM Int.* **1974**, 522–528.

(54) Khan, M. A. B.; Mehrotra, A. K.; Svrcek, W. Y. Viscosity Models for Gas-Free Athabasca Bitumen. *J. Can. Pet. Technol.* **1984**, *23* (3), 47–53.

(55) Mehrotra, A. K. Generalized one-parameter viscosity equation for light and medium liquid hydrocarbons. *Ind. Eng. Chem. Res.* **1991**, *30* (6), 1367–1372.

(56) Kavousi, A.; Tarobi, F.; Chan, C.; Shirif, E. Experimental measurement and parametric study of CO 2 solubility and molecular diffusivity in heavy crude oil systems. *Fluid Phase Equilib.* **2014**, *371*, 57–66.

(57) Gateau, P.; Hénaut, I.; Barré, L.; Argillier, J. F. Heavy oil dilution. *Oil Gas Sci. Technol.* **2004**, *59* (5), 503–509.

(58) Wallace, D.; Henry, D. Viscosity and Solubility of Mixtures of Bitumen and Solvent. *Fuel Sci. Technol. Int.* **1996**, *14* (3), 465–478.

(59) Eggertsen, F.; Groennings, S.; Holst, J. Analytical distillation by gas chromatography. Programmed temperature operation. *Anal. Chem.* **1960**, *32* (8), 904–909.

(60) Workman, S. Chapter 4: Simulated Distillation Measurement. In *Distillation and Vapor Pressure Measurement in Petroleum Products*; Montemayor, R. G., Ed.; ASTM International, 2008; pp 38–47.

(61) Grudoski, D. *Agilent SimDis Applications*; Houston, USA, 2013.

(62) Espinosa-Peña, M.; Figueroa-Gómez, Y.; Jiménez-Cruz, F. Simulated distillation yield curves in heavy crude oils: A comparison of precision between ASTM D-5307 and ASTM D-2892 physical distillation. *Energy and Fuels* **2004**, *18* (6),

1832–1840.

(63) Iupac. INTERNATIONAL UNION OF PURE COMMISSION ON ANALYTICAL NOMENCLATUREt Nomenclature for chromatography (IUPAC Recommendations 1993). *Pure Appl. Chem.* **1993**, *65* (4), 819–872.

(64) SHU. Gas Chromatography http://teaching.shu.ac.uk/hwb/chemistry/tutorials/chrom/gaschrm.htm (accessed Apr 10, 2015).

(65) Carbognani, L.; Lubkowitz, J.; Gonzalez, M. F.; Pereira-Almao, P. High temperature simulated distillation of athabasca vaccum residue fractions, bimodal distributions and evidence for secondary “on-column” cracking of heavy hydrocarbons. *Energy & Fuels* **2007**, *21*, 2831–2839.

(66) ASTM Standard D6352. Standard Test Method for Boiling Range Distribution of Petroleum Distillates in the Boiling Range from 174 to 700°C by Gas Chromatography. In *Annual Book of ASTM Standards*; ASTM International, West Conshohocken, PA; Vol. 5.

(67) ASTM Standard D7169. Standard Test Method for Boiling Point Distribution of Samples with Residues Such as Crude Oils and Atmospheric and Vacuum Residues by High Temperature Gas Chromatography. In *Annual Book of ASTM Standards*; ASTM International, West Conshohocken, PA.

(68) ASTM Standard D2887. Standard Test Method for Boiling Range Distribution of Petroleum Fractions by Gas Chromatography. In *Annual Book of ASTM Standards*; ASTM International, West Conshohocken, PA; Vol. 5.

(69) Peaden, P. Simulated Distillation of Petroleum and its Products by Gas and Supercritical Fluid Chromatography: A Review. *J. High Resolut. Chromatogr.* **1994**, *17*, 203–211.

(70) Vickers, A. K. Higher-Temperature Simulated Distillation with DB-HT Sim Dis Columns Application. *Hydrocarbon Processing*. 2002.

(71) Gas Chromatography http://chemwiki.ucdavis.edu/Core/Analytical_Chemistry/Instrumental_Analysis/Chromatography/Gas_Chromatography (accessed Apr 20, 2015).

(72) Holm, T. Aspects of the mechanism of the flame ionization detector. *J. Chromatogr. A* **1999**, *842* (1-2), 221–227.

(73) Chasteen, T. G. Flame Ionization Detector http://www.shsu.edu/chm_tgc/primers/FID.html (accessed Apr 10, 2015).

(74) Sutton, P. A.; Lewis, C. A.; Rowland, S. J. Isolation of individual hydrocarbons from the unresolved complex hydrocarbon mixture of a biodegraded crude oil using preparative capillary gas chromatography. *Org. Geochem.* **2005**, *36* (6), 963–970.

(75) Strydom, W.; Parker, W.; M, O. *Chapter 8 Electron Beams : Physical and Clinical Aspects*; 2006; Vol. 1.

(76) Industrial Irradiators for Radiation Processing. CANTEACH.

(77) Zimek, Z. *New trends in accelerators development*; Warsaw, Poland, 2013.

(78) Berman, I. Designing a system for upgrading of heavy crude oils through electron beam treatment, Texas A&M University, 2015.

(79) NuStar. Savannah Refinery Tour http://library.corporate-ir.net/library/19/197/197894/items/297891/SavannahTour_061908.pdf (accessed Jan 1, 2016).

APPENDIX A

RHEOMETER CALIBRATION

Accuracy of rheological measurements was verified using standard oils which are certified by National Institute for Standards and Technology (NIST). Two high viscosity standards were used for this purpose; s30000 and s8000 with viscosities of 74890cP and 23920cP respectively at 25°C. Shear rates in the range of 0.01 to 100s^{-1} were employed and the average value measured. The standard oils used exhibited Newtonian behavior at all the temperatures used for this study. Tables 5 & 6 give the measured value vs standard value and the % difference between the both. A maximum deviation of 4.5% was observed for s30000 at 100°C. Hence, 4.5% (using 5% as an overestimation) was determined to be the maximum possible measurement error using the rheometer.

Temperature [C]	Calibration Standard [mPa.s]	Avg Measured Value [mPa.s]	% difference
25	74890	76145	1.68
37.78	24720	25280	2.27
40	20660	21155	2.40
50	9698	9937.5	2.47
80	1459	1514	3.77
100	537.2	561.6	4.54

Table 5: Dynamic viscosity measurements of standard oil s30000

Temperature [C]	Calibration Standard [mPa.s]	Avg Measured Value [mPa.s]	% difference
37.78	7977	7767.5	-2.63
40	6688	6527	-2.41
50	3159	3090.5	-2.17
80	497.6	493.45	-0.83
100	192.6	191.45	-0.60

Table 6: Dynamic viscosity measurements of standard oil s8000

APPENDIX B

DENSITY METER CALIBRATION AND MEASUREMENTS

A density meter has been employed to measure the density of crude oils. An Anton Paar density meter (DMA 4500) has been used. Requiring 2ml of sample, it can operate within 20°C and 90°C. Sample is taken into a 3 ml syringe and is inserted into the test cell. Initial calibration tests indicate high accuracy. Table 7 gives the details of calibration using standard oils s600, s2000 and s8000.

Temperature [C]	s600 [g/mL]	Measured [g/mL]	% difference	s2000	Measured [g/mL]	% difference	s8000	Measured [g/mL]	% difference
20	0.8467	0.8467	*0.00 %*	0.8761	0.8763	*0.02 %*	0.8883	0.8882	*0.01 %*
25	0.8437	0.8437	*0.00 %*	0.8732	0.8734	*0.03 %*	0.8856	0.8854	*0.02 %*
37.78	0.836	0.8361	*0.01 %*	0.8659	0.8661	*0.03 %*	0.8785	0.8783	*0.01 %*
40	0.8347	0.8347	*0.01 %*	0.8646	0.8649	*0.03 %*	0.8773	0.8771	*0.02 %*
50	0.8288	0.8288	*0.00 %*	0.8589	0.8591	*0.03 %*	0.8718	0.8716	*0.02 %*
80	0.8111	0.8111	*0.00 %*	0.8419	0.8412	*0.01 %*	0.8553	0.855	*0.01 %*

Table 7: Density meter calibration results

However, since the sample insertion happens only by the use of a syringe, oil #2 cannot be used on this instrument. Hence, only oil #1 density measurements are presented in table 8 and a linear fit has been provided in figure 47.

Temperature [C]	Density [g/mL]
20	1.00225
30	0.99596
37.78	0.99111
40	0.98973
50	0.98346
60	0.97734
70	0.97115
80	0.965
90	0.95882

Table 8: Oil #1 density measurements

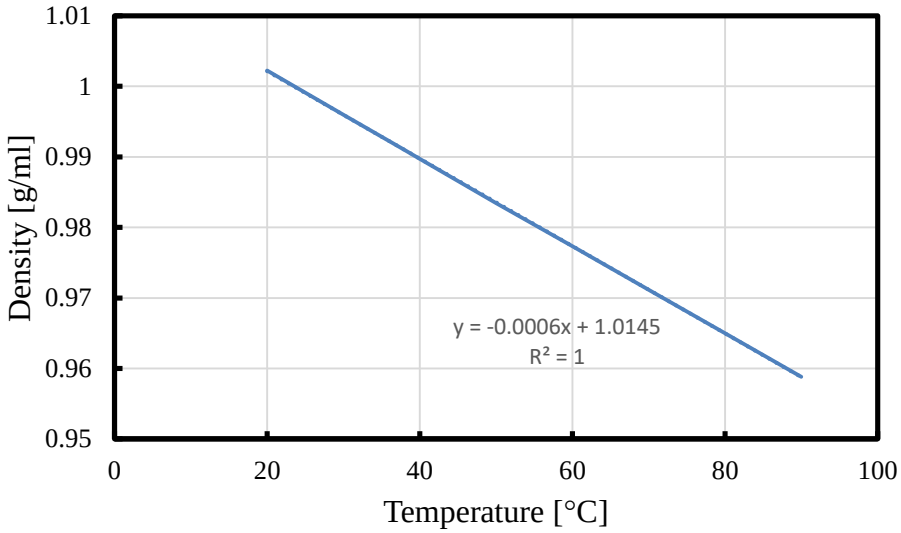

Figure 47: Density vs temperature for oil #1

APPENDIX C

RESULTS

C.1 Experimental Conditions

23 successful experiments have been performed so far using both oil #1 and oil #2. Various temperature ranges, shear rates and dose ranges were used. Initial experiments on oil #1 were performed using a semi-batch reactor. Later, the system was modified to a flow loop system. A wide range of doses have been used, 5 kGy – 1750 kGy. Both low and high shear rates have been employed. High shear rates had a range of 45-180 s^{-1} whereas experiments performed using low shear rates had a range of 20-50 s^{-1}.

The accelerator and electron energy configurations at the facility allowed little control over the dose rate. A highest dose rate of 20 kGy/s was achieved while few initial experiments were performed at low dose rates of 15 kGy/s. Some experiments had bubbling gases such as methane or hydrogen pumped into the oil while treatment to help the cracking process. Flow rates were varied in the range of 1-2 LPM. Further, separation chamber was absent in a few experiments. Table 9 gives the conditions for the experiments performed so far.

Exp No	Reactor	Flow rate LPM	Sep Chamber	Average shear rate [1/s]	Dose rate (kGy/s)	Dose (kGy)	Temperature range
Oil #1-E13	Loop	1	No	61-68	19.5	440	257-279°C
Oil #1-E12	Loop	2	No	15-27	19.5	757	140-156°C
Oil #1-E11	Loop	2	Yes	25-126	21.64	648	140-280°C
Oil #1-E10	Loop	2	Yes	21-130	20	1308	140-280°C
Oil #1-E9	Loop	2	Yes	30-60	19	198	150-215°C
Oil #1-E8	Loop	2	No	15-134	14.75	691	120-260°C
Oil #1-E7	Loop	2	Yes	18-155	17.68	605	130-300°C
Oil #1-E6	Loop	2	Yes	48-134	18.37	270	177-278°C
Oil #1-E5	Loop	2	Yes	48-181	17	348.5	175-310°C
Oil #1-E4	Loop	2	No	90.3-98	15	525	178-225°C
Oil #1-E3	Semi-batch	1	No	11.2	15	36.8	200°C
Oil #1-E2	Semi-batch	2	No	73	18.2	24.65	200°C
Oil #1-E1	Semi-batch	1	No	27	6.9	4.91	160°C
Oil #2-E8	Loop	1.5	No	20-50	20	757	200-250°C
Oil #2-E7	Loop	2	Yes	19-89	20	1774	200-290°C
Oil #2-E6	Loop	2	Yes	16-90	20	910	200-298°C
Oil #2-E5	Loop	2	Yes	12-87	20	1342	172-294°C
Oil #2-E4	Loop	2	Yes	12-90	20	1200	174-295°C
Oil #2-E3	Loop	2	Yes	12-90	20	1200	174-287°C
Oil #2-E2	Loop	2	Yes	15-85	19.5	1200	180-300°C
Oil #2-E1	Loop	2	Yes	28-137	19.5	562.8	180-300°C

Table 9: Experimental conditions

C.2 Mass Balance

As detailed in chapter 6, mass balance has a huge impact on the end result. A summary of the mass balance results can be found in the table 10.

Exp No.	Mass put in (gm)	Accounted mass %	Collector %	Separation Chamber %	Condenser %
Oil #1-E13	1850.8	94.33	89.61	NA	0.8
Oil #1-E12	1889	93.29	85.73	NA	8.83
Oil #1-E11	1604.43	99.67	81.62	12.1	3.11
Oil #1-E10	1575	86.4	41.01	15.04	3.24
Oil #1-E9	1583.63	102.37	96.05	3.46	0.7
Oil #1-E8	1673.02	102.24	94.62	NA	3.4
Oil #1-E7	1850.3	99.68	80	15.32	0.85
Oil #1-E6	1510.92	100.32	91.34	4.92	0.6
Oil #1-E5	1612.94	99.99	87.85	8.4	0.59
Oil #1-E4	2350	94.09	90.89	NA	0.17
Oil #1-E3	2760	104.44	100.54	NA	0.18
Oil #1-E2	2370	97.05	91.14	NA	0.21
Oil #1-E1	1950	100	94.62	NA	0.28
Oil #2-E8	2104.7	102.14	97.20	NA	2.75
Oil #2-E7	1849.50	111.36	84.15	8.2	5.8
Oil #2-E6	1811.70	99.56	89.65	5.05	1.32
Oil #2-E5	2131	96.5	59.4	13.5	3.5
Oil #2-E4	1803	95.75	32.32	15	4.15
Oil #2-E3	1832	102.47	85.38	11.85	2.94
Oil #2-E2	1832	98.42	75.91	13.54	3.28
Oil #2-E1	1831	100.36	92.29	5.05	1.32

Table 10: Mass balance results

C.3 Conversion

Simulated distillation results give the sample and residual conversion. Details of simulated distillation have been provided in chapter 5. Figures 48 & 49 plot the % wt off vs BP for treated and raw samples for oil #1 and figure 50 plots the results for oil #2.

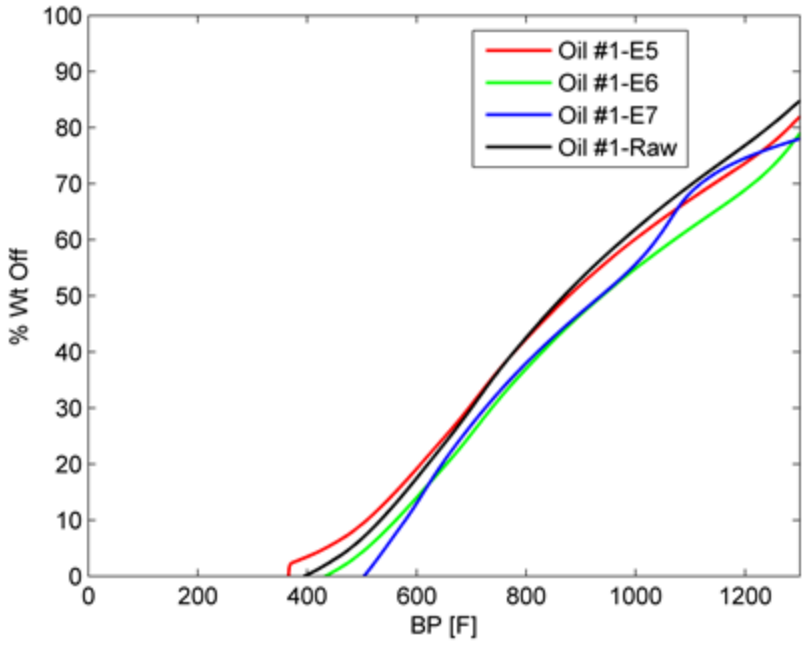

Figure 48: SimDis results for oil #1-E5-7

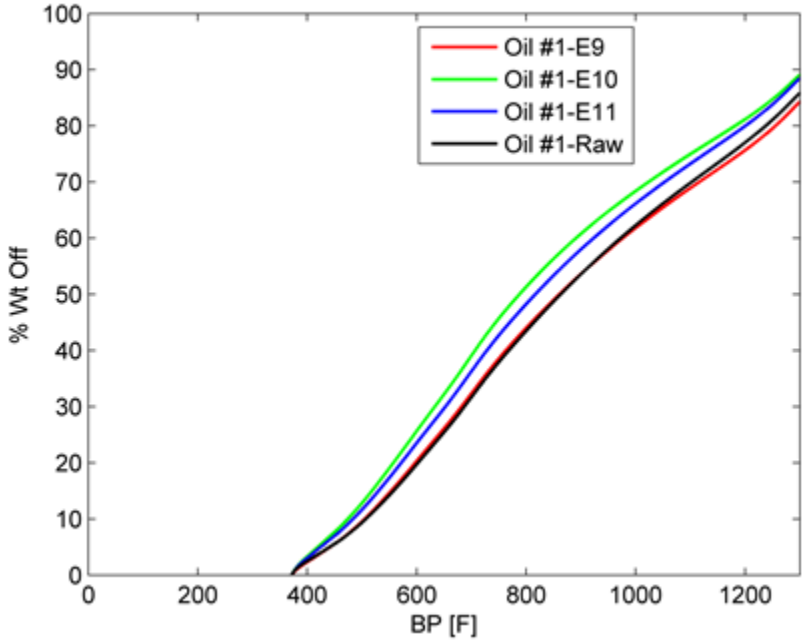

Figure 49: SimDis results for oil #1-E9-11

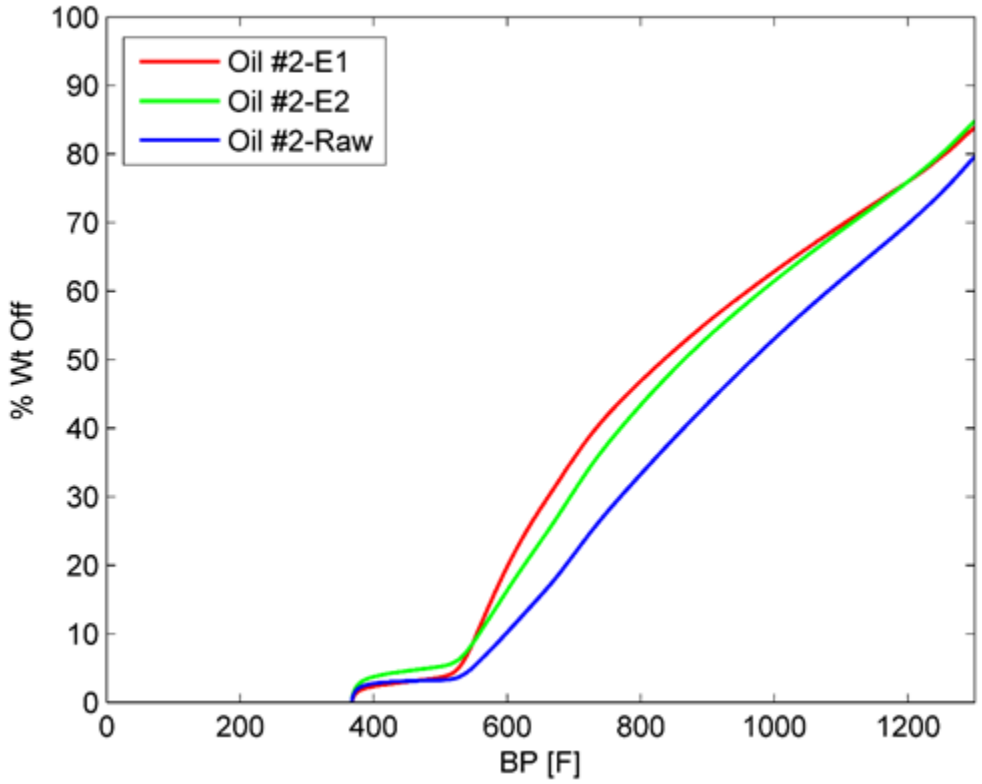

Figure 50: SimDis results for oil #2

C.4 Time Stability

Chapter 6 details the time stability of treated oil samples. Oil #1 has shown viscosity increase over time whereas oil #2 had steady viscosity over time. Tables 11 & 12 give the absolute viscosity measurements along with the time span and comparison to the raw sample.

	Oil #2-E7		Oil #1-E4		Oil #1-E1	
Temperature	100°C	150°C	100°C	150°C	100°C	150°C
Raw [cP]	1870	132	1870	132	1870	132
	After 2 days		After 15 days		After 6 days	
Wt mix [cP]	1380	110	1240	101	1040	NA
% reduction	*26.20%*	*16.67%*	*33.69%*	*23.48%*	*44.39%*	NA
	After 100 days		After 85 days		After 83 days	
Wt mix [cP]	1430	108	1160	93.9	1080	89.5
% reduction	*23.53%*	*18.18%*	*37.97%*	*28.86%*	*42.25%*	*32.20%*

Table 11: Oil #2 viscosity over time

	Oil #2-E11		Oil #1-E10		Oil #1-E9		Oil #1-E5	
Temperature	50°C	100°C	50°C	100°C	50°C	100°C	50°C	100°C
Raw [cP]	9350	247.3	9350.4	247.3	9350.4	247.3	9350	247.3
	After 10 days		After 12 days		After 13 days		After 6 days	
Wt mix [cP]	6136	186.2	2471.2	109.1	8228.4	211.2	7865	216.0
% reduction	*34.4%*	*24.7%*	*73.6%*	*55.89%*	*12.0%*	*14.6%*	*15.9%*	*12.6%*
	After 12 days		After 85 days		After 105 days		After 61 days	
Wt mix [cP]	6154	186.8	3430.2	136.04	9617	240.6	7940	215.1
% reduction	*34.2%*	*24.5%*	*63.3%*	*45.0%*	*-2.85%*	*2.73%*	*15.1%*	*13.0%*
	After 88 days		After 181 days		After 182 days		After 145 days	
Wt mix [cP]	7429.8	244.2	3420	129	10099	242.62	8452	235.3
% reduction	*20.5%*	*1.27%*	*63.42%*	*47.85%*	*-8.0%*	*1.91%*	*9.61%*	*4.85%*

Table 12: Oil #1 viscosity over time

APPENDIX D

STANDARD OPERATING PROCEDURE FOR GC-FID

Sample Preparation

1. Take approximately 0.1gm (note the mass) of the sample in a glass vial
2. Pour 10 ml of Dichloromethane (100 times the mass of sample) into the vial
3. Shake it well and sonicate at room temperature for 5-10 minutes
4. Pipette out 250µl of the sample into the GC vial
5. Place the vial in the GC autosampler tray

GC Programming

1. Open ChemStation software and select one of the pre-loaded methods (ASTM D7169 and D6352 have already been loaded into the software)
2. Make sure all the parameters are correct by referring to the table 13

Parameter	Modified ASTM D7169	Modified ASTM D6352
Injection volume	1ul	0.5ul
Solvent A washes (Pre-inj)	6	6
Solvent B washes (Pre-inj)	6	6
Sample washes (Pre-inj)	3	3
Solvent A washes (Post-inj)	6	6
Solvent B washes (Post-inj)	6	6
Plunger speed	Slow	Slow
Column Flow	20 ml/min	18 ml/min
Carrier Control	Constant Flow	Constant Flow
Initial Oven Temperature	25^0C	50^0C
Oven Temp Program	15^0C/min	10^0C/min
Final Oven Temperature	430^0C	400^0C
Final Hold Time	150 min	180 min
Inlet Initial Temperature	50^0C	Oven track mode
Inlet Temp Program	15^0C/min	Oven track mode
Inlet Final Temperature	425^0C	Oven track mode
Detector Temperature	435^0C	450^0C
Detector –Hydrogen	32 ml/min	32 ml/min
Detector-Air	400 ml/min	400 ml/min
Detector-He Make Up	24 ml/min	24 ml/min
Data Acquisition Rate	10 Hz	10 Hz

Table 13: GC-FID methods

3. Choose the required folder in ‘Sequence Parameters’ and set up a sequence using the ‘sequence table’
4. Make sure to include blank runs in between sample runs in order to make sure there is no residual left from the previous sample

Sample Injection

1. Prior to sample injection, make sure all the vials are in the same order as in the sequence
2. Make sure solvent A and solvent B are till the minimum level in the vials
3. Typical solvents are Toluene for A and DCM for B
4. Run the sequence

Data Analysis

1. Export the data in the form of .csv files
2. Plot signal vs retention time
3. Use the figure 51 to get the correlation between boiling point and retention time

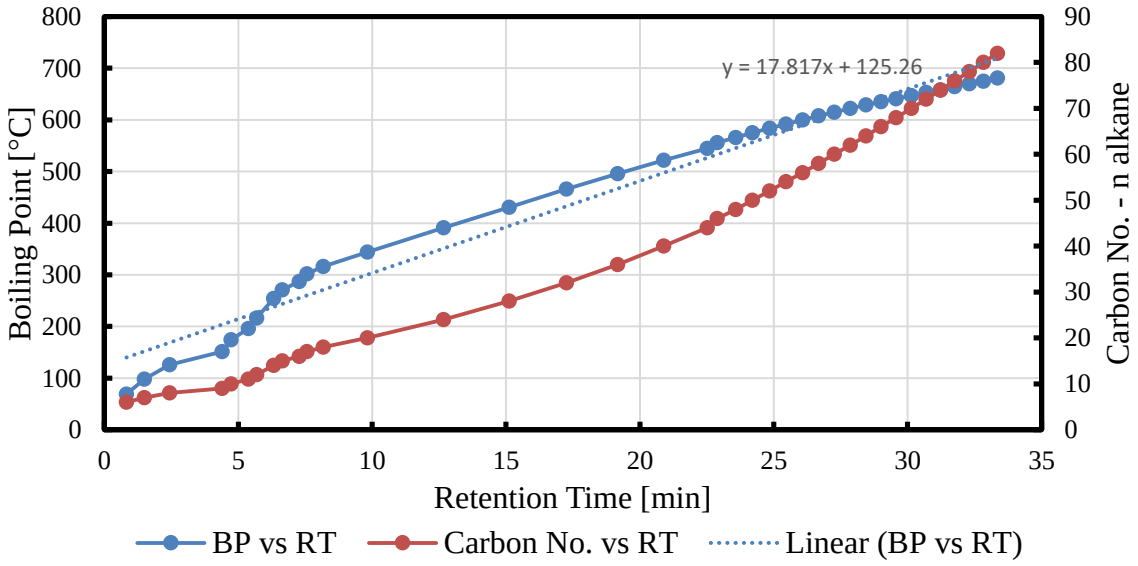

Figure 51: BP vs RT correlation

4. Calculate cumulative area of signal/total area of signal (% off) for retention time
5. Using the correlation between RT and BP, plot % off vs BP

Maintenance

1. After every sequence, manually clean the syringe with a solvent (DCM/Toluene)
2. Make sure there is reasonable flow in the column and detector when there is no sample elution
3. Reduce the FID temperature to 100-120°C when not in use
4. Perform leak checks and clean detector jet periodically
5. Replace the septum at the inlet after every 10 injections

APPENDIX E

STANDARD OPERATING PROCEDURE – RHEOMETER

1. Start the instrument and make sure there is adequate air flow (>= 1 m^3/h and 80psi)
2. Initialize the instrument and set the measuring system in place by lining up the markings on the spindle with the marking on the toolmaster
3. Verify the measuring system in the software and set zero gap (0.049 mm for cone-plate and 1 mm for plate-plate)
4. Set a moderate temperature on the bottom plate (50°C for oil #1 and 80°C for oil #2)
5. Scoop approximately 1.5gm (slightly more than the required 1.14gm) of oil and place it on the bottom plate
6. Lower the upper plate to measuring position and trim the sample to ensure the right amount of sample is between the plates
7. Set the measuring temperature and wait till the temperature is steady within 0.02°C of the set temperature
8. Select the appropriate program; ‘constant shear rate’ which allows for constant or ramped shear rate or ‘verification using standard oils’ when using standard oils or an apt program for thixotropy or creep tests.
9. Verify the requirements for each program. For example, 3 step creep test requires the use of a 25mm plate-plate measuring system and a gap of 0.3mm
10. Enter the required shear rate (constant, linear or log ramp) and start the test

11. After the measurements are taken, cool the base and remove the oil using solvents. Mineral spirits is used to clean the oil and IPA is used to remove any traces of mineral spirits
12. Perform calibration tests using standard oils frequently. Once every two months or sooner if possible
13. Even though the instrument is rated to high temperatures (450°C), for time dependent measurements it is advisable to perform testing at moderate temperatures (<250°C)

APPENDIX F

INTEGRATION

This section details the integration used to obtain the % off vs BP plot. Procedure to obtain the sample and blank offset have been detailed too.

```
%%% This part is for sample and blank offset
% n denotes the total no. of samples; 1 being the dcm blank
a = dlmread('plots.csv',',',1,0);
n = 4
n1 = [1 2 3 4]
no = [1 2 3];

for ii = 1:n
    t_o(:,ii) = a(:,2*ii-1);
    s_o(:,ii) = a(:,2*ii);
    t_o(s_o==0) = NaN;
    s_o(s_o==0) = NaN;
end

%%% Plot the signal before offset
plot(t_o,s_o)
ylim([0,400])
legend(num2str(n1'))
title('signal before offset')

%%%

for i = 1:n
    m = mean(a(1:10,2*i));
    sd = std(a(1:10,2*i));
    sum=0;
    count=0;
    for k=1:10
        if a(k,2*i)<=m+sd && a(k,2*i)>=m-sd
            sum=sum+a(k,2*i);
            count=count+1;
        else
            a(k,2*i)=0;
        end
    end
    average=sum/count;
    a(:,2*i)=a(:,2*i)-average;
    for k = 1:length(a)
        if a(k,2*i)<0;
            a(k,2*i)=0;
        end
    end
end
```

```
%%%

for ii = 1:n
    t(:,ii) = a(:,2*ii-1);
    s(:,ii) = a(:,2*ii);
    t(s==0) = NaN;
    s(s==0) = NaN;
end

%%% Plot the signal after offset
figure
plot(t,s)
ylim([0,400])
legend(num2str(n1'))
title('signal after offset')
%%%

%%% To get the time to start and end same
tmx = min(max(t));
tmn = max(min(t));
dt = min(min(diff(t)));
Nt = round(((tmx-tmn)/dt));
Nt = 50000;
tn = linspace(tmn,tmx,Nt);
%

%%% If trimming is needed
tn = tn(tn>1);
%

for ii = 1:n
    gi = ~isnan(s(:,ii)); % good indicies
    sn(:,ii) = interp1(t(gi,ii),s(gi,ii),tn);
    snn(:,ii) = sn(:,ii)/conc(ii); %%% if different concentrations
end
%%%
%%% Same tn for all signals sn
%%% Blank line subtraction
for i=2:n
    sb(:,i-1)=sn(:,i)-sn(:,1);
end

%%% Plot after blank line subtraction
figure
plot(tn,sb,'-')
ylim([0,400])
legend(num2str(no'))
title('signal after blank line subtract')

%%% %off vs BP
cols = 'rg:bkc'
for i = [1,3]
```

```
    st = sb(:,i);
    area = sum(st);
    s2{i} = cumsum(st)*100/area;
    bp = (14.701*tn+182.62)*9/5 + 32   %% BP vs RT correlation
    plot(bp,s2{i},cols(i), 'linewidth',1.5);
    xlim([0,1300])
    ylim([0,100])
    set(gca,'fontsize',12)
    xlabel('BP [F]')
    ylabel('% off')
    legend('xyz','abc');
    title('% off vs bp')
    hold on
end
```

APPENDIX G

ECONOMIC VIABILITY

Perhaps the most important evaluation during the development of any successful process is the economics. Good results are not of much use if not accompanied by economic viability. A thorough economic evaluation is necessary to ascertain the success of a process. This section details the cost of radiation processing and its economic viability.

An industrial facility of 1.5 MW is considered which consists of three 500 KW accelerators. Each of the accelerators cost approximately $5 million[76]. Since, all the accelerators are in the same facility shielding costs are assumed to be $4 million [Personal Communication, Amit Chaudhuri (Senior Research Instrumentation Specialist, NCERB, TAMU)]. This results in a total CAPEX of $19 million. It has been divided into 50% down payment and rest at 5% interest over 15 years. 10% downtime is assumed owing to the necessary maintenance processes. Moreover, 90% utilization efficiency is considered for the reactor design.

Use of linear DC accelerators over RF accelerators significantly increases the efficiency. Linear DC accelerators have an efficiency of 60-80% versus RF accelerators which only have 20-50% efficiency[77]. An average 70% accelerator efficiency has been used for this study. Further, the auxiliary and subsystems are assumed to consume one third of the accelerator output power i.e. 500 KW. An overestimate of electricity price has been used; $0.08/KWh. This is the typical commercial electricity rate and if there is onsite

power generation, the price significantly reduces. General and administration costs of $1000 have been estimated per day.

Different values of absorbed dose in the range of 100-1000 kGy are considered. Dose rates and electron energies can be optimized for the accelerator to obtain high dose rates and moderate electron energies. Operating temperatures in the range 100-250°C were considered and electricity was used to heat the oil prior to treatment. It should be noted that use of electricity is an overestimation as a simple heat exchanger could be designed to transfer heat from processed oil to feedstock. However, higher than typical costs were employed so as to be closer to the worst case scenario. Figure 52 gives the plot of $/barrel processing cost versus the absorbed dose at different operating temperatures.

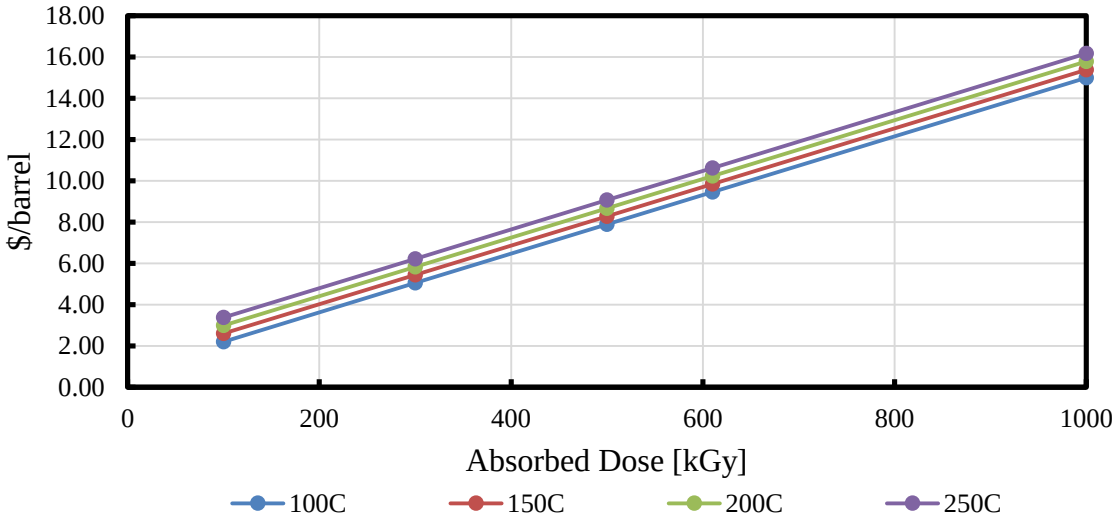

Figure 52: Oil processing cost using radiation cracking

General trends in oil market place reveal a $20 per barrel difference between heavy Boscan crude and light WTI crude[78,79]. Boscan crude is similar to oil #1 and oil #2 in API gravity at 10° whereas WTI is light crude of API gravity 39.6°. Price of Maya crude (API 21.5°) is half way between Boscan and WTI crude. If the end product of ebeam processing result in properties similar to Maya crude, there would be an increase in $10 per barrel price making it the breakeven price.

At a breakeven price of $10/barrel and operating temperatures lower than 200°C, absorbed dose of <600 kGy becomes economical. At 250°C, maximum economical dose is approximately 550 kGy. A low dose, low temperature (100°C and 100 kGy) run would only result in a processing cost of $2.21 whereas a high temperature, high dose (250°C and 1000 kGy) would result in processing costs as high as $16.17. A moderate dose and temperature (150°C and 300 kGy) lead to $5.44/barrel cost of upgrading. Considering a $10/barrel increase in market price, low to moderate dose and temperature leads to significant profits.